SURFACE MODIFICATION OF POLY(VINYL CHLORIDE) BY PHYSISORBED FREE RADICAL INITIATION FOR REDUCED PLASTICIZER MIGRATION AND ANTIMICROBIAL PROPERTIES

A Dissertation

Presented to

The Graduate Faculty of The University of Akron

In Partial Fulfillment

of the Requirements for the Degree

Doctor of Philosophy

Kathryn McGinty

December, 2008

SURFACE MODIFICATION OF POLY(VINYL CHLORIDE) BY PHYSISORBED FREE RADICAL INITIATION FOR REDUCED PLASTICIZER MIGRATION AND ANTIMICROBIAL PROPERTIES

Kathryn McGinty

Dissertation

Approved:	Accepted:
Advisor Dr. Roderic P. Quirk	Department Chair Dr. Ali Dhinojwala
Committee Member Dr. Scott Collins	Dean of the College Dr. Stephen Z.D. Cheng
Committee Member Dr. Ali Dhinojwala	Dean of the Graduate School Dr. George R. Newkome
Committee Member Dr. Judit Puskas	Date
Committee Member Dr. Mark D. Soucek	

ABSTRACT

Poly(vinyl chloride), PVC, is a particularly important commodity polymer that accounts for an annual world-wide production of 26 million tons. It is used frequently in the medical field as blood storage bags, endotracheal and dialysis tubing and intravenous catheters. Common plasticizers, namely di(2-ethylhexyl) phthalate (DEHP), are added to PVC to improve the processability and flexibility by lowering the glass transition temperature. However, most phthalate plasticizers are potential carcinogens. There has been extensive research on PVC with surface coatings to improve biocompatibility, surface crosslinking to create a barrier to the plasticizer leaching and surface grafting of hydrophilic polymers for both biocompatibility and reduced plasticizer migration.

A novel surface grafting technique is the grafting of hydrophilic monomers by physisorbed free radical initiators. This modification method can be applied to PVC to attach vinyl hydrophilic monomers by the "grafting from" method. This approach, extending on earlier work involving polymer brush formation on poly(dimethylsiloxane), involves a two-step process: physisorption of a hydrophobic free radical initiator onto a polymer surface followed by radical polymerization of hydrophilic monomers in water. The key step is creating a hydrophobic/hydrophilic diffusional barrier that promotes radical reactions at the polymer surface.

Polymers that have been successfully grafted from PVC films and tubing include: poly(hydroxyethyl methacrylate) (PHEMA), poly(dimethylacrylamide) (PDMA), poly(hydroxyethyl acrylate) (PHEA), poly(dimethylaminoethyl methacrylate) (PDMAEMA), poly(acrylic acid) (PAA), and poly(4-vinylpyridine) (P4VP). Characterization methods performed include bulk chemical composition by transmission infrared spectroscopy, surface composition using X-ray photoelectron spectroscopy, surface wettability by tensiometry and capillary rise, film thickness determination by infrared, gravimetric analysis and UV-Vis spectroscopy and M_n by gel permeation chromatography. The hydrophilic modification was demonstrated to decrease plasticizer migration via UV-Vis spectroscopy.

A particular system of interest is PVC with grafted poly(4-vinylpyridine) that has been quaternized due to its potential in killing bacteria such as *escherichia coli*, *staphylococcus aureus*, *staphylococcus epidermis*, and *pseudomonas aeruginosa*. Quaternization has been measured with IR spectroscopy.

DEDICATION

I would like to dedicate this work to my parents, Leo and Lynn McGinty. They have always been there for me every step of the way. From them I have learned the meaning of trust, loyalty and support.

ACKNOWLEDGEMENTS

I would like to thank Dr. Bill Brittain for his continued support, guidance and wisdom. His dedication to his students is commendable and I have greatly benefited from his mentorship. The entire polymer faculty nurtured my education with their shared expertise in each facet of polymer science. I would especially like to thank my advisor, Dr. Roderic Quirk and committee members: Dr. Scott Collins, Dr. Judit Puskas, Dr. Ali Dhinojwala and Dr. Mark Soucek. Ryan Van Horn and Wayne Jennings were also extremely helpful, providing AFM results and guidance when using the XPS.

TABLE OF CONTENTS

Page

LIST OF TABLES

Table Page

LIST OF FIGURES

LIST OF SCHEMES

Scheme Page

LIST OF ABBREVIATIONS

3	6-perfluorooctyl-1-bromohexane
5	PVC-*g*-P4VP quaternized with **3**
4a	1-bromobutane
4b	1-bromohexane
4c	1-bromooctane
4VP	4-vinylpyridine
6a	PVC-*g*-P4VP quaternized with **4a**, *n*-butylpyridinium film
6b	PVC-*g*-P4VP quaternized with **4b**, *n*-hexylpyridinium film
6c	PVC-*g*-P4VP quarternized with **4c**, *n*-octylpyridinium film
AA	acrylic acid
AFM	atomic force microscopy
AIBN	2,2-azobis(2-methylpropionitrile)
APTES	3-aminopropyltriethoxysilane
ATR-IR	attenuated total reflectance infrared radiation
ATRP	atom transfer radical polymerization
AU	absorbance unit
BBL	commercial medical agar company
BMA	butyl methacrylate
bronopol	2-bromo-2-nitropropane-1,3-diol
BSA	*bovine serum albumin*

$CDCl_3$	dueterated chloroform
CFU	colony-forming units
Coag. Staph	*coagulase-negative staphylococci*
CPAV	poly(acrylamide-*co*-poly(4-vinylpyridine))
CPDA	citrate-phosphate-dextrose-adenine
CVD	chemical vapor deposition
DEHA	di-2-ethylhexyl adipate
DEHP	di(2-ethylhexyl) phthalate
DIDP	diisodecyl phthalate
DINP	diisononyl phthalate
DITDP	diisotridecyl phthalate
DMA	*N*,*N*-dimethylacrylamide
DMAEMA	*N*,*N*-dimethylaminoethyl methacrylate
DMF	*N*,*N*-dimethylformamide
DNHP	di-*n*-heptyl phthalate
DOP	dioctyl phthalate
DTC	*N,N*-diethyl dithiocarbamate
E. coli	*escherichia coli*
ESA	electrostatic self-assembly
ESO	epoxidized soybean oil
EVA	poly(ethylene-*co*-vinyl acetate)
EVACO	poly(ethylene-*co*-vinyl acetate-*co*-carbon monoxide)
FDA	Food and Drug Association

FT-IR	Fourier transform infrared radiation
GPC	gel permeation chromatography
HEA	2-hydroxyethyl acrylate
HEMA	2-hydroxyethyl methacrylate
HMDI	hexamethylene diisocyanate
MEHP	monoethylhexyl phthalate
MEK	methyl ethyl ketone
NAG	*N*-acetyl-glucosamine
NAM	*N*-acetylmuramic acid
NMP	nitroxide-mediated polymerization
NMR	nuclear magnetic resonnance
NVP	*N*-vinylpyrrolidone
P. A.	*pseudomonas aeruginosa*
P4VP	poly(4-vinylpyridine)
PAA	poly(acrylic acid)
PAM	poly(acryamide)
PDMA	poly(dimethylacrylamide)
PDMAEMA	poly(dimethylaminoethyl methacrylate)
PDMS	poly(dimethylsiloxane)
PEG	poly(ethylene glycol)
PEO	poly(ethylene oxide)
PEO-Si	α,ω-bistriethoxysilane-terminated PEO
PHEA	poly(hydroxyethyl acrylate)

PHEMA	poly(hydroxyethyl methacrylate)
PIII	plasma immersion ion implantation
PMEA	poly(2-methoxyethyl acrylate)
PPO	poly(propylene oxide)
PS	polystyrene
PTFE	polytetrafluoroethylene
PTT	partial thromboplastin time
PVC	poly(vinyl chloride)
RAFT	reversible addition fragmentation chain transfer
RF	radiofrequency
S. A.	*staphylococcus aureus*
S. E.	*staphylococcus epidermis*
SEM	scanning electron microscopy
TBAB	tetrabutylammonium bromide
TBAH	tetrabutylammonium hydrogen sulphate
TEOS	tetraethoxysilane
THF	tetrahydrofuran
Ti(C, N)	$Ti[N(C_2H_5)_2]_4$
TPN	total parenteral nutrition
triclosan	2,4,4'-trichloro-2'-hydroxydiphenyl ether
Tween 20	poly(oxyethylene 20 sorbitan) monolaurate
UV-Vis	ultraviolet-visible
XPS	X-ray photoelectron spectroscopy

CHAPTER I

INTRODUCTION

Poly(vinyl chloride) (PVC) is the second most commonly used polymer and accounts for an annual world-wide production of 26 million tons. Many applications are in the medical field, such as blood storage bags, endotracheal tubes, dialysis tubing, and intravenous catheters. The properties of PVC are drastically altered by the incorporation of plasticizer which induces flexibility by lowering the second order transition temperature. However, phthalate ester plasticizers typically used for PVC have been under public scrutiny as potential carcinogens attributed to the pathogenesis of endocrine, pulmonary and hepato-toxicity.[1-3] Also the poor biocompatibility of the hydrophobic PVC surface leads to unwanted protein adsorption and cell adhesion.[4] To solve these problems, considerable basic and applied research has been devoted to the surface modification of the polymer. The polymer surface is the phase boundary that resides between the bulk polymer and the outer environment. By altering the properties of the boundary, the performance of the polymer can be modified.

Surface modifications of PVC have been developed by both chemical and physical processes to reduce plasticizer migration and increase the biocompatibility. Such techniques include surface coating,[5-11] surface crosslinking with ultraviolet radiation or plasma treatment,[12-17] and surface grafting with hydrophilic polymers.[18-23] Surface coating of antibacterial reagents, or hydrophilic polymers generally increases the

biocompatibility of PVC while surface crosslinking is intended to create a barrier to prevent interfacial mass transport of plasticizer.

Among these techniques, surface grafting has several advantages that include easy and controllable introduction of grafted chains with high density accompanied by minor changes in the bulk properties. Covalent attachment of grafted chains onto a polymer surface avoids desorption and ensures long-term chemical stability unlike surface coating modifications. Plasma treatment can introduce active species on the surface of the polymer, followed by polymerization of monomers. However, a limitation can be the expense of this technique. Irradiation treatments such as UV, gamma and microwave exposure are difficult processes to scale up. Also, irradiation can damage the polymer over prolonged exposure. Furthermore, all of the current modification techniques are incapable of easily modifying complicated sample geometries such as tubing or piping.

Grafting methods are generally divided into two classifications known as grafting-from and grafting-to.[24] The grafting-to process occurs when preformed polymer chains with reactive functional groups are covalently coupled to the surface. Grafting-from utilizes initiator species existing on the polymer surface to react with monomer. The monomer polymerizes to form a grafted chain, eminating from the surface. Hu and Brittain[25] reported a grafting-from technique in which hydrophilic polymers were created on the surface of poly(dimethylsiloxane) using a physisorbed free radical initiator. It was speculated that this method exploited the polarity disparity between the hydrophobic initiating species and the polar polymerization medium.

This dissertation describes the extension of this technique to the surface modification of PVC, including samples possessing complex object geometries.

Hydrophilic monomers, such as acrylic acid (AA), *N*,*N*-dimethylacrylamide (DMA), 2-hydroxyethyl acrylate (HEA), *N,N*-dimethylaminoethyl methacrylate (DMAEMA) and 2-hydroxyethyl methacrylate (HEMA) and 4-vinylpyridine (4VP) were grafted to the surface of PVC films and tubing to reduce plasticizer migration and increase biocompatibility. One of these systems was of particular interest for optimizing antibacterial properties of a film. Poly(4-vinylpyridine) (P4VP) contains a pyridine nitrogen which is susceptible to alkylation with halogenated compounds. The polycations produced belong to a class of antibacterial reagents called quaternary ammonium compounds which compare favorably with other antibacterial agents such as antibiotics, silver ions, or iodine.[26]

Most quaternization reactions take place upon dissolution of the starting material in a solvent in the presence of an appropriate alkylating reagent. Poly(acrylamide-*co*-poly(4-vinylpyridine)) (CPAV) was quaternized with dimethyl sulfate and precipitated into THF.[27, 28] Polystyrene-*b*-poly(4vinylpyridine) was alkylated with 6-perfluorooctyl-1-bromohexane in DMF and precipitated into diethyl ether.[29] Here a PVC-*g*-P4VP film was quaternized with *n*-butyl, *n*-hexyl and *n*-octyl bromide as well as 6-perfluorooctyl-1-bromohexane in ethyl acetate. Precipitation was not necessary because the solvent was selectively chosen to keep the mixture heterogenous.

The surface modification explained here is one approach to make PVC more acceptable for medical products. It is also important for PVC to have sterile surfaces as well as reduced plasticizer migration for potential human contact.

CHAPTER II

HISTORICAL BACKGROUND

2.1 Plasticized PVC

Amorphous PVC has a glass transition temperature (T_g) of 81 °C,[30] making it rigid and inflexible at room temperature. Therefore, additives are necessary to improve processability by lowering the glass transition temperature. Plasticizers account for one third of all global plastic additives due to their ability to increase structural flexibility.[1] Interactions between the plasticizer and the polymer chains increase free volume and reduce the T_g of PVC to 20 °C or lower.[31] It doesn't matter if the plasticizer is attached to the polymer through chemical bonding (internal) or not (external), they selectively partition into the amorphous phase of the polymer. For that reason plasticizers are extremely effective with PVC (90% amorphous).

Flory-Huggins solution theory models the thermodynamics of polymer chains mixing with a solvent. The equation for the gibbs free energy of mixing is shown below, where R is the gas constant, T is the absolute temperature, n_1 is the moles of solvent, n_2 is moles of polymer, ϕ_1 is volume fraction of solvent, ϕ_2 is volume fraction of polymer and chi is the polymer-solvent interaction parameter:

$$\Delta G_m = RT[n_1 \ln\phi_1 + n_2\phi_2 + \chi_{12}\, n_1\phi_2] \quad (1)$$

This equation is composed of the entropy and enthalpy of mixing. The probabilities that a space (on the lattice site) is occupied by polymer or solvent is expressed by the entropy

of mixing where while the interactions of the solvent-solvent, solvent-polymer, polymer-polymer are expressed by the enthalpy of mixing which is dependent of temperature. Since the plasticizer is highly compatible with PVC, the ΔG_m must be negative.

Patterson and Schreiber measured the chi parameter of di-n-octyl phthalate (DOP) and PVC with gas-liquid chromatography to determine the maximum volume fraction of plasticizer that would be compatible with PVC. The interaction parameter was strongly negative up to 0.25 volume fraction of plasticizer, indicating high compatibility. Chi became less negative as the volume fraction increased up to 0.60, where it turned positive, suggesting a lower compatibility limit. [32] The glass transition temperature (T_g) can be calculated by the Fox equation where w_1 is the weight fraction of polymer, w_2 is the weight fraction of plasticizer, T_g is the final T_g after plasticization, T_{g1} is the T_g of the polymer and T_{g2} is the melting point or T_g of the plasticizer:

$$1/Tg = w_1/T_{g1} + w_2/T_{g2} \quad (2)$$

If the weight fraction of plasticizer was 0.25, the T_g would be 35 °C. As the weight fraction of plasticizer increases to 0.60 (nearly incompatible), the T_g inversely decreases to -11 °C.

Other polymers that use plasticizers are poly(vinyl butyral), poly(vinyl acetate), acrylics, nylons, and polyamides. PVC accounts for 80% of plasticizer consumption.[33] Regardless of the polymer structure, plasticizers induce the same changes in properties: increasing flexibility, elongation at break, toughness, dielectric constant and reducing modulus, tensile strength, hardness, density, and melt viscosity.

Compatibility is a severe issue for plasticizer effectiveness especially at varying temperatures. Molecular weight and degree of branching play a prominent role with

respect to compatibility. The most common plasticizers used today are di(2-ethylhexyl) phthalate (DEHP), diisononyl phthalate (DINP), diisodecyl phthalate (DIDP), and diisotridecyl phthalate (DITDP) (Scheme 2.1).[1] As the length of the disubstituted alkyl ester increases, the diffusivity of the plasticizer is hindered. As the chain decreases in length, the plasticizer becomes more volatile. Branching nearest to the polar groups accompanied by a shorter main chain length produces increased viscosity thus diminishing plasticizer effectiveness.

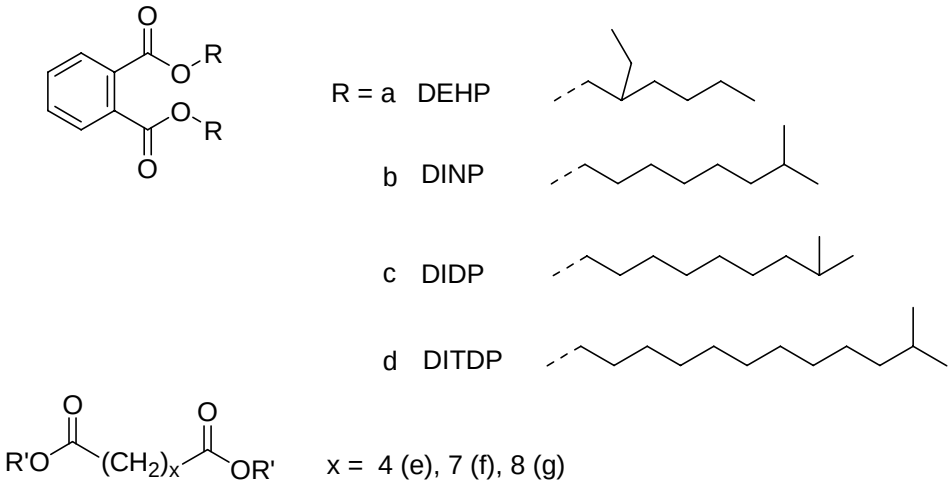

Scheme 2.1. Structure of common plasticizers: a) DEHP, b) DINP, c)DIDP, d) DITD, esters of adipic (e), azelaic (f) and sebaic (g) acids.

At high temperatures, PVC degrades by dehydrochlorination from structural defects present in the polymer chain. These defects occur upon manufacturing and storage to produce branching and allylic chloride, or by oxidation to produce carbonyl, peroxide, and ketoallyl groups (Scheme 2.2).[30]

Most plasticizers hinder degradation at room temperature. At higher temperatures, the low molecular weight liquid or resin is more susceptible to evaporation and degradation itself. PVC then becomes brittle and discolored (yellow) upon migration of plasticizer from the polymer. At low temperatures the thermodynamic compatibility

of the plasticizer decreases because the polymer chains are less mobile. Below the T_g, there is only vibrational and conformational relaxations (ß and γ) of the polymer chains which hinders the interactions between the polymer and plasticizer. The more compatible the additive is with the polymer, the more that it can be used to increase lubricity.[1] Thus, the "friction" or the interaction between polymer chain segments is less at lower temperatures.[34]

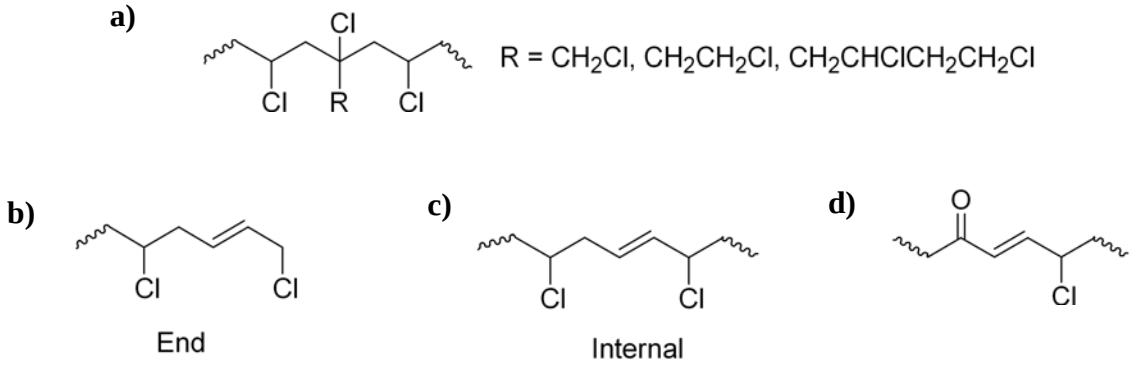

Scheme 2.2. Possible structural defects of PVC: a) branching, b) end allylic chlorine, c) internal allylic chlorine, and d) ketoallyl formation.

Plasticizers were founded in the late 19th century when camphor and castor oil were used for plasticization of celluloid lacquers.[1] The foundation for the ester plasticizers was set in 1912 when triphenyl phosphate was used as a substitute.[1] Phosphate esters are known for their flame retardant properties and are grouped into three main categories: trialkyl, triaryl and alkyl/aryl phosphates. Tricresyl phosphate is still used today. Around 1920, phthalic acid esters were introduced as plasticizers. Since this discovery, DEHP has been the most widely used plasticizer since 1930.[1]

Unfortunately these plasticizers, which were initially believed to be benign to humans, have recently demonstrated endocrine-disruption activity in rats. Large amounts of phthalate plasticizer were observed upon leaching from medical products such as

intravenous catheters, blood storage bags, dialysis tubing and endotracheal tubing. Therefore, phthalate esters have been under public scrutiny since the 1980's as potential carcinogens. In fact, various tests have shown correlations between phthalate esters and endocrine-, pulmonary- and hepato-toxicity. To meet modern safety requirements, a variety of new plasticizers had been developed: esters of adipic, azelaic and sebacic acid (Scheme 2.1). These plasticizers were only effective in the molecular weight range of 350-400 g/mol because of incompatibility and volatility. Other innovative polymeric plasticizers (polycaprolactone-polycarbonate blend, poly(1,3-butylene adipate, poly(ethylene-*co*-vinyl acetate-*co*-carbon monoxide) (EVACO)) which exhibit low volatility, are on the brink of replacing traditional plasticizers despite their expensive nature.[1]

2.2 Toxicity of Phthalate Esters

Humans have daily exposure to plasticizers, ranging from manufacturing off-gassing to common household products such as pacifiers, toys, car interiors, oxygen masks, food packaging, pill casings or some of the previously mentioned medical field products. Blood storage bags contain up to 80 wt% DEHP and dialysis tubing, used to transport blood to and from the body, is composed of 30-40 wt% DEHP.[35] Because the plasticizer is not chemically bound to PVC it can migrate into air and, at higher rates, into liquids such as blood, soapy water, hexanes or cottonseed oil. Elevated temperatures increase the rate of migration into the environment.

The amounts of DEHP recorded to leach from PVC blood bags and IV tubing into blood, water and drug products were 4-650 mg/L, 5 mg/L and 3.1-237 mg/L,

respectively.[35] The most severe amount of DEHP migration was 42-140 mg/kg in one treatment period for newborns undergoing extracorporeal oxygenation. The difference in weight and development from newborns and adults makes the high dosage for neonatal care especially dangerous. Other procedures such as hemodialysis, blood transfusions, cardiopulmonary bypass, and artificial ventilation reported levels of DEHP migration under 8 mg/kg. Newborns were also recorded to ingest up to 6 mg of DEHP/day when using pacifiers, teething rings and toys in their mouths.[35]

Kambia *et al.*[36] quantified the amount of lipid-soluble plasticizer that leached from infusion bags composed of poly(ethylene-*co*-vinyl acetate) (EVA) and PVC plasticized with DEHP and tubing composed of PVC/DEHP. The extracting media (amino acids, glucose, electrolytes, vitamins) and trace amounts of lipids used for total parenteral nutrition (TPN) were initially stored for 1 week at 4 °C in the bags. Samples were drawn aseptically from the bags and outlet tubing during the simulated infusion treatiment time for eight intervals from 0 to 11 h. Di-*n*-heptyl phthalate (DNHP, 50µl) was added to the samples as an internal standard. The organic layer was collected, evaporated, dissolved into acetonitrile and used for high-performance liquid chromatography with a diode-array UV detector (202 nm). The detected amounts leached from the bag and outlet tubing were 0.2 - 0.7 mg and 0.8 – 2.0 mg over 11 h. These findings were dependent upon the lipid concentration and flow rate used. The increase of lipid content was paralleled by the increase in DEHP concentration.

Kambia, *et al.*[37] also monitored the leachability of DEHP from hemodialysis tubing used on patients with chronic renal failure. In a four hour session, the tubing was

found to leach 123 mg of DEHP while adults retained 27 mg in their bodies. The critical limit for hazardous effects of DEHP exposure is 69 mg/kg per day.[1, 13]

A second method to monitor the effect of toxic plasticizer was to administer DEHP to laboratory animals and monitor the level adsorbed in the liver, reproductive tract, kidneys, lungs and heart. DEHP is classified as a peroxisome proliferator which makes it responsible for the oxidation of fatty acids and the biosynthesis of cholesterol. Peroxisome proliferation is also connected to liver cancer in animals, and to a lesser degree in humans. Because its effects are more prominent for rodents, the relevance of animal studies has been questioned. It is prudent to assume that peroxisome proliferation will have an effect on some fraction of the human population or that another mechanism, such as genotoxicity, may contribute to malignant transformation. Also, each organ may undergo multiple varying mechanisms for adverse effects with DEHP which are indeterminate for both laboratory animals and human beings.

Adverse effects such as loss of vitamin E (an important antioxidant) are also detrimental to living organisms. Vitamin E protects against free radical damage which leads to the pathogenesis of a number of chronic diseases such as: cardiovascular disease, carcinogenesis, neurological disorders, immune system disfunction, neurological disorders, cataracts and arthritis.[2]

As DEHP infiltrates the human body, enzymes mainly present in the intestine, but also in the liver, kidney, lungs, pancreas and plasma, metabolize DEHP into mono-ethylhexyl phthalate (MEHP) and 2-ethyl hexanol as seen in Scheme 2.3. MEHP is recognized as the primary source of DEHP's toxicity.[2]

Because the intestinal track is more susceptible to enzyme breakdown, Manojkumar, *et al.*[2] administered DEHP intraperitoneally (injection to the peritoneum) in low doses (0-750 g/100g body weight) to rats. The peritoneum is a multilayered membrane which lines the abdominal cavity, holding the organs of the digestive tract in position while conveying nerves, blood vessels, and lymphatic ducts to the viscera (which covers internal organs). Table 2.1 displays the results which are in agreement with the correlation theory of vitamin E and DEHP. As the subject is exposed to larger doses of DEHP over 24 h, more DEHP is adsorbed in the liver and testes, and the amount of vitamin E is reduced.

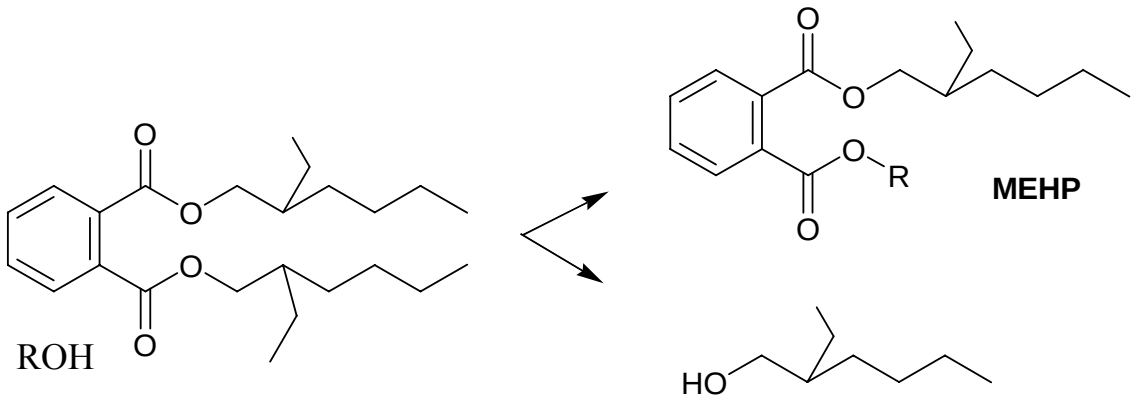

Scheme 2.3. Metabolites of DEHP after exposure to enzymes.

The loss of vitamin E was also measured for blood stored in Penpol blood storage bags composed of DEHP and PVC. A citrate-phosphate-dextrose-adenine (CPDA, 49 mL) solution was added to 350 mL of human blood and was stored in Penpol blood bags. As shown in Table 1, the amount of DEHP extracted increased from 1 to 9.65 mg/100 mL in 42 days and the amount of vitamin E decreased 265 μg/100 mL.

Table 2.1. Concentration of DEHP and vitamin E in blood bags, rat liver and testes.[2]

Sample	Days	Vitamin E		DEHP	
		μg/ 100 mL		mg/ 100 mL	
Penpol bag					
(1) CPDA[a]	0	645 ± 54.5		1.08 ± 0.06	
	28	527 ± 25.8		8.12 ± 0.78	
	42	380 ± 32.6		9.65 ± 1.01	
Sample		**[DEHP]** μg/ g	**[DEHP]** μg/ g	**[vitamin E]** μg/ g	**[vitamin E]** μg/ g
Rats		**Liver**	**Testes**	**Liver**	**Testes**
(1) control		0	0	17.34 ± 0.91	13.18 ± 0.6
(2) 450 μg		28.6 ± 0.91	96.1 ± 4.4	10.80 ± 0.74	11.28 ± 0.40
(3) 750 μg		34.4 ± 1.4	128.6 ± 8.6	5.72 ± 0.63	9.62 ± 0.43

[a] CPDA (citrate-phosphate-dextrose-adenine solution added to blood) stored in bag.

Human exposure to plasticizers is the most prevalent in point-source pollution from manufacturing off-gassing[3] and medical treatment with plasticized equipment. The leaching, migration and evaporation of plasticizers had become a concern to the United States Government after much debate over the toxicity of general plasticizers. Initially, the United States and the European Union felt that the migration limits for phthalates were safe and that medical devices are neither carcinogenic nor have any harmful effects at the average level of exposure.[1] The European Union Scientific Committee of Toxicity Ecotoxicity and the Environment, the American Council on Science and Health, and the US Consumer Product Safety Commission were concerted in agreement that plasticizers were not harmful to humans. It wasn't until after reviewing the results previously mentioned for the leaching of DEHP that the US Food and Drug Administration suggested that manufacturers 1) label the content of DEHP, 2) consider the feasibility of

replacing PVC/DEHP with alternative materials, or 3) use coatings to minimize patient exposure to DEHP.[38]

There have been many doubts about the usage of alternative plasticizers. The American Chemistry Council declares, "alternative materials may not have the long track record and unique performance profile that makes PVC with DEHP a proven and lifesaving combination."[38] In spite of this statement, there have been many efforts to overcome the technical challenges of toxic plasticizers. Surface modifications of PVC have been developed by both chemical and physical processes to reduce plasticizer migration and increase the biocompatibility of PVC. Such techniques include surface coating, surface crosslinking with ultraviolet radiation or plasma treatment, and surface grafting with hydrophilic polymers.

2.3 Surface Modification of PVC

Attempts have been made to reduce the mass transfer of plasticizer from PVC medical and food packaging. Fugit *et al.*[39] claimed to successfully delay and reduce the plasticizer migration when treated PVC packaging was in contact with liquid food simulant. In reality, they were removing the plasticizer from the outer layer of the PVC film by 1) soaking in heptane (1-4 min.) for various temperatures (30-50 °C) and 2) drying films for 1-2 days at 90-200 °C. We theorize that the plasticizer will leach from the surface, leaving spaces void of plasticizer and a bulk layer (plasticized) which has been unaffected by the solvent (Figure 2.1). Therefore, plasticizer migration in foodstuff was reduced and delayed, but the initial desired mechanical properties were altered by the treatment, rendering the application of this method not useful.

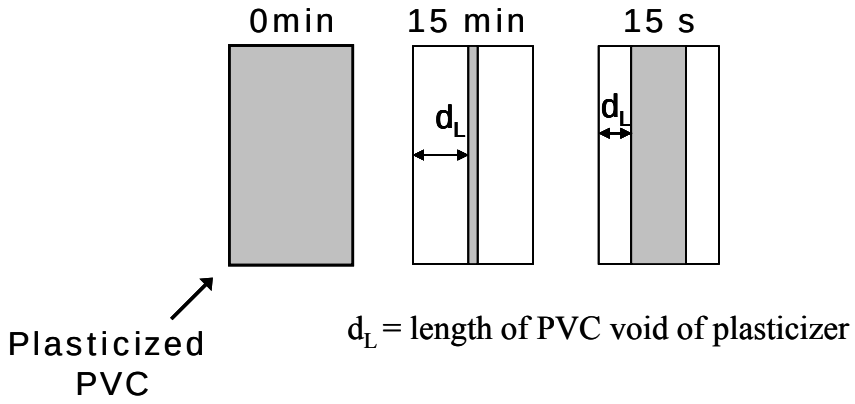

Figure 2.1. Theory of solvent treatment for plasticized PVC with exposure to hexanes or acetone for 0 min, 15 min or 15 s.

Beneficial information, such as the coefficient of diffusion, was obtained from the soaking treatment analysis. The diffusion was measured when plasticizer was first detected leaching from the film as well as the time (t_{dL}) necessary for the plasticizer to pass through the rigid PVC to the heptane/PVC interface. For a film soaked in heptane at 30°C for 4 min, the lag time (t_{dL}) was 216,600 s and the coefficient of diffusion was 0.85 x 10^{-9} cm^2/s.[39]

Successful surface modifications minimize initial plasticizer loss by limiting exposure to extracting solvents. These techniques include: surface coating,[5-11] surface crosslinking[12-17] and surface grafting.[18-23]

2.3.1 Surface Coating

Surface coating of antibacterial reagents or hydrophilic polymers generally increases the biocompatibility of PVC. Surface coating of inorganic-organic layers can also create a barrier to mass transfer of plasticizer.

Chemical vapor deposition (CVD) is widely used to coat complex substrates at high temperatures. Unfortunately most polymers are temperature sensitive materials. For instance, PVC has a glass transition temperature of 80 °C and maximum service temperature of 140 °C.[30] Plasma assisted CVD allows possible coating temperatures around 60 °C to circumvent degradation. Breme *et al.*[5] have coated PVC with titanium-based layers for improved bio- and blood compatibility of medical devices which potentially reduce plasticizer migration.

The precursor $Ti[N(C_2H_5)_2]_4$ gave very smooth and thin layers (5-100 nm) with good adhesion (6-10 N/mm^2) accompanied by reduced chlorine content resulting from the bombardment of radicals and ions during the plasma treatment. Oxygen was incorporated onto the polymer surface before the coating process with an air plasma treatment to increase the surface tension of the material. The critical surface tension of a biomaterial is above 55 mJ/m^2.[5] Other polymers, such as poly(ethylene terephthalate), polyethersulfone, polytetrafluoroethylene, polyethylene and polypropylene, also exhibited acceptable surface tension values (69 mJ/m^2), improved biocompatibility with increased proliferation (growth) and vitality of fibroblasts and endothelial cells upon coating with Ti(C, N). The blood compatibility was measured by the partial thromboplastin time (PTT) which was significantly longer for coated samples, meaning the time to form a thrombus (clot) increased. The normal range for PTT is 25-39 s. Prolonged times indicate less coagulation.

The barrier properties of PVC coated substrates were examined upon exposure of the films to dioctyl phthalate (DOP) for 48 h at 40 °C (Figure 2.2). The weight of the film was measured before and after showing a 20% increase for the uncoated control film

after 24 hours. The coated PVC film showed no deviation from the initial weight after 48 h implying that the Ti(C, N) coatings can potentially prevent the leaching of plasticizers from PVC since they can successfully block the entrance of the same substance.

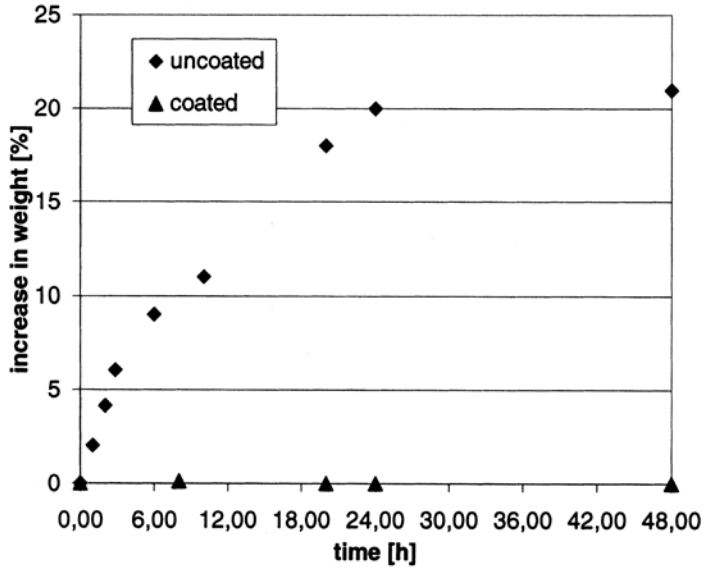

Figure 2.2. Exposure of uncoated and Ti(C, N)-coated PVC in DOP at 40 °C.[5] Reprinted with permission from *Thin Solid Films* **2000**, *277-278*, 755. © 2008 Elsevier Limited.

Despite the effective barrier provided by titanium-based layers, the technique does present drawbacks such as cost, loss of transparency, poor adhesion and sample size limitation. Alternatively, Messori *et al.*[6] coated organic-inorganic hybrids (ceramers) by a wet chemical process. The hybrids were synthesized by a sol-gel process which crosslinked metal alkoxides and organic oligomers with reactive functional groups. When combined, the molecular composites possessed nanosize domains which preserved transparency upon coating PVC.

Poly(ethylene oxide) (PEO) was used as the oligomer (600 g/mol) because it is readily soluble in tetraethoxysilane (TEOS) and it adheres well to PVC through hydrogen bonding of the ether oxygens. First α,ω-triethyoxysilane-terminated PEO (PEO-Si) was

synthesized by reaction of PEO with 3-isocyanatopropyltriethoxysilane at 120 °C for 3 h. The sol-gel reaction proceeded at 70 °C for 3 h upon addition of TEOS, water and HCl to PEO-Si. Scheme 2.4 portrays the possible hydrolysis reactions of ethoxy groups on PEO-Si and TEOS. The networks are formed through reaction of the hydroxyl groups with a neighboring ethoxy-substituted silane. Both the hydrolyzed TEOS and PEO-Si were suitable for crosslinking the PEO-Si. PVC was finally dip-coated with the PEO-Si/SiO_2 sol-gel solutions.

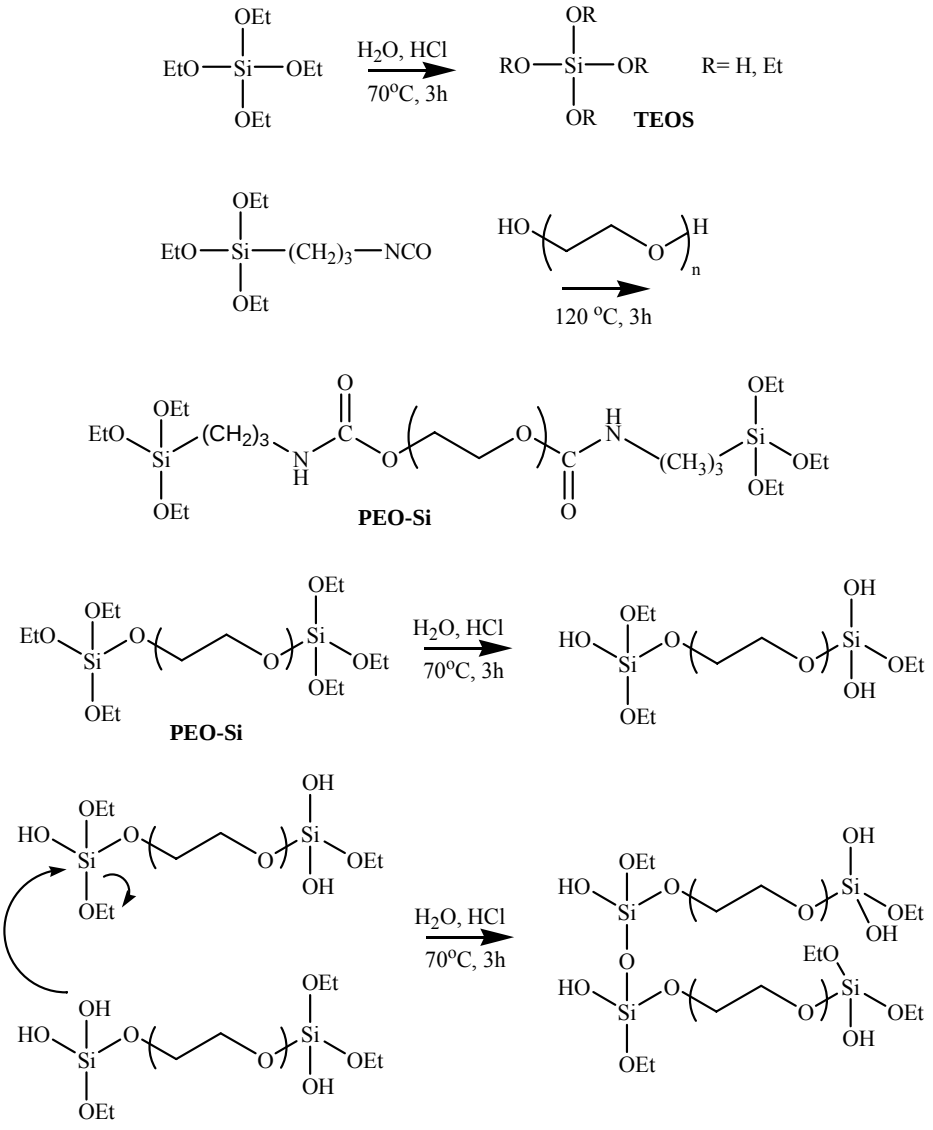

Scheme 2.4. Possible sol-gel reactions with PEO-Si/TEOS to make hybrids PEO-Si/SiO_2.

Extraction studies of the coated film and tubing with hexanes were used for HPLC analysis to determine the percent migration of plasticizer from the PVC hybrid coated film. The extent of migration was dependent on the stoichiometry of the organic phase (PEO-Si) to the inorganic phase (SiO_2). If the coating was organic-rich or inorganic rich, the barrier to DEHP migration was weakened because of adhesion problems and cracking from a brittle coating. The optimum ratio of PEO-Si/SiO_2 was 2:1 which exhibited less than 5% DEHP migration of the total plasticizer in the PVC sample after 10 h of extraction in hexanes.

2.3.2 Coatings for Biocompatibility

Coatings are most often made to PVC to increase biocompatibility and reduce protein adsorption and bacterial cell adhesion. Recent publications show the application of coatings through radio frequency glow discharge,[7, 8] layer-by-layer deposition,[9,10] and plasma immersion ion implantation (PIII).[11] These methods were used to coat pluronics, sodium hydroxide, silver nitrate, *bovine serum albumin* (BSA), heparin, poly(2-methoxyethyl acrylate) (PMEA), or triclosan and bronopol.[7] Pluronics® is a trade name used by BASF to refer to a triblock copolymer composed of hydrophilic poly(ethylene oxide) (PEO) and hydrophobic poly(propylene oxide) (PPO).[7] The PPO segment anchors to any hydrophobic surface from an aqueous media through hydrophobic interactions as the PEO segments extend away from the surface like a brush. The more hydrophobic the surface, the more extended the PEO blocks stretch, making the surface more brush-like.

Balazs *et al.*[7] coated PVC with polytetrafluoroethylene (PTFE) using RF-plasma deposition with hexafluoroethane as the precursor and hydrogen as the carrier gas to

maximize the hydrophobicity of the native PVC. The PTFE-like surface is presumed to be more effective for coating the amphiphilic triblock copolymer PEO/PPO/PEO to increase extension and reduce bacterial adhesion to PVC medical products (Figure 2.3).

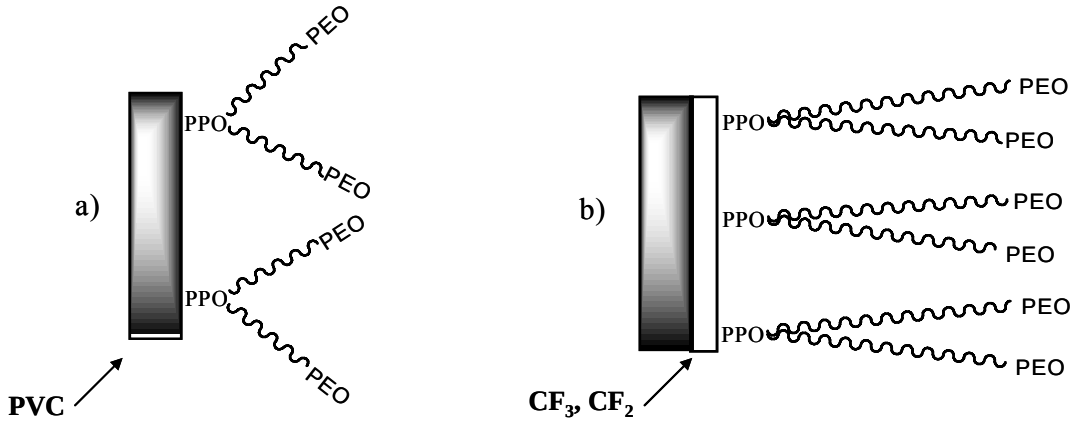

Figure 2.3. Neat PVC coated with PEO/PPO/PEO (a), CVD modified PVC coated with PEO/PPO/PEO (b).[7]

A year earlier, Balazs *et al.*[8] reported another successful yet more expensive method to coat PVC endotracheal tubes for antibacterial and colonization-resistant properties. A two step wet-treatment in NaOH and $AgNO_3$ was applied to native PVC tubes and RF oxygen glow discharge pre-functionalized PVC tubes. Silver, used in bandages and burn-wound treatments, is widely known for its activity against gram-negative and gram-positive bacteria such as *pseudomonas aeruginosa*. The methodology of incorporating monovalent silver into PVC is illustrated in Scheme 2.5.

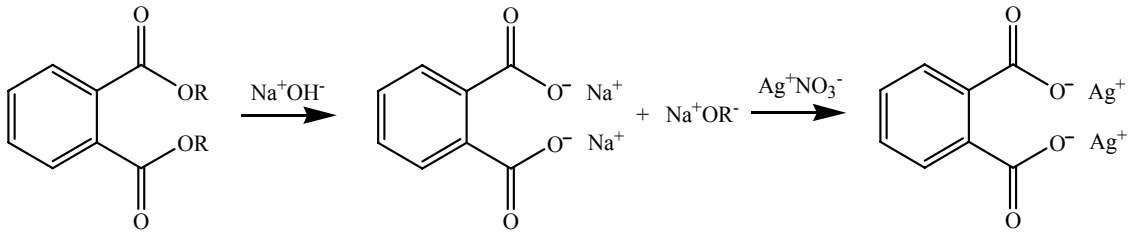

Scheme 2.5. Two-step wet chemistry for silver phthalate salts.

Neat PVC has additives with ester groups such as the common plasticizers: DEHP, DOP, DINP, DIDP and DITDP. The ester group is the featured component that allows integration of monovalent silver. First these groups underwent saponification with NaOH to produce a sodium phthalate salt and alcohol. Silver ions were then exchanged with the sodium to embed the anti-microbial agent at the surface of PVC. The concentration of ester groups controls the extent of silver substitution. RF-O_2 plasma was used to degrade the surface and created more carboxylic acid/ester groups by 250%. However, neither the neat nor plasma-treated PVC tubes coated with NaOH/$AgNO_3$ showed any adherent bacteria unlike the uncoated specimen which showed approximately 1 x 10^6 cells/cm^2 for four different strains of *pseudomonas aeruginosa* (PAO1, AK44, 1.1.A1, 19G12).

RF glow discharge was also used with ammonia as a carrier gas for ammonia plasma treated PVC surfaces that could be coated with heparin and *bovine serum albumin* (BSA) by electrostatic self-assembly (ESA) or layer-by-layer deposition as shown in Scheme 2.6.[9] Heparin is a sulphonated anionic polysaccharide and albumin is a positively charged protein. These materials commonly prevent platelet adhesion, thrombosis and infection. PVC was coated with BSA and ESA to reduce protein/platelet adsorption. Surface analysis of PVC films by size exclusion microscopy (SEM) affirmed that the coated films had reduced platelet adhesion from the control (80 x $10^4/cm^2$). In fact, the platelet adhesion was inversely related to the number of layers coated. For example, a sample with 5(heparin/BSA) layers had less than 5 x $10^4/cm^2$ platelets adhered and 4(heparin/BSA) layers had approximately 15 x $10^4/cm^2$ platelets adhered.

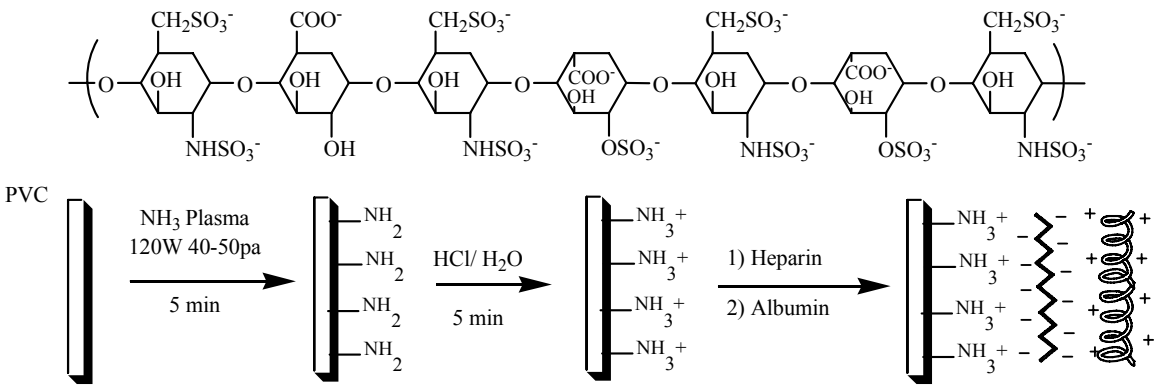

Scheme 2.6. Chemical structure of heparin and scheme for electrostatic layer-by-layer self-assembly of heparin and serum albumin.

RF glow discharge plasma deposition was extremely useful for introducing functional groups such as carboxylic acids, fluoropolymer and amine groups onto the PVC surface. In all three cases, this was only the initial step which aided in coating other antimicrobial or thromboresistant agents which creatively made PVC more biocompatible.

Because heparin is known for reducing thrombus activity when in contact with human blood, it was used in a comparison study with a promising new anti-thrombogenic poly(2-methoxyethyl acrylate) (PMEA) coated PVC tubing.[10] For the thrombin generation assay, all samples were analyzed before and after incubation and circulation with human whole blood for 6 h at 37°C. The heparin-coated tubing did show minimal thrombin generation whereas the PMEA-coated sample exhibited negative thrombin generation. The amount of fibrin binding followed the trend: non-coated > heparin-coated > PMEA-coated. The superior performance of PMEA against thrombin generation and fibrin adhesion makes it a promising polymer for the medical device industry.

Another method to obtain anti-infective properties for PVC medical devices, reported by Zhang *et al.*,[11] was to first treat the surface of PVC by plasma immersion ion implantation (PIII) to introduce hydrophilic functional groups (C-O and C=O) for better adherence of non-toxic antibacterial reagents, 2,4,4'-trichloro-2'-hydroxydiphenyl ether (triclosan) and 2-bromo-2-nitropropane-1,3-diol (bronopol) (Scheme 2.7). After coating the immobilized reagents, argon plasma ion bombardment ensured better attachment to the surface. Most antibacterial reagents are immobilized, which poses a threat if they are toxic.

The antibacterial performance against S.A and E. coli was determined by plate-counting the active bacteria after a 2.0 mL solution of 2-5 x 10^5 colony-forming units (CFU)/mL was added to the surface and incubated for 24 h at 37°C. Sample 3 was treated with O_2-plasma, triclosan and Ar-plasma. Sample 4 was treated with bronopol under the same conditions. The triclosan-PVC showed 82.2% and 79.5% activity against S.A and E. coli, and the bronopol-PVC demonstrated 98% and 77.3% activity, respectively (Figure 2.4).

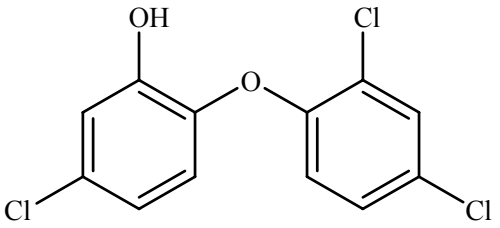

Triclosan

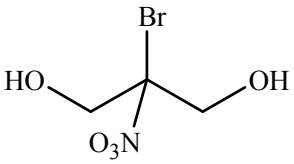

Bronopol

Scheme 2.7. Chemical structures of triclosan and bronopol.

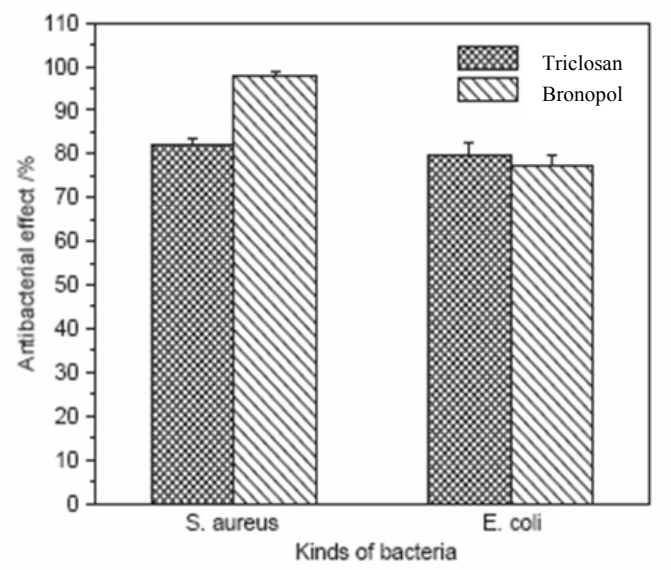

Figure 2.4. Antibacterial effect against S.A and E. coli for PVC film treated with oxygen plasma, triclosan (sample 3) or bronopol (sample 4) and argon plasma.[11] Reprinted with permission from Biomaterials 2006; 27:44. © 2008 Elsevier Limited.

Coatings tend to be less beneficial because of their nature to detach from the surface of PVC over time and especially when brought into contact with a good solvent. Also, performing CVD, RF plasma or PIII to improve coating ability makes this technique expensive and size limited. With these drawbacks, it was evident that other methods for resisting plasticizer leaching and introducing antimicrobial or biocompatible properties are imperative.

2.3.3 Surface Crosslinking

Crosslinking provides a covalently bonded network of chains which inhibits motion and flexibility necessary for small molecules to permeate through polymer chains. By crosslinking the surface of a polymer, bulk additives may be prevented from leaching out and outside materials can be prohibited from migrating into the plastic. This surface modification technique has successfully altered plasticized PVC for reduced global

migration of plasticizer to/from PVC food packaging, blood bags and transfusion tubing. Crosslinking is incurred upon cold plasma treatment,[12] UV irradiation[13-15] and chemical crosslinking.[16-17]

PVC is used as commercial food wrap films with di-2-ethylhexyl adipate (DEHA) and epoxidized soybean oil (ESO) as low molecular weight plasticizing additives. The migration of these plasticizers into the edible media polluted the food and reduced the mechanical properties of the packaging. Fatty food media, such as cheese, butter or olive oil, produce the highest migration results which can be simulated with accelerated migration into isooctane. Under the same conditions, isooctane extracts an equivalent amount of plasticizer in only 2 h compared to treatment with olive oil for 10 days. Audic *et al.*[12] reported the migration of these plasticizers from PVC food wrap films into isooctane before and after cold plasma treatment.

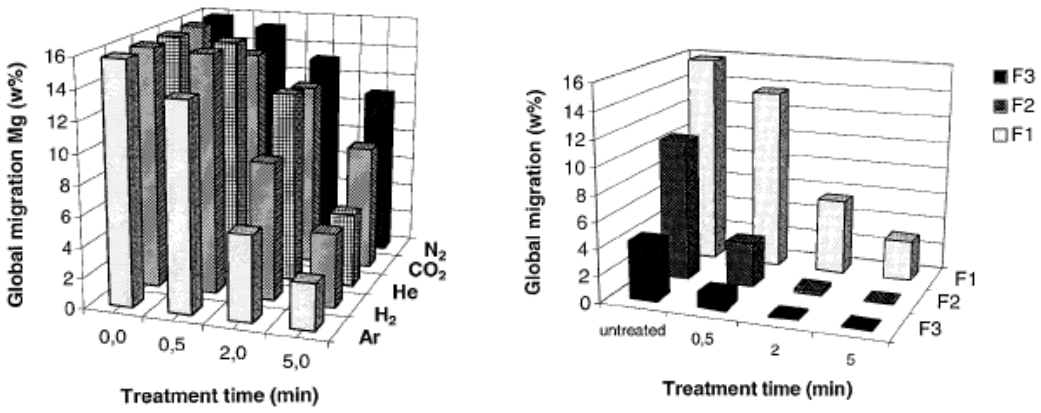

Figure 2.5. a) Global migration of plasticizer into isooctane for plasma treated PVC F1 versus the treatment time and gas. b) Global migration of plasticizer into isooctane for Ar plasma treated F1, F2 and F3 versus treatment time.[12] Reprinted with permission from *J. App. Polym. Sci.* **2000**, *79*, 1384. © 2008 John Wiley & Sons, Inc.

Multiple gases with varying effects (functionalization, ablation, crosslinking) were used in the cold plasma treatment of the PVC film with 100 parts PVC, 10 parts ESO and 28 parts DEHA. Argon, H_2 and He were effective in preventing the migration of plasticizer by creating a barrier upon crosslinking. Nitrogen preferentially induced the linking of functional groups and was less effective towards crosslinking as was CO_2 which provoked chain scission and produced highly reactive atomic oxygen, increasing the surface wet-ability. The degree of ablation and weight loss followed this trend: $CO_2 > H_2 > He > Ar > N_2$. Figure 2.5a depicts Ar as the most successful gas used in treatment to lower the global migration into isooctane from 15.8 % (untreated) to 3% (5 min).

A twist to this experiment involves the varied replacement of DEHA and ESO with a higher molecular weight elastomeric plasticizer: poly(ethylene-*co*-vinyl acetate-*co*-carbon monoxide) (EVACO). The higher molecular weight plasticizer is compatible with PVC and will potentially resist migration because of the limited mobility in the polymer matrix. Three film compositions of PVC/ESO/DEHA/EVACO were investigated: 100/10/28/00 (F1), 100/10/10/40 (F2), and 100/10/0/60 (F3). The films underwent treatment with Ar plasma for 0.5, 2 and 5 min and were tested for global migration of plasticizer into isooctane. Results from Figure 2.5b proved that EVACO is a less diffusive plasticizer than ESO and DEHA. F3 has less than 1 % plasticizer detected (upon extraction) after 2 min of treatment. Also, the migration is significantly reduced with the gradient in treatment time for all samples. Successful crosslinking of PVC food packaging and replacement of DEHA with EVACO exhibited limited plasticizer contamination in consumer products.

Irradiation treatments such as UV, gamma and microwave exposure have extensively been used to crosslink the surface of PVC sheets and tubing. Irradiation has been performed on unmodified PVC[13] as well as PVC substituted with sodium azide,[14] *N,N*-diethyl dithiocarbamate (DTC),[15] sodium sulfide,[16] and sodium thiosulphate.[17] Unfortunately, irradiation treatments are difficult processes to scale up and they can damage the polymer over prolonged exposure. Regardless of these shortcomings, the irradiation technique has profoundly impacted the field of surface chemistry and will be reviewed.

Ito *et al.*[13] have investigated the effects of temperature and UV irradiation on PVC medical sheets (blood bag samples) and tubing used for transfusion, infusion and donation of blood. Samples were held at 60 °C and irradiated with a UV lamp at a distance of 75 cm for 1 month. DEHP (*m/z*: 149.024) was extracted with Sandimmun (drug solvent from Novartis Pharma Co.) and analyzed against the internal standard (DEHP-d_4 *m/z*: 153.049) by GC-MS. The amount of DEHP migration was determined via a calibration curve of the peak ratio of DEHP to the internal standard (DEHP-d_4) versus the DEHP concentration. UV irradiated samples which were treated for one month on one side showed approximately half the level of DEHP migration (2.0 μg/mL) as that of the control (4.0 μg/mL). The authors surmised that PVC oxidation and crosslinking was the result of UV irradiation which established the barrier to DEHP migration.

To ensure surface crosslinking, many research groups have substituted PVC with photoactive groups. Jayakrishnan *et al.*[14-17] discovered sufficient crosslinking after UV irradiation of PVC substituted with sodium azide, *N,N*-diethyl dithiocarbamate, sodium

sulfide, and sodium thiosulphate. In 1996, tetrabutyl ammonium bromide (TBAB) was used as a phase transfer catalyst with a 40% aqueous solution of sodium azide to create a photolytically unstable azidated PVC surface.[14] The catalyst transferred the azide ion from the aqueous phase to the organic phase where the nucleophilic substitution of chlorine occurred. Then chlorine was transported to the aqueous phase by the tetrabutyl ammonium cation. The extent of azide substitution increased with a higher concentration of TBAB (up to 0.00004 mol/mL), reaction time and temperature (50-90 °C). Scheme 2.8 shows the azidation reaction accompanied by competing dehydrochlorination.

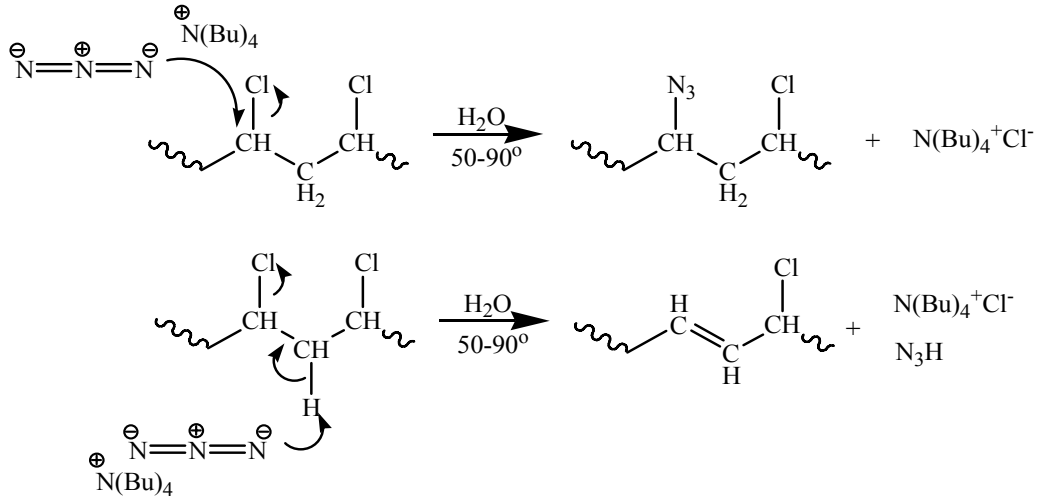

Scheme 2.8. Nucleophilic substitution and dehydrochlorination with sodium azide/TAB.

PVC samples were irradiated with a 125 W UV lamp at a distance of 15 cm under ambient conditions. Crosslinking resulted from addition of the dehydrochlorination product and the nitrene and/or C-H insertion with the nitrene (Scheme 2.9). The degree of nitrene formation was followed with fourier transform infrared radiation (FT-IR) spectroscopy. The azide peak at 2100 cm^{-1} decreased with irradiation time but was still prevalent after reacting for 180 min. This suggests that not all azide groups were

converted to nitrenes, essential for crosslinking reactions. Regardless, DEHP migrations studies proved that the nitrene concentration was sufficient in producing a crosslinked barrier.

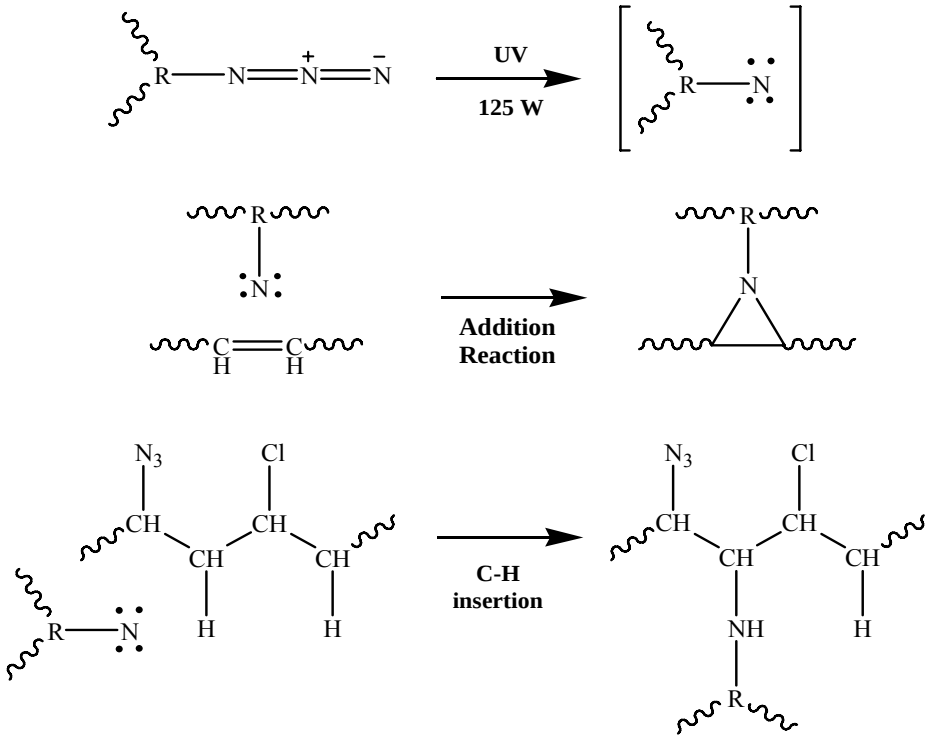

Scheme 2.9. UV irradiation of azidated PVC and possible crosslinked products.

DEHP was extracted with hexanes at 30 °C and the amount was assayed by UV-Vis spectrophotometry. The absorption maximum of DEHP was found at 275 nm. One experiment traced the migration of plasticizer with varying irradiation times of the azide-modified PVC sheets. Azide-modified samples that were irradiated for 30 min, 1h, 2h and 3h were extracted with hexane for 1 week to determine the wt% DEHP that migrated from the PVC sheet. As the irradiation time increased, the plasticizer migration decreased. The control, which was not treated with sodium azide but was exposed to UV irradiation for 3h, demonstrated a 26 % weight loss after seven days while the azide

modified sample which was irradiated for 3 h only had a 4 % weight loss (Figure 2.6). UV irradiation on the control PVC will not induce crosslinking unless it was exposed for several days unlike the azide-modified PVC which displayed positive results within a few hours.

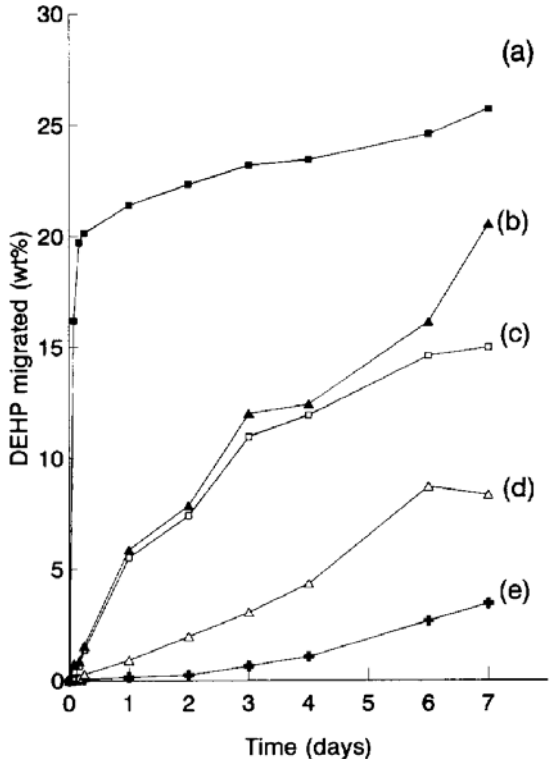

Figure 2.6. Effect of radiation dose on the extent of DEHP migration for PVC sheets treated with TBAB at a concentration of 0.000037 mol/mL at 80 °C. Control sheet irradiated for 3h (a), sheets azide-modified and irradiated for 30 min (b) 1 h (c), 2 h (d) and 3 h (e).[14] Reprinted with permission from *Polymer* **1996**, *37*, 5213. © 2008 Elsevier.

Overall the azide-modified PVC sheets were effective upon irradiation to produce a barrier to the plasticizer migration. The mechanical properties of the material were reduced from a strain of 606 to 393 % and a stress at break of 33 to 23 MPa for the unmodified and 3h irradiated modified sheets. These results confirm that the surface of PVC has been crosslinked after successful substitution with sodium azide and irradiation with UV light.

Lakshmi and Jayakrishnan[15] continued this investigation of the nucleophilic substitution of PVC with another photo-labile compound, *N*,*N*-diethyl dithiocarbamate (DTC), which was reported in 1998. This reaction was very similar to their previous work with sodium azide, where the phase transfer catalyst transported the photoactive compound from the aqueous phase to the organic phase while subsequently partitioning the substituted chlorine anion to the aqueous phase. However, a significant discrepancy in the basic nature of DTC does inhibit the dehydrochlorination of PVC. Scheme 2.10 displays the mechanism of nucleophilic substitution of PVC with DTC and tetrabutylammonium hydrogen sulphate (TBAH) and crosslinking upon UV irradiation. FT-IR spectroscopy analysis and determination of gel content proved that close to 4% of PVC was crosslinked at the surface. Comparison of the IR spectra for the substituted PVC and the photoirradiated PVC revealed a loss of the strong absorption peak at 1202 cm^{-1} (C=S) upon irradiation. Furthermore, the amount of DEHP extracted with petroleum ether at 30 °C decreased substantially due to the crosslinked sulfur bridge. There was less than 2.5 wt% plasticizer migration after irradiation for 4 h. The control that was not treated exhibited at least 25 wt% DEHP migration which almost amounts to the total plasticizer concentration in the sample. PVC tubing and sheets can contain up to 40 wt% plasticizer.

The substitution of PVC by DTC was just as efficient in creating a barrier to plasticizer migration as the azide-substituted PVC without the competing dehydrochlorination reaction which affords unfavorable discoloring. Also the dithiocarbamate groups can be used for photografting bioactive vinyl monomers to increase the biocompatibility of PVC.

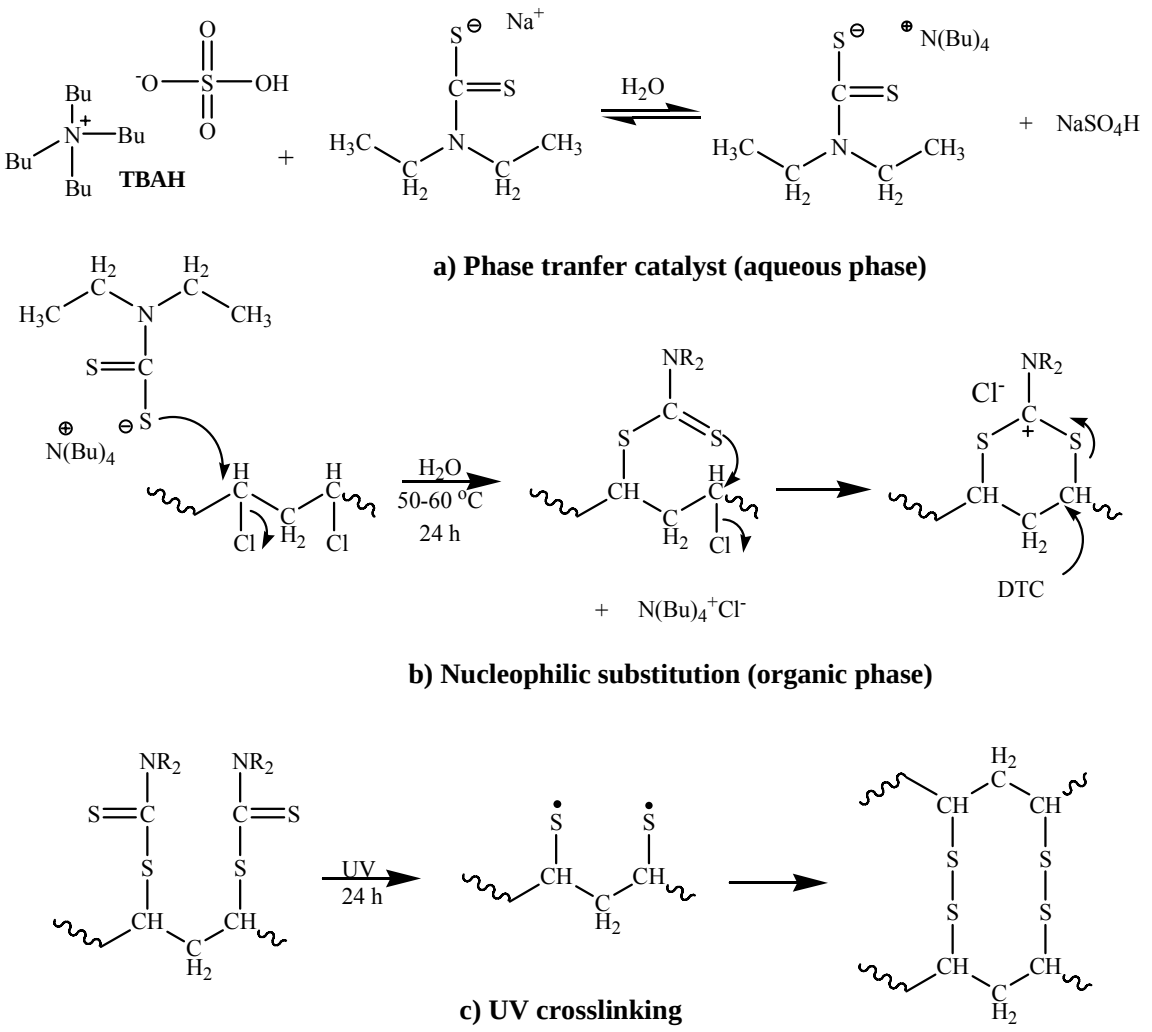

Scheme 2.10. Mechanism for a) phase transfer of DTC by TBAH b) nucleophilic substitution of PVC with DTC and c) UV crosslinking from a 125 W source at 15 cm.[15]

An impenetrable crosslink was formed at the surface of PVC using sodium sulfide and TBAH as a phase transfer catalyst in water (Scheme 2.11).[16] The labile chlorine atoms were easily substituted by the sulfide dianion, which resulted in crosslinking without the assistance of irradiation. XPS proved the presence of sulfur and the swelling with tetrahydrofuran (THF) verified a crosslinked gel. The extraction of DEHP into petroleum ether demonstrated practically no migration after 6 mos.

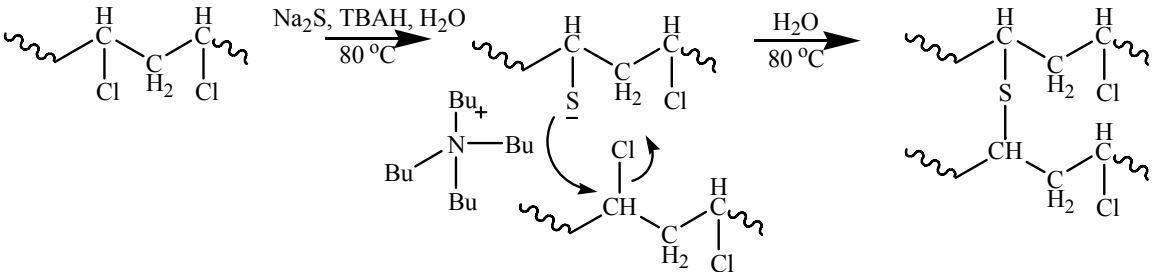

Scheme 2.11. Sulfide substitution resulting in crosslinked PVC.

Unfortunately, the sulfide substitution accompanied a dehydrochlorination which caused discoloration in the films and tubing. An alternative method was to use sodium thiosulphate instead, which afforded many possible reactions resulting in R-S-S-R and R-S-SO_3-R crosslinks (Scheme 2.12).[17] The thiosulphate dianion can directly react with two chlorines from adjacent PVC chains or with one chlorine to form the alkyl thiosulphate (bunte salt). The latter product could then cleave at the S-SO_3^- bond, in the presence of an acid, to form R-S-H, which leads to the formation of the R-S-S-R crosslink. Further treatment with acid or alkali enables the remaining alkyl thiosulphates to crosslink.

The migration of DEHP was measured using hexanes as the extracting media at 30 °C. The absorption maximum at 275 nm for DEHP was assayed with a UV-Vis spectrophotometer. After 2 months, the DEHP extracted only amounted to less than 1 % weight loss of the entire sample. Treatment with gamma irradiation for sterilization further reduced the migration of DEHP due to chain scission and additional crosslinking of the base polymer.

Overall, the irradiation technique was successful in crosslinking the surface for reduced plasticizer migration, but the surfaces were not biocompatible due to their

cytotoxic nature. Also UV, gamma and microwave exposures are difficult processes to scale up and the sample can be damaged from prolonged exposure.

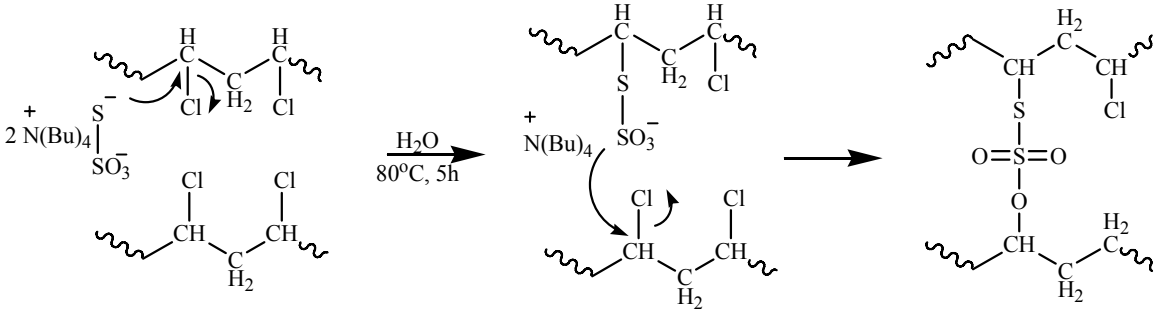

a) Thiosulphate crosslinked bridge

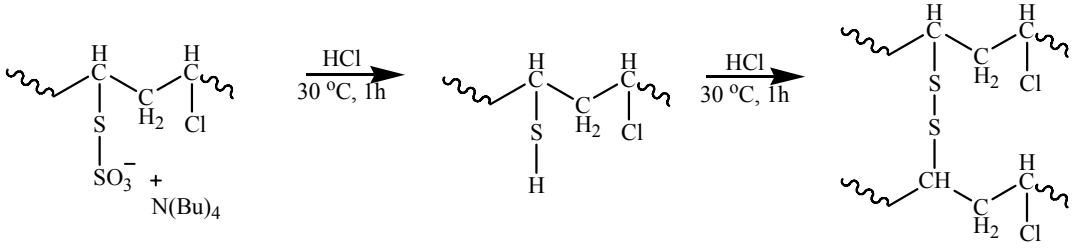

b) Disulfide crosslinked bridge

Scheme 2.12. Mechanism for crosslinking with a) thiosulphate and b) disulfide bridge.

2.3.4 Surface Grafting

Surface grafting is probably the most advantageous technique for surface modification of PVC for many reasons. Grafted chains are covalently bound to the polymer surface to ensure long-term stability unlike surface-coated polymers or antibacterial reagents which only remain physisorbed to the surface through mechanical interlocking or dispersive forces such as van der Waals and London forces. The density and molecular weight of the grafted chain can be controlled by use of living free radical techniques such as atom transfer radical polymerization (ATRP)[40], reversible addition fragmentation chain transfer (RAFT)[41] and nitroxide mediated polymerization (NMP)[42]

as well as anionic,[43] cationic and coordination chemistries.[44] The use of wet chemistry to graft polymers is superior to the more expensive and hard to scale up irradiation treatments commonly used for surface crosslinking. Furthermore, prolonged irradiation exposure will cause damage to the samples. Grafting methods are generally divided into two classifications known as grafting-from and grafting-to.[24] The grafting-to process occurs when preformed polymer chains with reactive functional groups are covalently coupled to the surface. Grafting from utilizes initiator species existing on the polymer surface to react with monomer. The monomer polymerizes to form a grafted chain from the surface.

There are many procedures to graft hydrophilic monomers to and from PVC to create a biocompatible hydrophilic surface. One method involved the reaction of PVC with lithiated α,ω–diaminopoly(alkene oxide).[18] The dehydrochlorinated product was then used to graft 2-hydroxyethyl methacrylate with a free radical initiator, such as benzoyl peroxide, that reacted with the double bonds formed along the backbone.[19] In another method, Sreenivasan *et al.*[20] coupled HEMA to PVC through the hydroxyl group of the monomer by the Williamson reaction by first reacting HEMA with metallic sodium to form the sodium alkoxide, which effected nucleophilic substitution with PVC (Scheme 2.13). The functional vinyl group of the HEMA coupled PVC was utilized to graft hydrophilic polymer, HEMA or *N*-vinylpyrrolidone (NVP) from PVC.

NVP is a carcinogenic monomer but as a polymer it is non-hazardous. Poly(*N*-vinylpyrrolidone) can be ingested by humans and has been used as a blood plasma extender.[55] Analogous to HEMA, it is hydrophilic as well as a key component for contact lenses. HEMA is grafted to PVC through the vinyl functional group of HEMA

by gamma irradiation. NVP is grafted in a similar fashion by a free radical initiator. The availability of the vinyl functional group of HEMA expands the possibilities for grafting other polymers or functionalizing other biocompatible reagents to PVC.

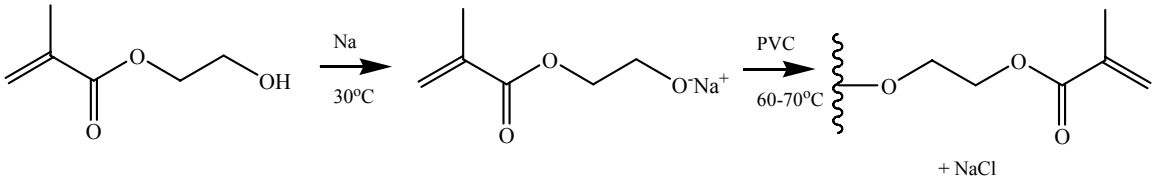

a) Williamson ether synthesis of HEMA grafted PVC

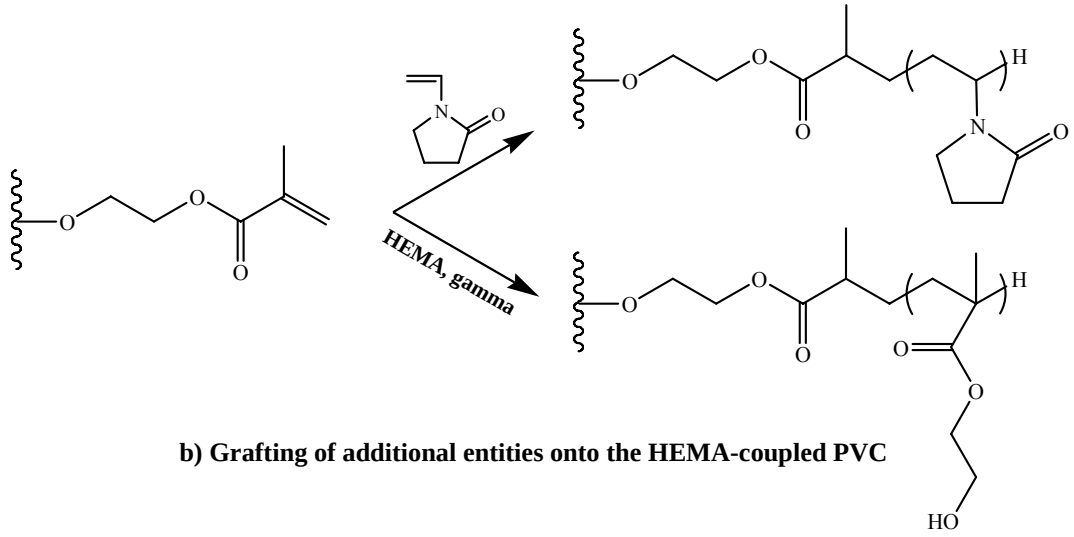

b) Grafting of additional entities onto the HEMA-coupled PVC

Scheme 2.13. Grafting hydrophilic monomer to PVC through a) the hydroxyl group of HEMA and b) the functional vinyl group of HEMA.

In 1998, Lakshmi and Jayakrishnan[21] reported using the Williamson reaction to graft hydroxyl terminated poly(ethylene glycol) (PEG) onto plasticized PVC. PEG is a blood compatible polymer that is approved for internal consumption by the Food and Drug Administration (FDA).[21] Besides resisting protein, platelet and bacterial adhesion,[21] PEG (M_n = 400 g/mol) acted as a barrier to plasticizer mass transfer. PVC-*g*-PEG tubing was extracted with cotton-seed oil at 70 °C for accelerated migration. The

unmodified tubing showed approximately 10% weight loss in cotton-seed oil and the modified tubing exhibited less than 1% in cotton-seed oil. Figure 2.7 displays the results for PVC and PVC-*g*-PEG (400 g/mol) in cottonseed oil over 4 days. Since PVC contained approximately 20 wt% plasticizer, the unmodified PVC leached >50% of the total plasticizer.

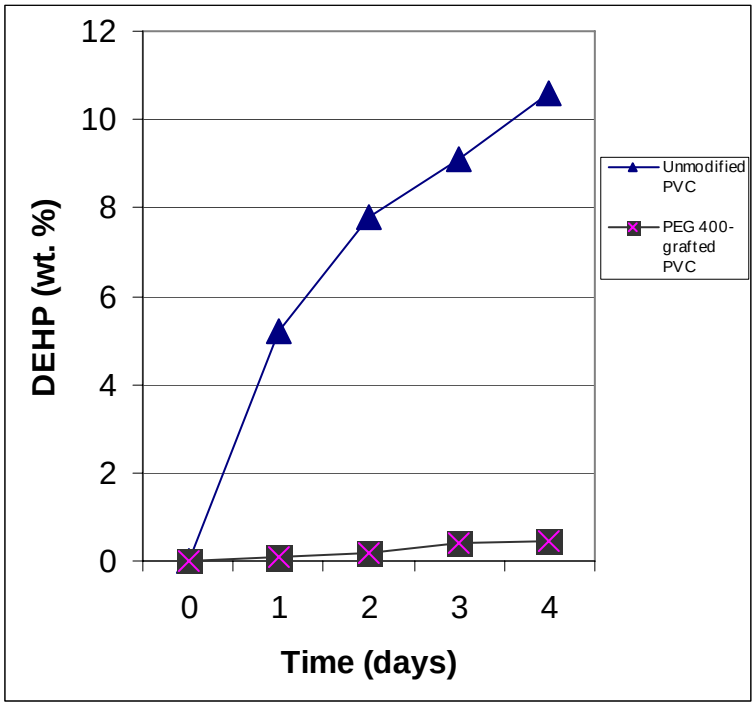

Figure 2.7. Accelerated migration of DEHP into cotton-seed oil at 70°C from plasticized PVC tubes and PEG 400-grafted PVC tubes.[21]

PVC-*g*-PEG (4,000 g/mol) sheets also have an anticoagulant nature. SEM images of unmodified PVC and PVC-*g*-PEG exhibited extreme platelet adhesion only for unmodified PVC (Figure 2.8). Following this success, others have grafted PEG and poly(oxyethylene 20 sorbitan) monolaurate (Tween 20, Figure 2.9) for reduced platelet adhesion and antithrombogenic properties.[22, 23]

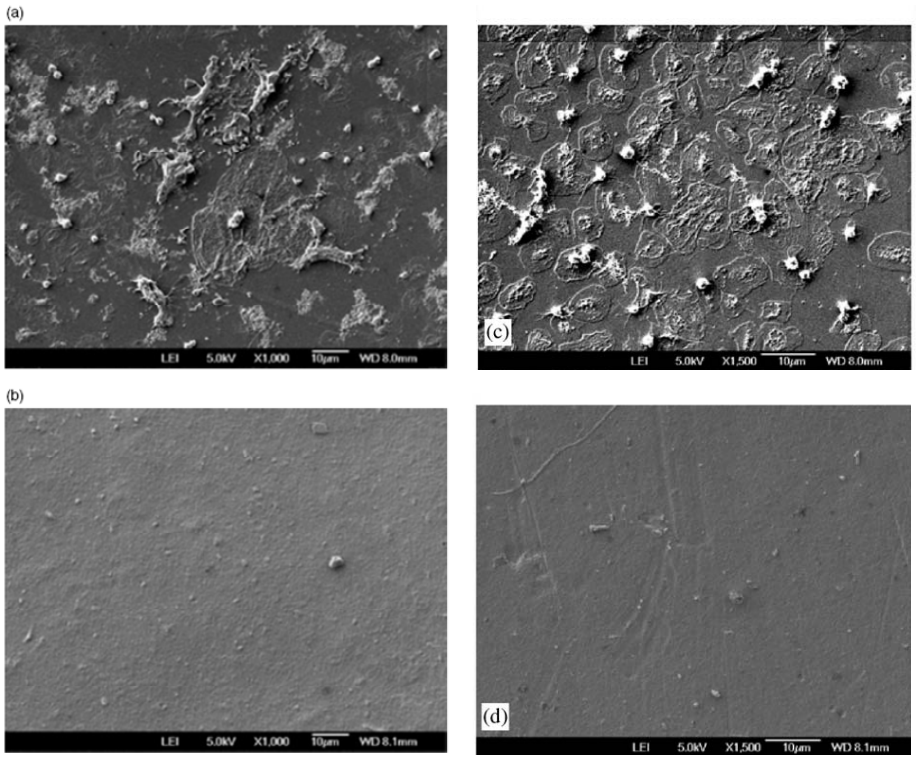

Figure 2.8. SEM images of platelet adhesion onto unmodified PVC film (a, c), Tween 20 modified PVC film (b) and PEGylated PVC film (d).[22, 23] Reprinted (a) and (b) with permission from *Biomaterials* **2005**, *23*, 3495. © 2008 Elsevier Limited. Reprinted (c) and (d) with permission from *Polym. Int.* **2005**, *54*,1304. © 2008 John Wiley & Sons Ltd.

Tween 20

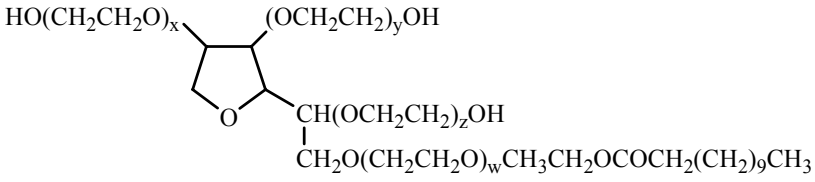

Figure 2.9. Structure of Tween 20.

Three steps were used to graft these hydrophilic polymers to PVC resin as described in Scheme 2.14: 1) amination of PVC with 80% ethylenediamine in water, 2)

chain extension with hexamethylene diisocyanate (HMDI) and 3) grafting of PEG or Tween 20. These antifouling grafted polymers reduced platelet adhesion significantly as seen by the SEM images of unmodified PVC, PVC-*g*-PEG and PVC-*g*-Tween (Figure 2.8).

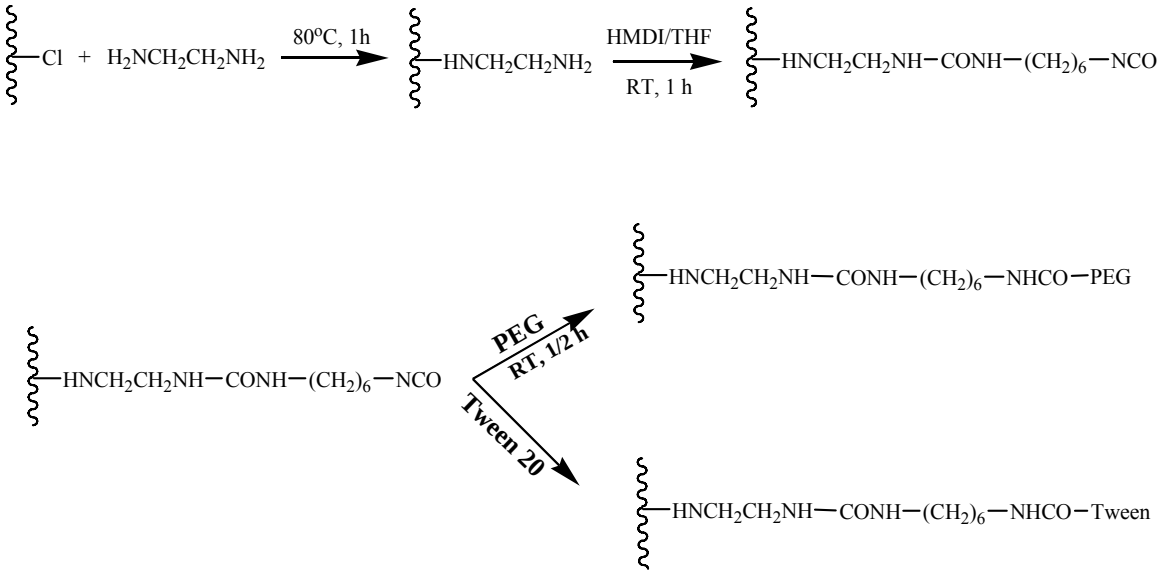

Scheme 2.14. Three step wet chemistry for grafting PEG and Tween 20.

PVC has been grafted successfully with many hydrophilic monomers for enhanced biocompatibility. However, the methods mentioned above all require multiple steps beginning with the initial modification of the PVC surface by wet chemistry before grafting polymer to or from the functional groups made by dehydrochlorination, coupling of HEMA or amination. A versatile method of grafting hydrophilic polymer from poly(dimethylsiloxane) (PDMS) was reported by Hu and Brittain[25] that did not need to chemically alter PDMS before grafting, thereby eliminating steps. In 2005, Hu and Brittain[25] reported a grafting-from technique in which hydrophilic polymers were created

on the surface of poly(dimethyl siloxane) using a physisorbed free radical initiator. This simple procedure consisted of two steps, 1) the physisorption of hydrophobic initiator, 2,2-azobis(2-methylpropionitrile) (AIBN), onto the surface of PDMS and 2) surface grafting of hydrophilic monomer from radicals formed on the surface of PDMS. It was speculated that this method exploited the polarity disparity between the hydrophobic initiating species and the polar polymerization medium.

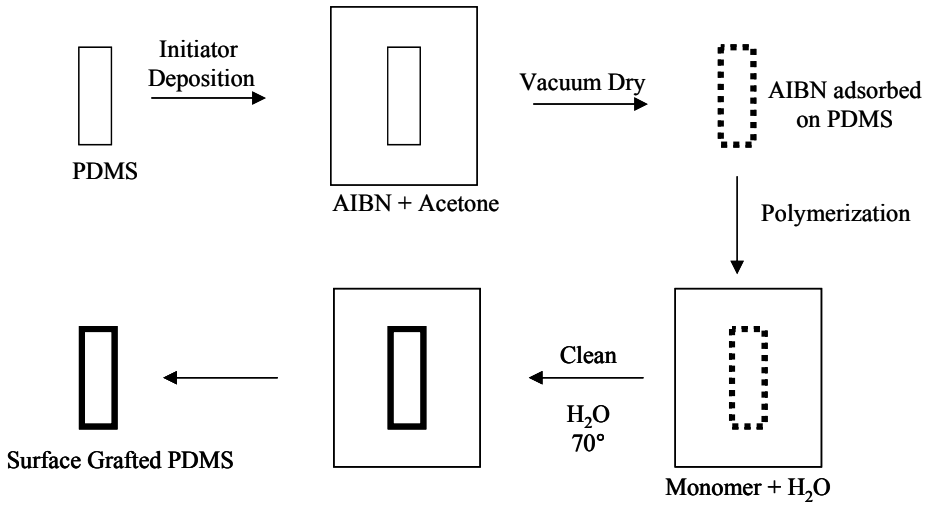

Scheme 2.15. Free radical surface graft polymerization onto a PDMS surface. Reprinted with permission from Macromolecules 2005; 38: 3263.[25] © 2008 American Chemical Society.

As portrayed in Scheme 2.15, hydrophobic PDMS was immersed into a solvent which allowed it to swell, such as acetone. The hydrophobic initiator (AIBN), which was dissolved in acetone, penetrated and adsorbed to the surface of PDMS. The initiator was physisorbed to the surface upon removal of the film from the solution. When the dried film was placed in a hydrophilic media, such as water, the initiator remained trapped at the surface of PDMS due to its preferred proximity to the hydrophobic PDMS versus the hydrophilic media. Upon heating, the initiator dissociated, leaving tertiary radicals to

react with the surface of PDMS. The generated grafted radicals were readily available to react with the monomer in solution to form a hydrophilic polymer brush surface.

The authors postulated three possible reactions for the tertiary AIBN radicals that occur upon heating (Scheme 2.16). In the first scenario, the tertiary radicals recombine with each other. In the second case, the tertiary radical abstracts a hydrogen from the pendent methyl groups, leaving a grafted radical to react with monomer to form the polymer graft. Lastly, not shown, the radical breaks free into the aqueous media and reacts with the monomer present to form free hydrophilic polymer.

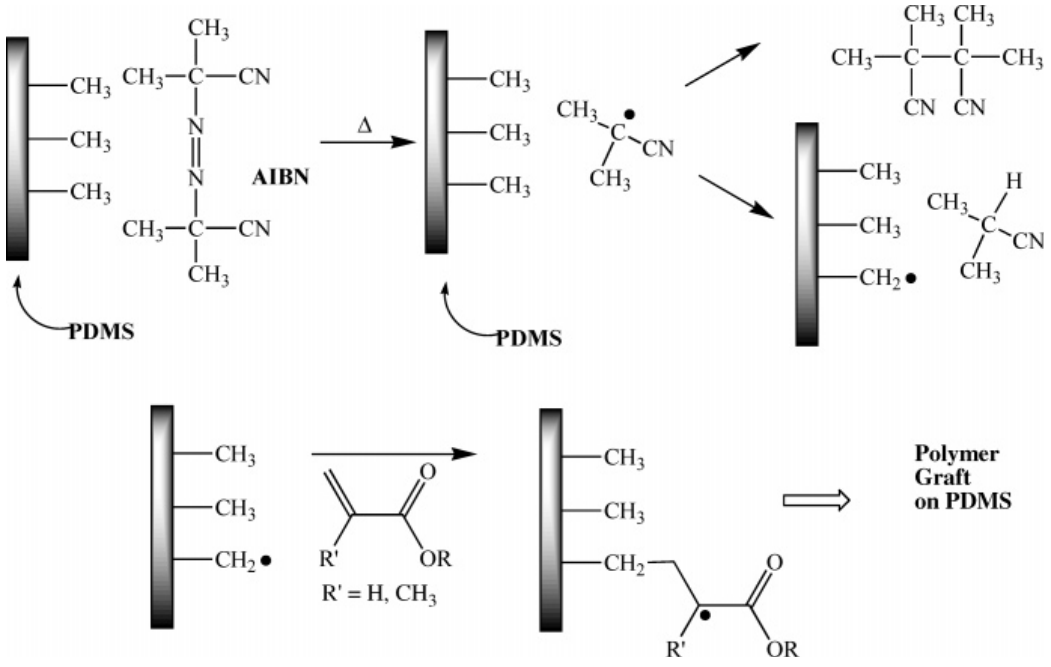

Scheme 2.16. Possible mechanism of surface grafted free radical polymerization.[25] Reprinted with permission from Macromolecules 2005; 38: 3263. © 2008 American Chemical Society.

Qualitative observation after grafting showed that PDMS bulk properties were altered. The polymer was more rigid and less transparent upon polymerization with various hydrophilic monomers: hydroxyethyl acrylate (HEA), hydroxyethyl methacrylate (HEMA), *N*,*N*-dimethylacrylamide (DMA), and acrylic acid (AA). Quantitative

measurements such as contact angle, X-ray photoelectron spectroscopy (XPS) and attenuated total reflectance infrared spectroscopy (ATR-IR) proved successful grafting of the hydrophilic monomers. For example, native PDMS had an advancing water contact angle of 114 degrees and a receding contact angle of 98 degrees. The decrease in contact angles for the hydrophilic modified PDMS suggested surface attachment of hydrophilic monomers as seen in Table 2.2. XPS analysis indicated the presence of nitrogen for the poly(acrylamide) grafted surface, but also showed oxygen and silicon binding energies, consistent with a non-uniform surface modification. All tests were run after extensive cleaning of the film by sonication and Soxhlet extraction to remove any free polymer.

Table 2.2. Water contact angle measurements and XPS of surface-grafted PDMS.[25]

sample description	θ °a	θ °r	C/O[a]	C/N[b]
PDMS	114	98	N/A	N/A
PDMS-*g*-PAA	74	62	1.56	*c*
PDMS-*g*-PAM	77	68	1.57	10.61
PDMS-*g*-PDMA	90	79	*c*	*c*
PDMS-*g*-PHEMA	93	80	1.76	*c*
PDMS-PHEA	87	76	1.83	*c*

[a] XPS data for carbon and oxygen element percentages expressed in a ratio.
[b] XPS data for carbon and nitrogen element percentages expressed in a ratio.
[c] One of the elements was not detected by XPS.

The attenuated total reflectance infrared spectra of modified films displayed carbonyl absorptions corresponding to the hydrophilic polymer. PHEMA PHEA, PAA, PAM and PDMA have absorptions in the range of 1650-1730 wavenumbers (Figure 2.10).

The advantages of this new modification technique are: lack of harsh chemicals or radiation treatments, simplicity, and cost efficiency. The research described here is an extension of the PDMS work to graft hydrophilic monomers, such as HEMA, DMA,

DMAEMA, 4VP, HEA, and AA to the surface of PVC films and tubing. One of these systems is of particular interest for optimizing antibacterial properties of a film. Poly(4-vinylpyridine) (P4VP) contains a tertiary nitrogen which is susceptible to alkylation with halogenated compounds. The antibacterial effect of this polycation depends on the length and structure of the alkyl substituent.[26]

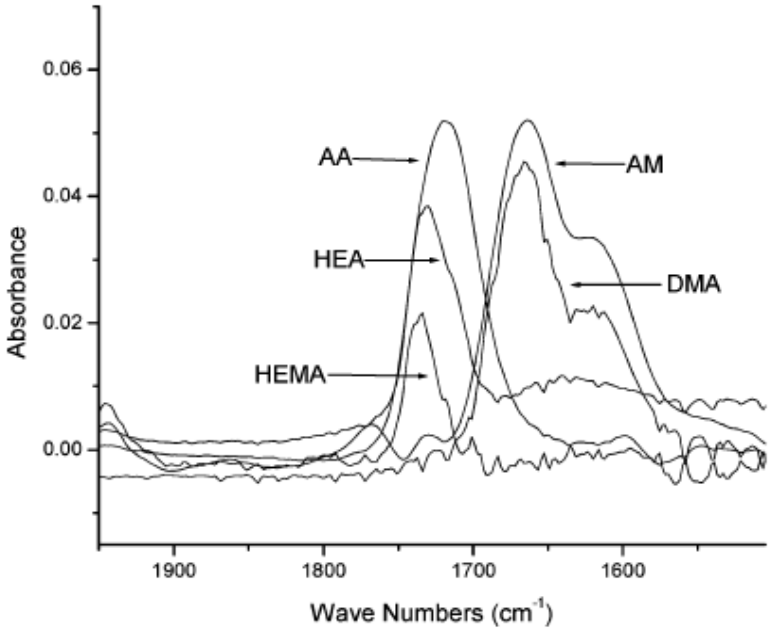

Figure 2.10. ATR-IR spectra of PDMS modified films on silica wafers. Reprinted with permission from Macromolecules **2005,** *38*, 3263.[25] ©2008 American Chemical Society.

2.4 Antibacterial Properties of Cationic P4VP

P4VP has been reported to remove bacterial cells from water by forming a swellable matrix with clay as a substitute to toxic soluble polymer biocides.[45] Remarkably, P4VP was immobilized onto clay by using the grafting from technique. First, γ-methyacryloxypropyl trimethoxysilane was coupled to the surface of the clay via condensation to afford functional vinyl groups. The monomer (P4VP) was then grafted

from the vinyl group after radical initiation with AIBN (Scheme 2.17). Subsequent quaternization was performed with benzyl bromide to yield the ammonium salts.

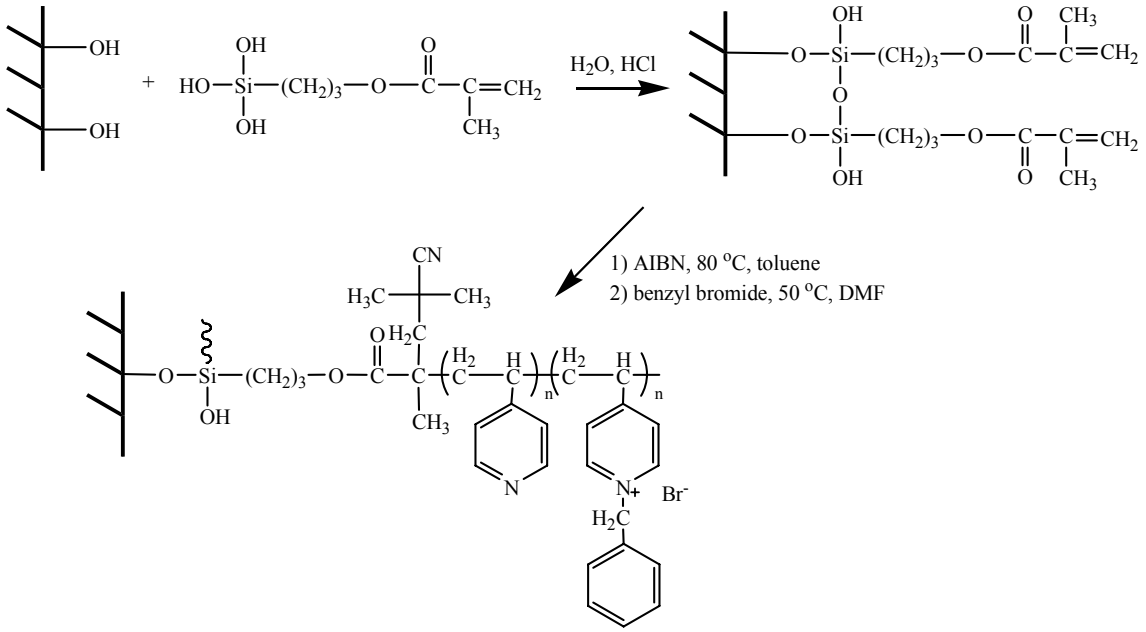

Scheme 2.17. Preparation of polyacrylate-clay sol-gel material.

The antibacterial activity was determined with a suspension test of the clay-P4VP salt matrix in water containing a bacteria culture of known *escherichia coli*, *pseudomonas aeruginosa* or *staphylococcus aureus* counts. Aliquots of the solution were taken at variable times and spread onto agar plates to manually count the number of viable colonies formed after incubation at 37 °C for 24 h. All strains of bacteria were dead after 3 h exposure to the clay supported bactericides. The clay-polymer material did not only swell for increased antibacterial effectiveness, but was reusable after rinsing out the contamination.

Most antimicrobial agents, such as antibiotics, quaternary ammonium compounds, silver ions and iodine have only been verified to kill bacteria that are suspended in

aqueous solutions. The effectiveness of P4VP against bacteria in aqueous solution is enticing but not as fascinating as its potential ability to kill airborne bacteria. Rühe and Biesalski[46] reported the grafting of P4VP from a silicon wafer with subsequent quaternization with *n*-butyl bromide in nitromethane at 65 °C, but did not mention its effectiveness against bacteria. Tiller *et al.*[26] (2001) were the first to announce positive results for killing airborne bacteria on contact with long chains of *N*-alkylated P4VP. Tiller copolymerized P4VP to a glass substrate through acryloyl moieties and subsequently quaternized P4VP with different *N*-alkyl bromides of varying length (propyl to hexadecyl) in nitromethane at 75 °C for 72 h for 90% conversion. These surfaces were successful in killing up to 99% of a number of airborne gram-positive (*staphylococcus epidermis*) and gram-negative bacteria (*pseudomonas aerug*inosa and *escherichia coli*). The length of the alkyl chain was a critical variable. *N*-hexylated P4VP was the optimum alkyl length for destroying bacteria because of the stronger electrostatic repulsion that overrides the hydrophobic interactions associated with longer alkyl chains which theoretically stick together.

In 2002, Tiller *et al.* [47] used their poly(vinyl-*n*-hexylpyridinium) graft on a high density polyethylene (PE) slide that was first flame treated and then coated with silica. The SiO_2-coated slide was aminated with 3-aminopropyltriethoxysilane (APTES), then immersed into 1,4-dibromobutane and grafted to P4VP which underwent quaternization with 1-bromohexane (Scheme 2.18). This system exhibited antibacterial efficiency against many wild and antibiotic-resistant strains of *staphylococcus aureus* such as: ATCC 700698 (resistant to methicillin), ATCC BAA-38 (resistant to methicillin, penicillinm, streptomycin and tetracycline) and ATCC BAA-39 (resistant to penicillin,

tetracycline, imipenem, cefaclor, oxacillin, tobramycin, cephaliexin, cefuroxime, gentamicins, amoxicillin, clindamycin, erythromycin and cephamandole). The polyethylene slide coated with hexylpyridinium exceeded 90% killing efficiencies in all instances.

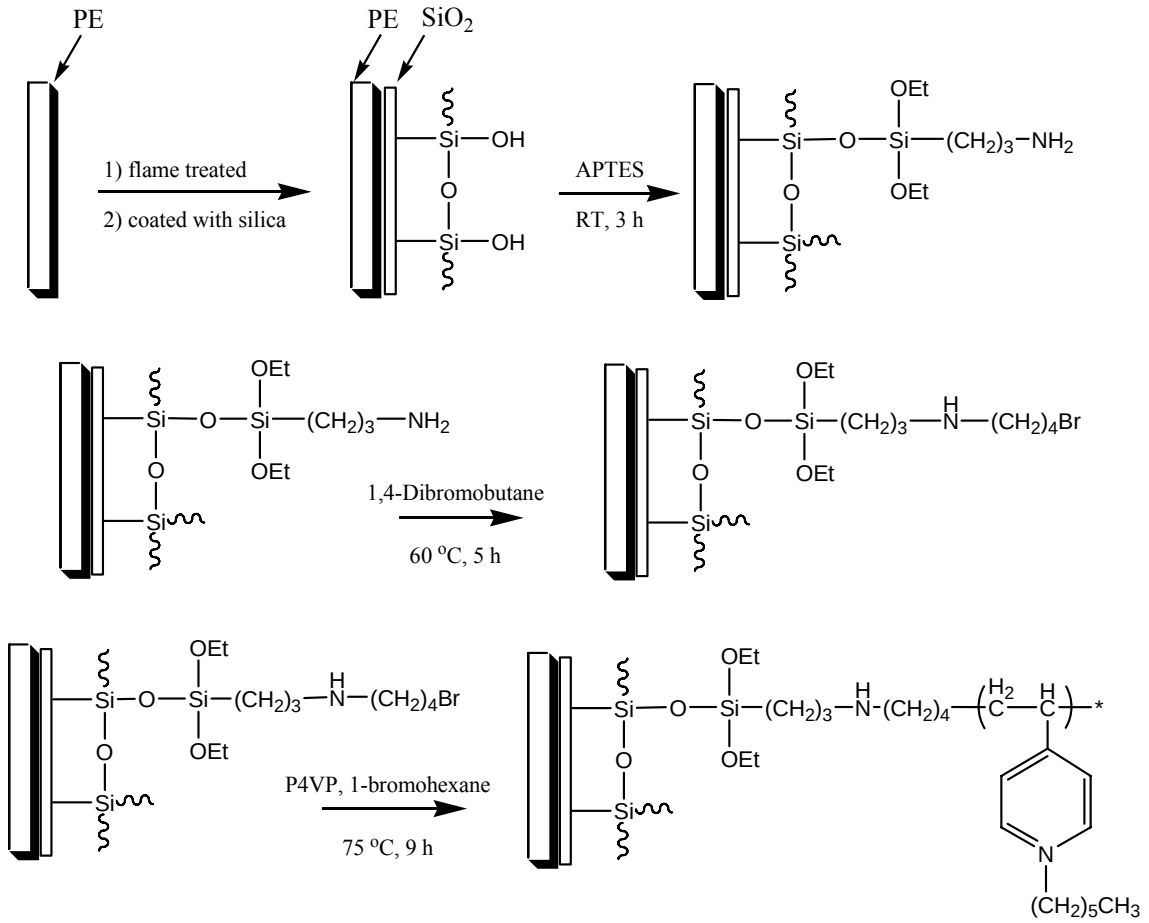

Scheme 2.18. Modification of PE with P4VP and quaternization with 1-bromohexane.

This study prompted the investigation of poly(vinyl-N-alkylpyridinium) coatings or grafts to other polymer surfaces such as poly(acrylamide) (PAM), silica gel and polystyrene (PS) to improve antimicrobial properties. In 2003, Gao *et al.*[27] copolymerized acrylamide and 4-vinylpyridine to combine the excellent flocculation properties of cationic PAM, typically used in wastewater treatment, and the quaternary

salt of P4VP used for corrosion inhibition and sterilization. The two monomers were copolymerized with a potassium persulfate initiator in equal volumes of water and DMF. The cationization reaction was carried out at room temperature using the toxic dimethyl sulfate as a quaternizing reagent. Unique to previous quaternization methods, the hydrophilic copolymer was dissolved in methanol/glycol since a hydrophilic alkylating reagent was used (Scheme 2.19).

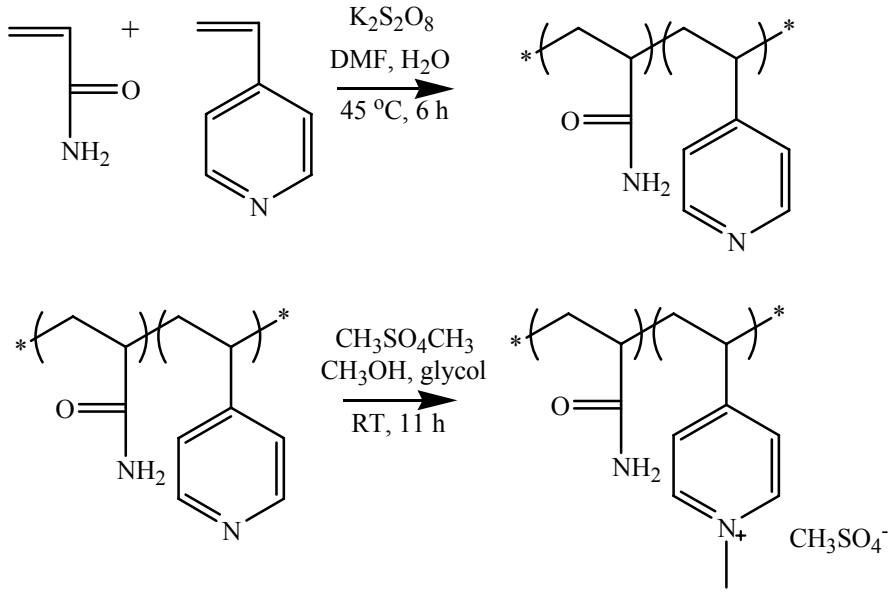

Scheme 2.19. Synthesis of cationic copolymer PAM-CP4VP.

The cationic copolymer exhibited a higher flocculation for waste simulation than the well known PAM. The stronger the charge density of the copolymer, the more stretched the cationic chain is, favoring the bridging and neutralization reaction with negatively charged waste. To prevent corrosion, the cationic copolymer forms a dense adsorption layer through electrostatic attraction to the metal surface (negative portion) to

shield acids from contacting the surface. Also the pi electrons from the pyridine ring may enter into the empty d orbital of iron creating stronger adsorption.

Two years later, Gao *et al.*[28] tested the same system for antibacterial activity against *escherichia coli* in solution. The PAM-P4VP water soluble salt was almost 100% effective when there was 80 mol % cationic degree, the pH of the solution was above 5 and the copolymer had been in contact with the solution for at least 5 min. Gao *et al.* extended this research to create a water insoluble antibacterial material by grafting PAM-*co*-P4VP to silica gel with subsequent quaternization with dimethyl sulfate.[48] Similar to the water soluble copolymer salt, the system was successful in killing approximately 100 % of the viable E. coli cells. Finally, PS was used as a water insoluble support for the cationic P4VP.[29] However, this time a fluorinated alkylating agent was used in place of 1-bromohexane. The fluorinated pyridinium surfaces showed enhanced antibacterial activity that was dependent on the charge density and increasing concentration of pyridinium rings at the surface. Other fluorinated oligomer substituents on acrylamide polymers were found to inhibit replication of HIV-1 in cell culture and exhibited antibacterial activity against *staphylococcus aureus*, rendering the fluorinated alkylating agents very attractive.[29]

For the PS system, fluorinated alkylating agents were prepared as shown in the literature (Scheme 2.20). 6-Perfluorooctyl-1-hexanol (**2**) was synthesized by a two step reaction described by Hopkens.[49] First, perfluorooctyl iodide was refluxed with 5-hexene-1-ol and AIBN at 80°C for 6 h to afford 1-perfluorooctyl-2-iodo-ω-hexanol (**1**). The iodo-adduct was then reduced with tributyltinhydride and AIBN. Finally, (**2**) underwent nucleophilic substitution (S_N2) with carbon tetrabromide and triphenyl

phosphine (Scheme 2.20) as described by Wang and Ober[12] for production of the alkylating agent, 6-perfluorooctyl-1-bromohexane (**3**). Ober *et al.*[50] used this alkylating agent to quaternize PS-*b*-P4VP (4) and compared its performance with PS-*b*-P4VP and poly(4-vinylpyridine-*r*-butyl methacrylate) (P(4VP-*r*-BMA)) quaternized with 1-bromohexane.

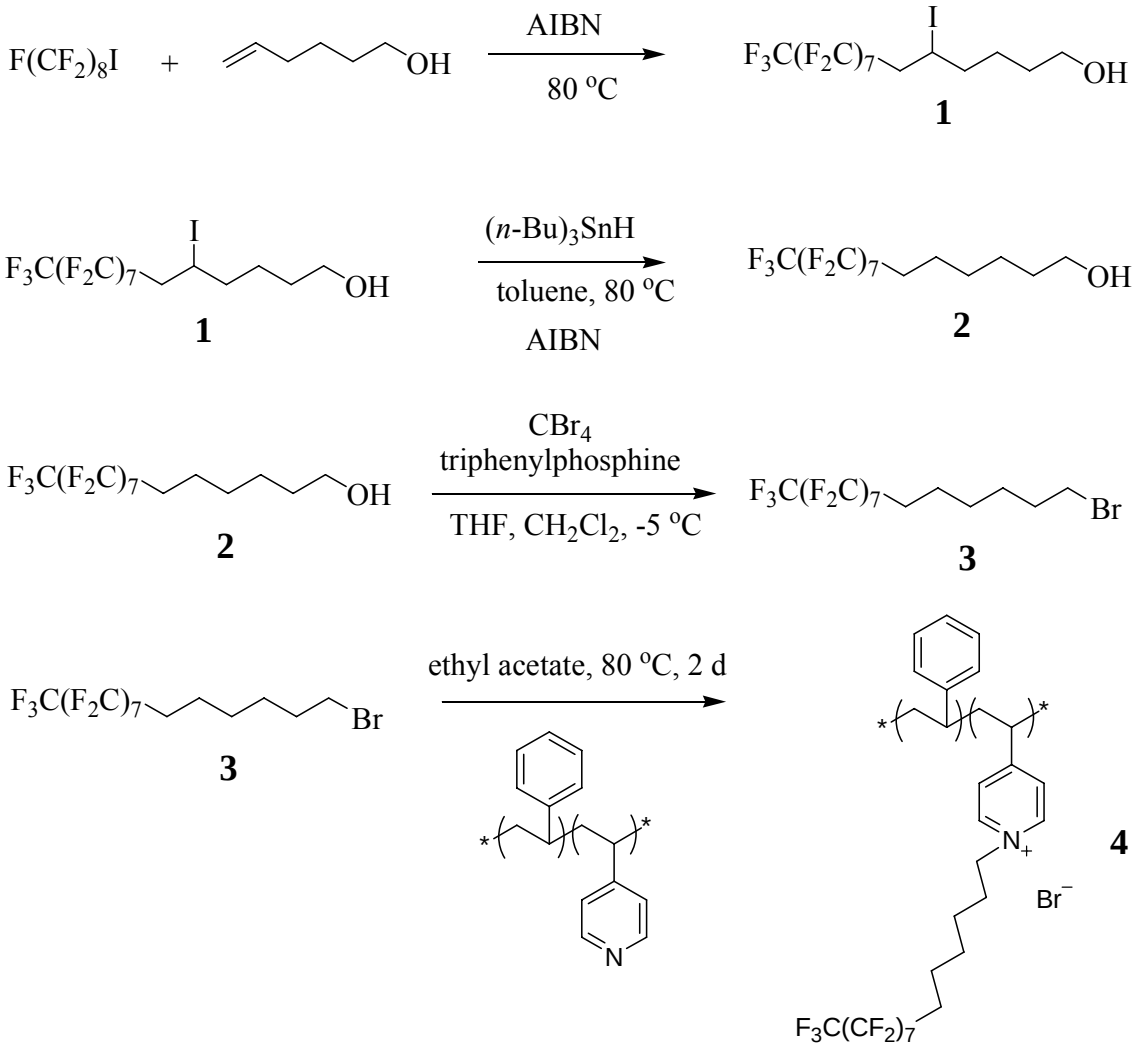

Scheme 2.20. Synthesis of 6-perfluorooctyl-1-bromohexane (**3**) and (PS-*b*-P4VP) quaternized with **3**.[29]

The antibacterial effect was tested by a viable counting method and a LIVE/DEAD BacLight assay. In viable counting test, PS-*b*-poly(ethylene-*r*-butylene)-*b*-

PS was spun cast onto the glass slide before solutions of PS-*g*-P4VP quaternized polymers were sprayed onto the slide. Then 10^6 cells/mL of *staphylococcus aureus* were sprayed onto the surface and covered with 1.5% w/v of growth agar. The number of bacterial colonies formed on the hexyl pyridinium coated glass slide (B) was 15-30% lower than the colonies formed on the uncoated glass slide (A). However, a more pronounced effect was seen on the fluorinated pyridinium coated slide (E) where there was almost 100% decrease in viable colonies (Figure 2.11).

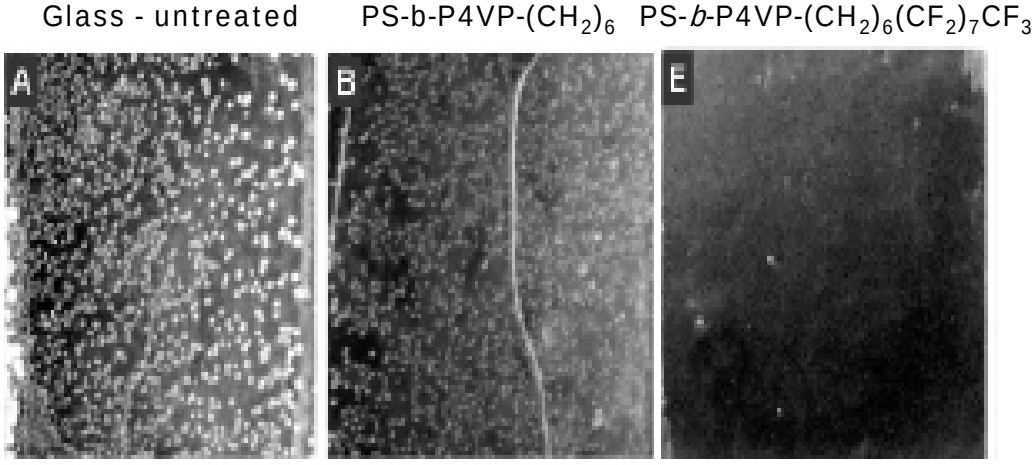

Figure 2.11. Viability test depicts the number of S.A. bacteria colonies for glass, PS-*b*-P4VP-$(CH_2)_6$ and PS-*b*-P4VP-$(CH_2)_6(CF_2)_7CF_3$.[29] Reprinted with permission from *Langmuir* **2006,** *22*, 11255. © 2008 American Chemical Society.

The latter test involves a green fluorescent SYTO 9 nucleic acid stain which permeates live/intact cell membranes and a red-fluorescent PI nucleic acid stain which only penetrates damaged membranes. These stains were added to the bacteria solution before spraying onto untreated and treated glass slides coated with P(4VP-*r*-BMA) that was quaternized with 1-bromohexane. After only 30 min of incubation, samples were analyzed with phase-contrast and fluorescence microscopy. Figure 2.12 shows the green fluorescence (480 and 500 nm) for an uncoated glass slide and red fluorescence (537 and

620 nm) for a P(4VP-*r*-BMA) quaternized glass slide. This test proved that the quaternized films killed *staphylococcus aureus* and the mechanism resulted in disruption of the cell membrane.

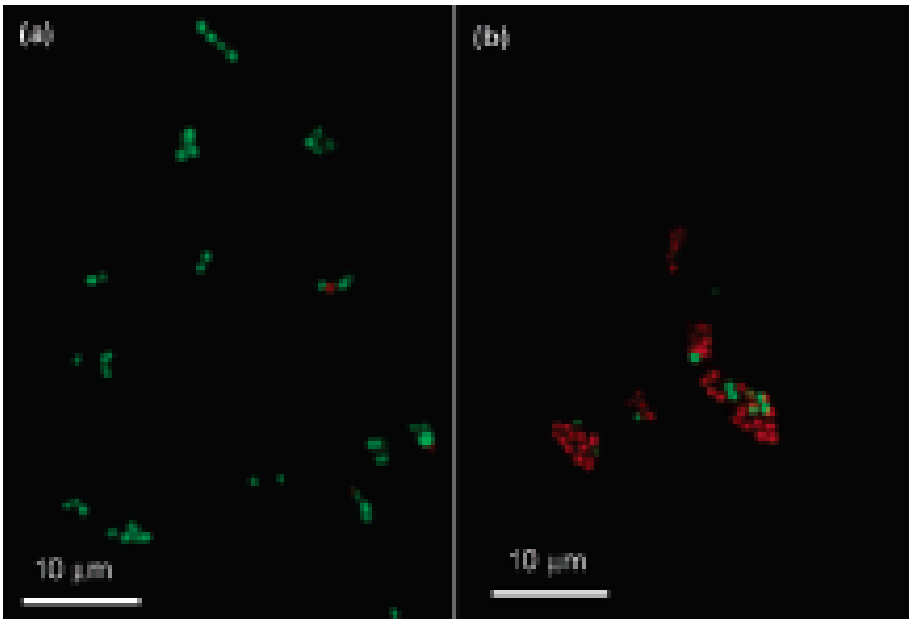

Figure 2.12. S.A cells on a) uncoated glass slide and b) slide coated with P(4VP-*r*-BMA) quaternized polymer.[29] Reprinted with permission from *Langmuir* **2006**, *22*, 11255.

In light of the positive results P4VP quaternary compounds have had against a number of bacterial strains when they are grafted or coated on glass slides, clay, and polymers, they have been considered for making PVC antibacterial. Unlike other methods previously mentioned to coat antibacterial reagents to PVC (pluronics, triclosan and bronopol, *bovine serum albumin* and heparin and NaOH/ $AgNO_3$), grafting cationic P4VP bears several advantages. For instance, the antibacterial agent would be immobilized and insoluble in aqueous media. Also, the hydrophilic nature of PVC-*g*-P4VP may increase the biocompatibility by reducing platelet adhesion and thrombosis.

2.5 Mechanism of Bactericidal Effect

Both gram positive and gram negative bacteria have distinctive rigid cell walls with differing composition and resistance properties. Endotoxins, such as gram positive bacteria, have a 15-80 nm thick cytoplasmic membrane cell wall consisting of multiple layers of peptidoglycan (Scheme 2.21).[51, 52] The gram negative endotoxin cell wall (10 nm) only has one layer of peptidoglycan surrounded by an outer lipopolysaccharide membrane that renders the bacteria impervious to penicillin, other ß-lactams and lysozyme.

For E. coli the peptidoglycan layer is composed of two disaccharides linked by a peptide side chain.[53] *N*-acetyl-glucosamine (NAG) and *N*-acetylmuramic acid (NAM) are connected by a beta 1, 4-glycoside bond which can easily be cleaved by lysozyme to disrupt the cell membrane. NAM is bonded to a peptide side chain of L-alanine, D-glutamate, diaminopimelic acid and D-alanine which forms an amide crosslink to another peptide chain. The crosslinks allow the cell membrane to be one continuous glycan molecule. Different types of bacteria have distinctive peptide chains and interpeptide bridges. Gram negative bacteria are less susceptible to lysozymal cleavage because the layer of peptidoglycan is protected by an outer membrane. The amphiphilic lipopolysaccharide has a hydrophobic lipid tail which inserts into the interior membrane while the hydrophilic linear polysaccharide extends away from the outer membrane into the aqueous media. The negatively charged phosphates of the lipid head group attract Mg^{2+} cations which chelate with other lipids affording lateral stability for the membrane (Scheme 2.21).[53] The lipid is the main toxic component of the bacteria.

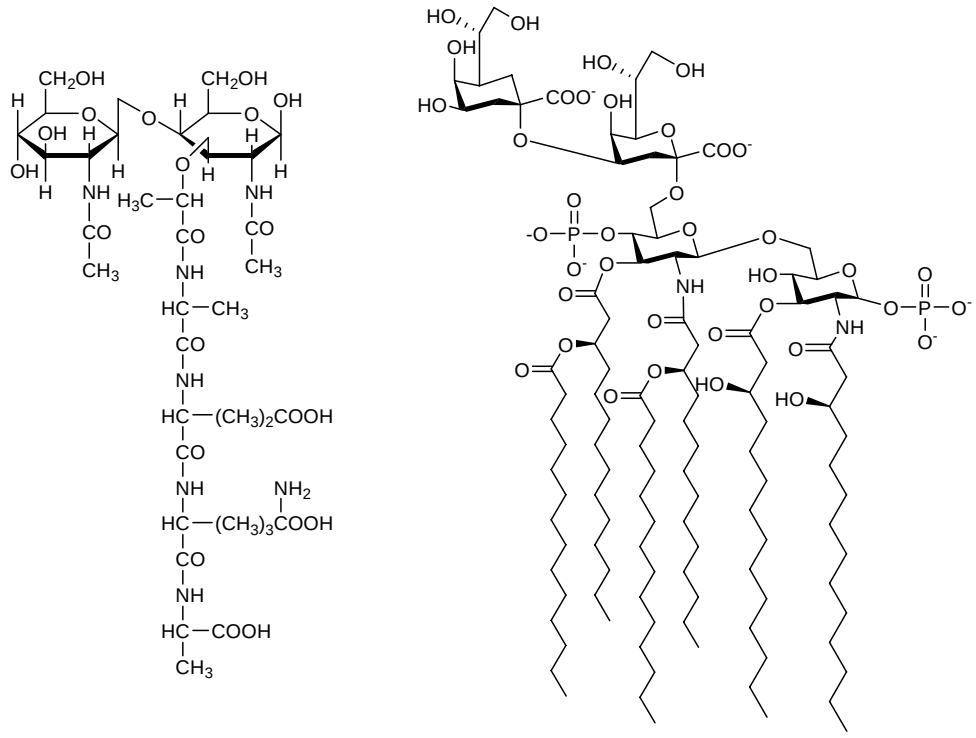

Scheme 2.21. Structure of E. coli peptoglycan (left) and lipopolysaccharide (right) wall.

There are a few proposed theories for the mechanistic breakdown of bacteria. Ivanov *et al.*[54] used molecular simulations of polymethacrylate copolymers with quaternary ammonium compound functionalities and extended hydrophobic alkyl chains to illustrate the hydrophobic disruption of the gram negative cytoplasmic cell wall. Electrostatic interaction between the phosphate of the lipid head groups and the polycation allow proximity for the hydrophobic alkyl chains to penetrate and disrupt the lipopolysaccharide.

Another viable mechanism employs the displacement of bridging Mg^{2+} and Ca^{2+} cations for polycations with a high surface charge density, resulting in destabilization of the outer membrane.[29] As previously mentioned, the surface charge density of the PS-*b*-P4VP system increased with the gradient of pyridinium rings at the surface. These

polycations may have replaced the Mg^{2+} and Ca^{2+} cations to breakdown the cell wall. Also, the cationic groups may then further penetrate into the inner membrane, producing leakage.

Although researchers have successfully modified the surface of PVC for reduced plasticizer migration and increased biocompatibility by coating or chemically crosslinking the surface, a more advantageous technique is based on the surface grafting of hydrophilic polymer. The technique proposed by Hu and Brittain does not use harsh chemical or expensive UV or cold plasma treatment which can damage the sample. The beauty of the method is the low cost and simplicity, and therefore it was used to alter the surface of PVC. The following experimental and results and discussion chapters give details into the favorable and successful surface modification of PVC films and tubing.

CHAPTER III

EXPERIMENTAL SECTION

3.1 Materials

Acrylic acid (AA, Aldrich) was passed through a column of neutral aluminum oxide (150 mesh, Aldrich). *N*,*N*-Dimethylacrylamide (DMA), 2-hydroxyethyl acrylate (HEA), *N,N*-dimethylaminoethyl methacrylate (DMAEMA) and 2-hydroxyethyl methacrylate (HEMA) were purchased from Aldrich and passed through a column of activated basic alumina (150 mesh, Aldrich). 4-Vinylpyridine (4VP, Aldrich, bp 62-65 °C) was purified by distillation. 2, 2-Azobis(2-methylpropionitrile) (AIBN, Aldrich, mp 102-104 °C) was recrystallized from methanol.

Methanol (MeOH), acetone, diethyl ether, anhydrous toluene, anhydrous methlyene chloride, *N*,*N*-dimethylformamide (DMF), ethyl acetate, anhydrous tetrohydrofuran (THF), hexanes and deuterated chloroform ($CDCl_3$) were purchased from Aldrich and used as received. The alkylating agents, 1-bomooctane, 1-bromohexane and 1-bromobutane, were purchased from Aldrich and used as received. Heptadecafluoro-1-iodooctane, 5-hexen-1-ol, tributyltin hydride, carbon tetrabromide, and triphenylphosphine were purchased from Aldrich and used as received. PVC sheets (7 mil, 0.164 mm thick) were obtained from Universal Plastics. PVC tubing was obtained from VWR International. A RTE-5DD Endocal circulating bath was used at 75 °C to heat the polymerization media inside the tubing.

3.2 Characterization Methods

Transmission Fourier transform infrared (FT-IR) spectroscopy measurements were performed on a Nicolet model 730 FT-IR spectrometer. X-ray photoelectron spectroscopy (XPS) was performed on a Perkin-Elmer instrument using Al α radiation with a takeoff angle of 45° at the MATNET Surface Analysis Center at Case Western Reserve University. Before measurement, the samples were vacuum dried for 22 h. Ellipsometry was performed using a Gaertner model L116C ellipsometer with a He-Ne laser (λ = 632.8 nm) and a 70° fixed angle of incidence. Atomic force microscopy (AFM) was performed using a multimode scanning probe microscope (Digital Instruments, Nanoscope IIIA) in tapping mode with a silicon tip. The AFM images were obtained at room temperature in air. A scan rate of 1 Hz and a resolution of 512 × 512 pixels were selected to generate high-quality images. Digital pictures of the cross-sectioned tubing and films were taken using an Olympus BX51 Research Microscope with 5× and 2.5× magnification equipped with an Olympus DP70 digital camera. Elemental analysis was performed by Galbraith Laboratories. All proton nuclear magnetic resonance (^{1}H NMR) spectra were recorded on a Varian Mercury 300 spectrometer, using $CDCl_3$ as the solvent and reference (7.26 ppm).

Contact angles were determined using a Rame Hart NRL-100 contact angle goniometer equipped with an environmental chamber and tilting base mounted on a vibrationless table (Newport Corp.). A 7.5 μL droplet of filtered, deionized distilled water was placed on the surface of the samples at room temperature. After 1 min the contact angles (advancing and receding) were measured using the tilting stage (35°) method. Each reported value is the average of five independent measurements. Capillary

rise measurements of the modified and unmodified PVC tubing were recorded using a traveling telescope cathetometer M912 from Gaertner Scientific. The probe fluid (water or ethylene glycol) rose for a few h to equilibrate before measurements were made.

The molecular weight for PVC was determined by gel permeation chromatography (GPC) in THF using a Waters 501 pump, Waters HR4 and HR2 styragel columns, a Waters 410 differential refractometer and a Viscotek 760A dual light scattering and viscosity detector. Other molecular weights were determined by GPC in DMF using a Waters 501 pump, two PLgel (Polymer Laboratories) mixed D columns (5 μm), and a Waters 410 differential refractometer. Molecular weights were calibrated by comparison to narrow polydispersity poly(methyl methacrylate) standards (200 to 1.0×10^6 g/mol) (Polymer Laboratories).

3.3 Determination of Grafted Film Thickness

The construction of calibration curves for thickness determination by transmission FT-IR spectroscopy was based on spin-cast free polymer layers on silicon wafers and their relative absorbance and thickness values An initial solution of free polymer was spin cast onto the wafer with the appropriate solvent: 5% poly(2-hydroxyethyl methacrylate) (PHEMA) (50:50 methanol/THF, w/w), 1% poly(2-hydroxyethyl acrylate) (PHEA) (methanol), 5% poly(dimethylacrylamide) (PDMA) (30:70 methanol/THF, w/w), 5% poly(acrylic acid) (PAA) (75:25 methanol/H_2O, w/w), 3% poly(4-vinylpyridine) (P4VP) (THF), 3% poly(dimethylaminoethyl methacrylate) (PDMAEMA) (toluene), and 2% PVC (THF). These solutions were diluted to spin cast polymer layers of reducing thickness. Each polymer layer was characterized by ellipsometry for thickness in nm and transmission IR spectroscopy for absorbance. The refractive index

values used for film thickness determination are 1.53 for PAA and PDMA, 1.51 for PHEA and PHEMA, 1.52 for PDMAEMA and 1.47 for P4VP.[55, 56]

Another calibration curve for thickness determination of the P4VP graft used absorbance values from a Hewlett Packard 8453 Diode Array UV-Visible spectrophotometer equipped with tungsten and deuterium halogen lamps. The free polymer, P4VP, had an absorption maximum at 267 nm[57] for dilute solutions of varying concentrations in DMF. Plasticizer migration was assayed with UV-Vis spectrophotometry using hexane as the extracting solvent.

3.4 Grafting-from Polymerization of Hydrophilic Monomers

The PVC film (2 cm × 1 cm × 7 mil (0.164 mm)) was immersed into an acetone solution of 5% AIBN (w/w) for 15 min. Shorter immersion times of 15 s were also performed. After immersion, the film was removed from the solution and placed between two glass plates, where the percent swelling was measured with a ruler. Percent swelling (S) was defined as: $S\% = ((A_f-A_i)/A_i) \times 100$; where A_i and A_f represent the area of the film before and after immersion, respectively. The PVC film was then dried in a vacuum oven at room temperature for 24 h. The monomer solution (10% monomer in water or methanol, v/v) and the AIBN-preadsorbed PVC film were transferred into a sealed glass vessel, purged with nitrogen for 1 h and heated at 70 °C for 24 h. The samples were then exhaustively treated with methanol for 2 h at 70 °C, sonicated for 2 h, and again immersed in solvent for 2 h at 70 °C to remove physisorbed monomer and polymer. The hydrophilic grafted PVC films were dried for 17 h in vacuo. Samples were kept under vacuum in a desiccator prior to characterization.

For polymerizations within PVC tubing, 2.5 ft sections were used. Initiator deposition was conducted by filling the tubing with a 5% AIBN/acetone (w/w) solution. After 15 min exposure, the tube was vacuum dried for 3 h. For polymerization, the tubing was filled with a 10% monomer/methanol (w/w) solution and immersed in a water bath set for 75° C. After 24 h, the tubing was removed from the water bath and cleaned by passing methanol (70 °C) several times through the tubing. Following sonication in methanol for several h, the tubing was vacuum dried and characterized by capillary rise and gravimetric analysis.

3.5 Noncovalent Coating of Hydrophilic Polymers to PVC

Free polymers collected from previous polymerizations were used in the coating experiment with PVC. P4VP and PHEMA were added to separate flasks containing MeOH and a PVC film. The flask was purged with nitrogen for 1 h and heated at 70 °C overnight. The samples were then exhaustively treated with methanol for 2 h at 70 °C, sonicated for 2 h, and again immersed in solvent for 2 h at 70 °C. The sample was characterized by FT-IR spectroscopy and contact angle analysis to distinguish covalent grafting of a hydrophilic polymer versus physisorbtion of polymer chains to the surface.

3.6 Controlled Radical Abstraction of PVC

A piece of treated PVC film was placed into a round bottom flask under the same conditions used in polymerization, without the monomer. By excluding the monomer, it was possible to examine how the AIBN radicals would interact with the PVC surface. According to the proposed mechanism (Scheme 4.2), the radicals should either abstract a

chlorine or hydrogen from the PVC backbone. After the reaction ran overnight, the solution was evaporated into a weighing pan. Part of the residue left behind was analyzed by NMR and IR spectroscopy.

3.7 Plasticizer Migration of Modified and Unmodified PVC Films

The mass transfer of plasticizer from bulk PVC to the surface of the film was assayed with UV-Vis spectrophotometry. Hexanes were used as the extraction media for all PVC films. For each sample, 10.5 cm^2 of film was placed into a sealed screw top cuvette with 4 mL of hexanes. The absorbance maximum which represents the plasticizer in the UV-Vis spectrum was found at 278 nm.[14] The absorbance unit of this peak was monitored over time as the films were continuously exposed to hexanes. Migration studies were performed on the control PVC samples which were exposed to acetone for 0 s, 15 s, and 15 min as well as the modified films which underwent initiator deposition for the typical 15 min and also the fast dip method of 15 s.

3.8 Synthesis of 6-Perfluorooctyl-1-hexanol (**2**)

The procedure used was described by Höpken *et al.*[49] and Ober and Wang[50] (Scheme 4.5). Heptadecafluoro-1-iodooctane (25 g, 12.8 mL, 45.8 mmol) was reacted with 5-hexen-1-ol (6.85g, 8.1 mL, 68.4 mmol) at 80 °C in a 100 mL three-neck, round bottom flask fitted with a reflux condenser sealed with a rubber septum. A nitrogen inlet was attached to this septum. AIBN (125 mg, 76.2mmol) was added to the reaction in four portions over 6 h. The solution was then distilled to remove excess 5-hexene-1-ol. The remaining iodo-alkane (**1**) was reduced by adding 9.4 mL toluene, tributyltin hydride

(9.96 g, 34.2 mmol, 9.1 mL) and AIBN (205 mg, 1.25 mmol) to the reaction flask which was heated at 80 °C for 24 h. The sample was recrystallized from toluene.

Analysis of **2**: ^{1}HNMR ($CDCl_3$): δ 1.24 (t, 1H, CH_2*OH*, $J_{(H-H)}$ = 5.3 Hz,), 1.37-1.5 (m, 4H, $CF_2CH_2CH_2$*CH_2CH_2*), 1.53-1.70 (m, 4H, CF_2CH_2*CH_2* and *CH_2*CH_2OH), 2.08 (tt, 2H, CF_2CH_2, $J_{(H-F)}$ = 18 Hz , $J_{(H-H)}$ = 9 Hz), 3.67 (pseudo-q, 2H, CH_2OH).

3.9 Synthesis of 6-Perfluorooctyl-1-bromohexane (**3**)

The procedure used was described by Ober *et al.*[29, 50] (Scheme 4.6). 6-Perfluorooctyl-1-hexanol (**2,** 4.9 g, 94.2 mmol) and carbon tetrabromide were added to a 100 mL, round bottom flask equipped with a stir bar. Anhydrous THF (2.6 mL) and 5.2 mL of methylene chloride were added to flask which was cooled to -5 °C with a brine ice bath. Small portions of triphenylphosphine (1.05 g, 39.9 mmol) were added over 15 min. The mixture was stirred for 1 h at -5 °C and became slightly pink due to the presence of free bromine and a white precipitate of triphenylphosphine oxide that was produced. The mixture was stirred for another 6 h at room temperature. The solvent was then removed by use of a rotary evaporator. The collected solid was purified by silica gel chromatography using methylene chloride as the elution solvent.

Analysis of **3**: ^{1}HNMR ($CDCl_3$): δ 1.46 (m, 4H, $CF_2CH_2CH_2$*CH_2CH_2*), 1.64 (m, 2H, CF_2CH_2*CH_2*), 1.89 (m, 2H, *CH_2*CH_2Br), 2.08 (tt, 2H, CF_2CH_2, $J_{(H-F)}$ = 15 Hz , $J_{(H-H)}$ = 7.5 Hz), 3.43 (t, 2H, CH_2Br).

3.10 Quaternization of PVC-*g*-P4VP with 1-Bromoalkanes

PVC-*g*-P4VP films (approximately 3 × 2 cm) were reacted with 10% (v/v) solutions of either 1-bromobutane, and 1-bromohexane in ethyl acetate at 80 °C for 120 h under nitrogen. Multiple PVC-*g*-P4VP films were reacted separately with a 10% solution of 1-bromooctane in ethyl acetate at 80 °C for 6, 12, 19, 24, 36, 48, 60, 72, 95, and 120 h. All films were then washed with MeOH, dried under vacuum and characterized by contact angle, IR spectroscopy and XPS analysis. As reaction time advanced, the films turned darker brown.

3.11 Quaternization of PVC-*g*-P4VP with 6-Perfluorooctyl-1-bromohexane

A 10% (w/w) solution of 6-perfluorooctyl-1-bromohexane in ethyl acetate was reacted with multiple PVC-*g*-P4VP films (approximately 3 x 2 cm) simultaneously at 80 °C for 24, 48, 72, 96 and 148 h. The PVC-*g*-P4VP films that reacted with the 6-perfluorooctyl-1-bromohexane for 24 and 48 h were further quaternized with 1-bromohexane under similar conditions for 24 and 72 h, respectively. After quaternization, all films were washed with methanol and vacuum dried. A dark brown color was observed for films with long reaction times.

3.12 Intramolecular Quaternization of PVC-*g*-P4VP

To determine the extent of quaternization by alkylating agents, it was imperative to quantify any possible intramolecular reaction of the pyridine nitrogen of P4VP and chlorines on the PVC backbone. PVC-*g*-P4VP was heated in ethyl acetate at 80 °C for 5

days under nitrogen. The degree of intramolecular quaternization was determined by the absorbance maximum at 1640 cm^{-1} with FT-IR spectroscopic analysis.[50]

3.13 Bacterial Inhibition Studies

Bacteria strains used included: s*taphylococcus aureus* (ATCC, strain 29213), s*taphylococcus epidermis* (*coagulase negative staphylococcus*), e*scherichia coli* (ATCC, strain 25922) and p*seudomonas aeruginosa* (ATCC, strain 27853). Standardized suspensions were prepared in trypticase soy broth using a 0.5 McFarland standard (final concentration 10^8 colony-forming units per mililiter (CFU/mL)). Suspensions were further diluted to 10^6, 10^5 and 10^4 CFU/mL in saline. Samples (10 μL) of each dilution were applied to the surface of each film, previously cropped on a glass slide, using an automated pipette. Slides were placed in petri dishes and allowed to dry in a 35 °C incubator for approximately 30 min. Following drying, pieces of Mueller Hinton II agar were cut from a commercial agar plate (BBL) and placed over the cross-section of film exposed to the bacteria. Lids were placed on the petri dishes and they were incubated overnight at 35°C. The bacteria colony growth was monitored with a digital microscope.

CHAPTER IV

RESULTS AND DISCUSSION

4.1 Surface Grafting onto PVC via Physisorbed Free Radical Initiation

The graft polymerization of hydrophilic monomers AA, DMA, HEA, HEMA, DMAEMA and 4VP from PVC was conducted using a simple two-step process: 1) physisorption of a hydrophobic free radical initiator (AIBN) onto the surface of PVC, followed by 2) radical polymerization in a hydrophilic media (Scheme 4.1). In step one, the hydrophobic PVC was swollen in a good solvent (acetone). We have determined that the PVC expanded up to 142% of the original size after 15 minutes of exposure to AIBN/acetone by immediately measuring the dimensions of the film as it was pressed between two glass plates following immersion.

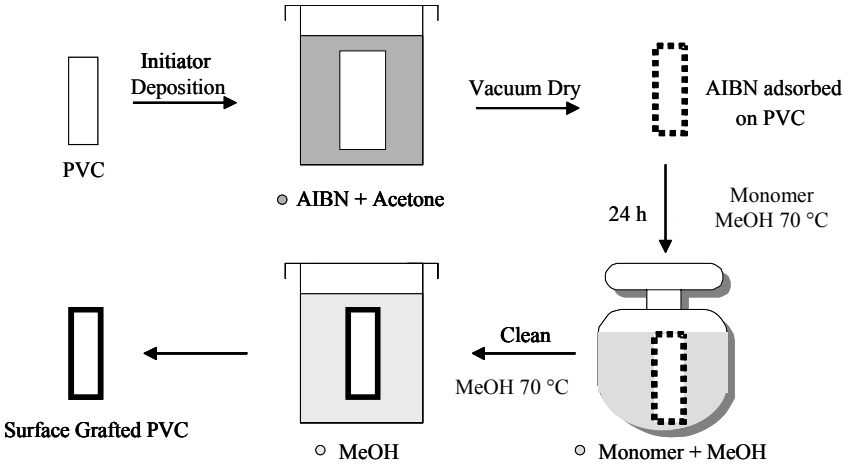

Scheme 4.1. Simple 2-step surface modification of PVC.

As the solvent evaporated *in vacuo*, we speculate that the initiator remains on the surface and is potentially entrapped in the subsurface of PVC. Subsequently, when the film was placed into the polymerization media, a hydrophobic/hydrophilic diffusional barrier between the surface and the media prevented diffusion of the initiator into solution. Because the majority of initiator was in proximity to hydrophobic PVC, heating promoted radical generation at the surface.

The low bond dissociation energy associated with AIBN is related to the high stability of the tertiary radicals formed upon heating. In this reaction, the isobutyronitrile radicals can undergo three possible reactions: combination/disproportionation with another tertiary isobutyronitrile radical, initiation of monomer in solution forming free polymer, or abstraction of a hydrogen or chlorine from the PVC backbone (Scheme 4.2). To determine the correct mechanism, a controlled radical test was performed.

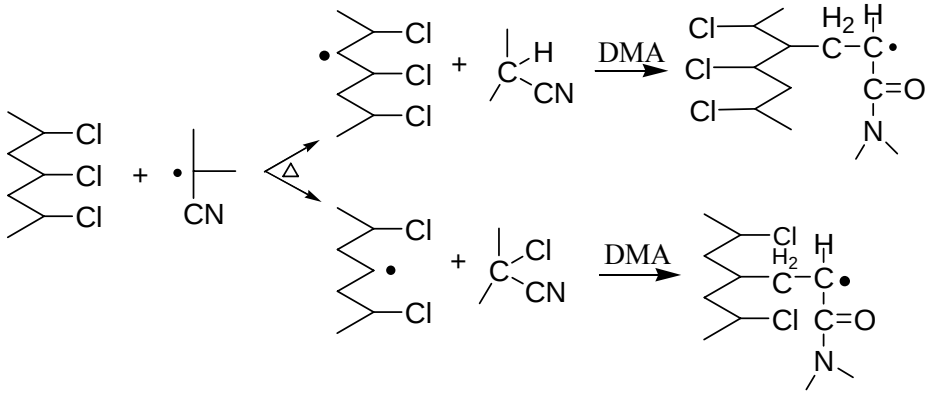

Scheme 4.2. Mechanism of hydrogen and chlorine abstraction.

In this experiment, PVC with physisorbed initiator was heated at 70 °C for 15 minutes and the sample was then placed into MeOH under nitrogen for 24 h at 70 °C. By excluding the monomer, we eliminated the polymerization pathway for initiator loss. Theoretically, the only potential products formed upon heating could be the PVC film

with active radical sites (solid state) and either 2-methylpropionitrile (bp 107 °C) or 2-chloro-2-methypropionitrile (depending on whether hydrogen or chloride abstraction occurred), and products from combination (tetramethylsuccinonitrile) or disproportionation. After the reaction ran overnight, the solution was evaporated in a weighing pan. The residue was analyzed by NMR (Figure 4.1) and IR (Figure 4.2) spectroscopy.

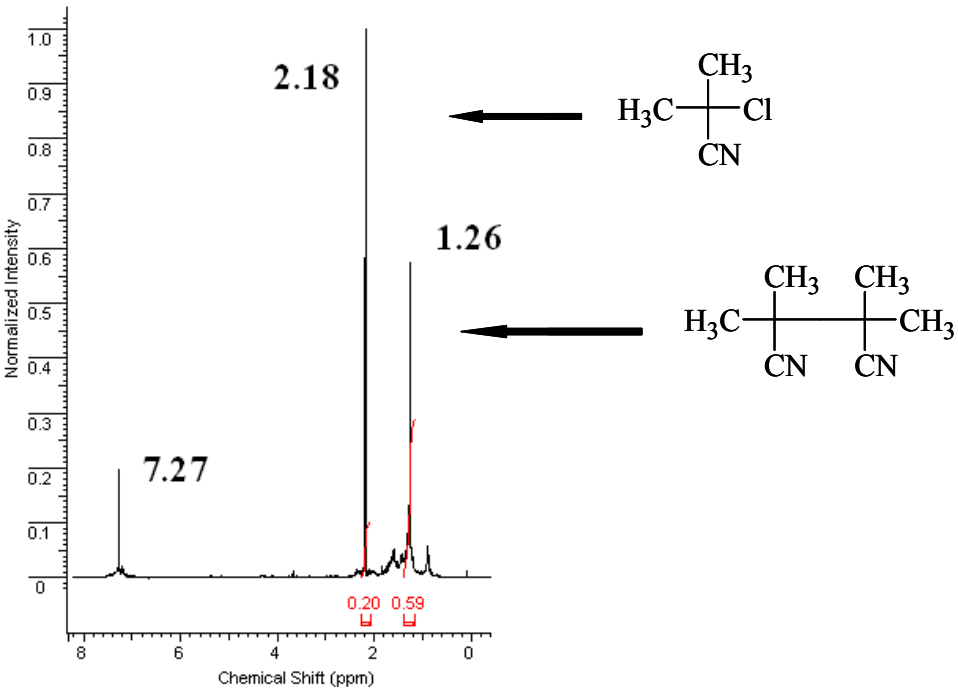

Figure 4.1. ^{1}H NMR spectrum of chlorine-capped AIBN radicals ($CDCl_3$).

As expected from bond dissociation energies, both characterization methods were consistent with preferential abstraction of chlorine ($\Delta H_{C\text{-}Cl}$ = 81 kcal/mol) over hydrogen ($\Delta H_{C\text{-}H}$ = 95 kcal/mol) because of a lower heterolytic bond dissociation energy.[58] The NMR exhibited two singlets at 2.18 and 1.26 ppm indicative of the methyl hydrogens of 2-chloro-2-methypropionitrile and tetramethylsuccinonitrile, respectively.[58]

If only the hydrogen capped product (2-methypropionitrile) were present, there would have been a septet at 2.8 ppm for the hydrogen and a doublet at 1.3 ppm for methyl substituents (integration 1:6).[59]

The transmission IR spectroscopy also confirmed the presence of the chlorine capped AIBN radical. Absorptions at 2930-2850, 2254, 1462-1380 and 910- 736 cm^{-1} were indicative of the aliphatic (C-H), nitrile, gem dimethyl and C-Cl absorptions, respectively.

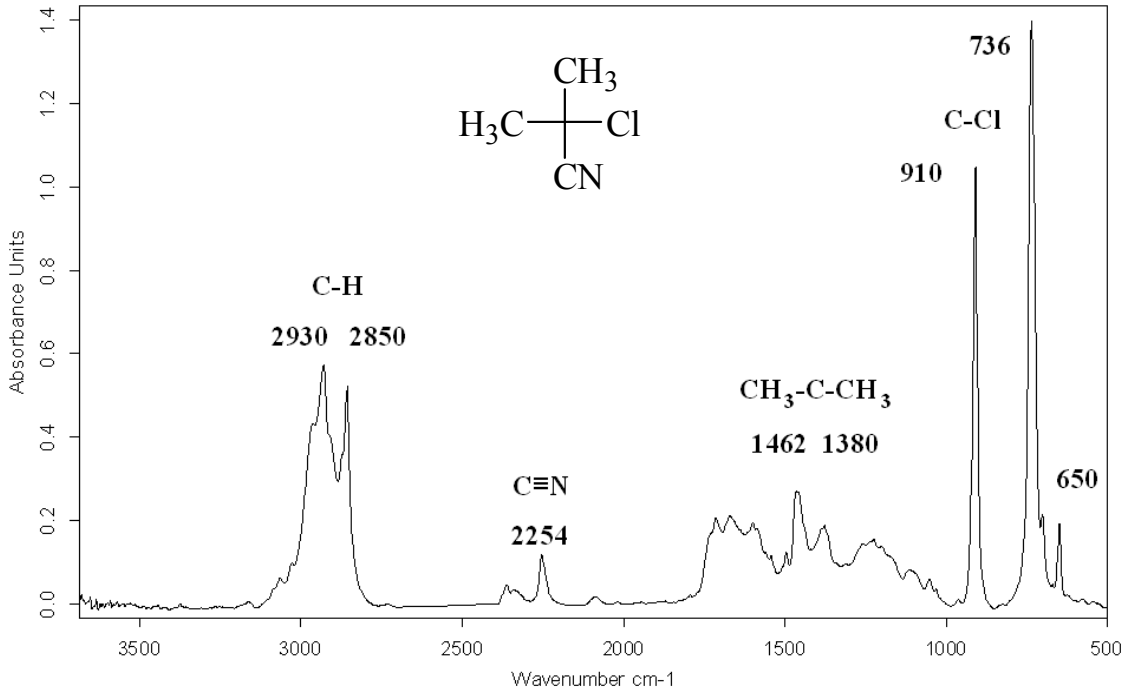

Figure 4.2. Transmission IR spectrum of 2-chloro-2-methylpropionitrile.

The surface PVC radicals formed from the chlorine abstraction can react with adsorbed hydrophilic monomer from solution forming grafted polymer chains. Energetically, the abstraction of the chlorine or hydrogen is unfavorable in comparison to homogeneous radical polymerization in solution. However, at the interphase of solid and liquid solution, the reaction of the hydrophobic radicals and the PVC is enhanced by

limited diffusion of the hydrophobic initiator radicals into the aqueous environment. Also, there is a possibility of polymer chain transfer from the free polymer to the PVC; although we speculate that the majority of surface-generated radicals arise from isobutyronitrile radical abstraction.

After polymerization, the polymer samples were exhaustively extracted by solvent (either water or methanol) and sonicated in solvent to remove the noncovalently attached free polymer. It was qualitatively observed that the modified PVC films became cloudy upon polymerization with all monomers. The films occasionally appeared opaque because the polymerization was run relatively close to the T_g of PVC, 81 °C,[30] where there is a possibility of long range segmental motion which can induce crystallinity. However, PVC is only 10% crystalline.[30] Most experiments produced a more rigid and less flexible PVC film. This can be explained by the loss of plasticizer during the initiator deposition stage. As the film swells in acetone, free volume increases allowing diffusion of the plasticizer. In fact, almost all plasticizer (93.3%) was lost after 15 minute immersion. Later, data will be presented on using reduced initiator deposition times for plasticizer migration studies.

4.2 Surface Wettability of PVC Films Grafted with Hydrophilic Monomers

The modified PVC films were characterized using water contact angles (Table 4.1). The advancing water contact angle of our plasticized PVC film[7] was 82 ± 2 °C, the static angle is 74 ± 2 °Cand the receding angle is 67 ± 2 °C. After surface modification the contact angles decreased significantly, consistent with the presence of a hydrophilic material on the surface. Literature values for contact angles of the hydrophilic polymers

are consistent with the presence of PHEMA (63°),[60] PHEA (69°),[61] PDMAEMA (65°),[62] PAA (45-50°),[63] PDMA (42°)[64] and P4VP (68°)[65] at the surface. For example, PVC-*g*-PHEMA exhibits advancing and receding angles of 61 ± 3 °C and 47 ± 4 °C.

Table 4.1. Water contact angles for modified PVC substrates.

Sample Description	Θ_a^o	Θ_s^o	Θ_r^o
PVC	82 ± 2	74 ± 2	67 ± 2
PVC-*g*-PHEMA	61 ± 3	57 ± 3	47 ± 4
PVC-*g*-PHEA	61 ± 3	57 ± 4	45± 3
PVC-*g*-PDMAEMA	71 ± 2	66 ± 3	57 ± 2
PVC-*g*-PAA	62 ± 4	57 ± 4	49 ± 5
PVC-*g*-PDMA	46 ± 4	42 ± 3	34 ± 1
PVC-*g*-P4VP	67 ± 5	64 ± 4	56 ± 5

4.3 Transmission IR Spectroscopy

Surface characterization of the modified PVC films, free polymer collected along with polymerization and unmodified PVC was carried out by transmission IR spectroscopy. Also, a background subtraction of the PVC film was used during the transmission IR spectroscopy analysis of modified PVC films to obtain a spectrum solely representative of the hydrophilic polymer graft. This was accomplished by taking a background spectrum of unmodified PVC and loading it into software prior to performing a transmission spectrum of the modified film. Figures 4.3 - 4.8 compare all spectra for PVC modification.

Pure PVC is not typically known to have a carbonyl absorption. However, if the polymer has been partially oxidized during manufacturing or contains plasticizer, a

carbonyl absorption will be observed. Neat PVC film displayed a carbonyl absorption at 1733 cm^{-1} which we have assigned to a phthalate plasticizer. Prominent absorptions at 1436, 1330, 1250, 1198, 1099 and 977 cm^{-1} were found along with 699 and 637 cm^{-1} for the C-Cl stretch.

All hydrophilic polymers possessed unique absorptions independent of PVC. Successful grafting was supported by the appearance of unique absorptions from both the hydrophilic polymer grafts and PVC in the transmission IR spectra of the modified films. Hydrophilic polymers such as PDMA and PAA had carbonyl absorptions that can be differentiated from the plasticizer. However the IR spectra of PHEMA, PHEA and PDMAEMA displayed carbonyl absorptions overlapping that of the plasticizer. This obstacle was not significant because there were other unique absorptions for each hydrophilic polymer. These discrepancies were better observed by comparing the spectrum of the modified film with the free polymer, the modified film with a subtraction of PVC and the neat PVC starting material. The modified film with a background subtraction of PVC removes absorptions associated with PVC so that only the hydrophilic graft absorptions are observed. Quantitative absorbance measurements of the background spectrum are not accountable since the film thickness of the PVC is most likely different than the starting material thickness. Regardless, in a comparative analysis, we can deduce covalent attachment has occurred.

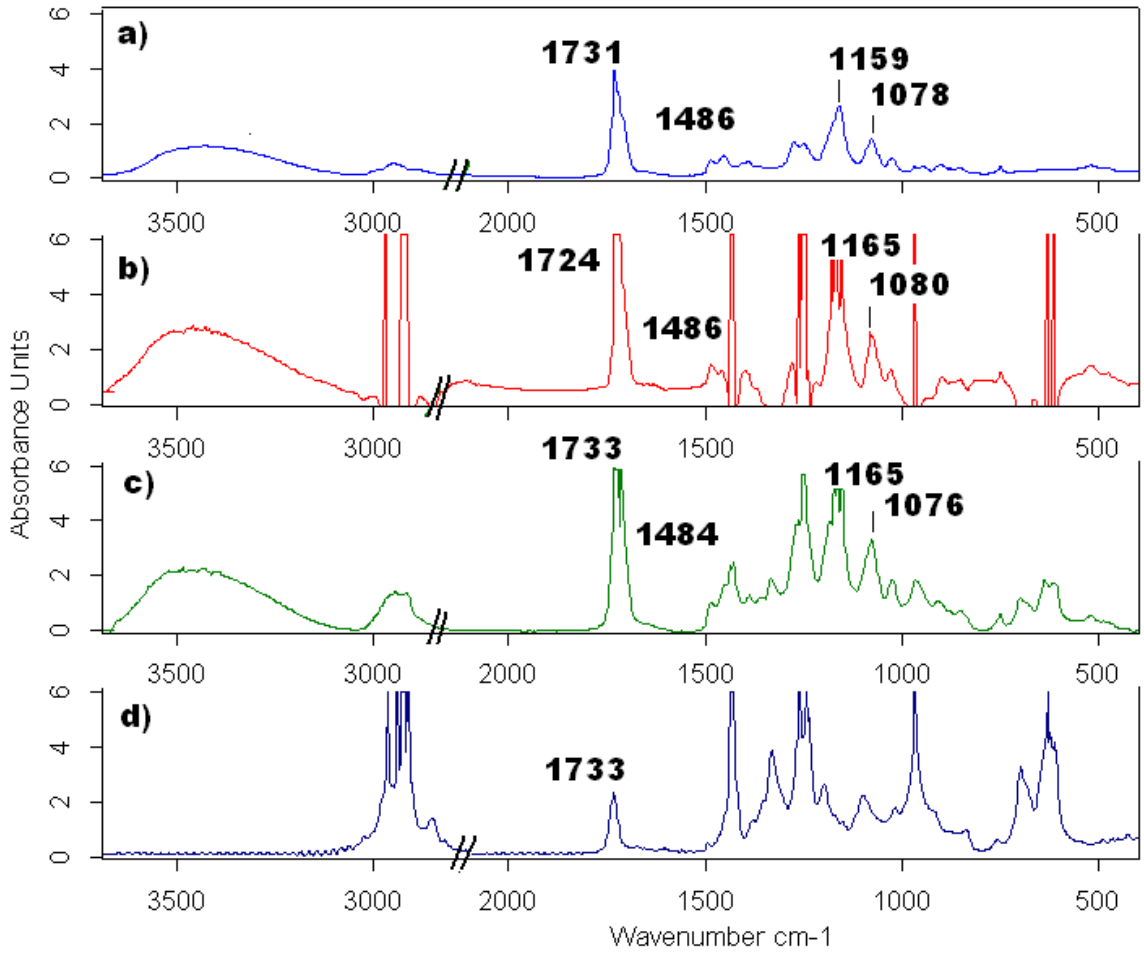

Figure 4.3. IR spectra of a) PHEMA, b) PVC-*g*-PHEMA with PVC background subtraction, c) PVC-*g*-PHEMA and d) PVC.

Figure 4.3 displays an O-H bend around 3500 cm^{-1}, C-O stretches at 1159 and 1078 cm^{-1} and a peak at 1478 cm^{-1} from the free PHEMA[66] that was present in both the modified film and the background subtraction spectra. The same absorptions were absent in the PVC spectrum, verifying their uniqueness to PHEMA. The PVC-*g*-PHEMA spectrum also illustrates all PVC absorptions (C-Cl stretch) confirming that PHEMA is covalently grafted to the surface of PVC.

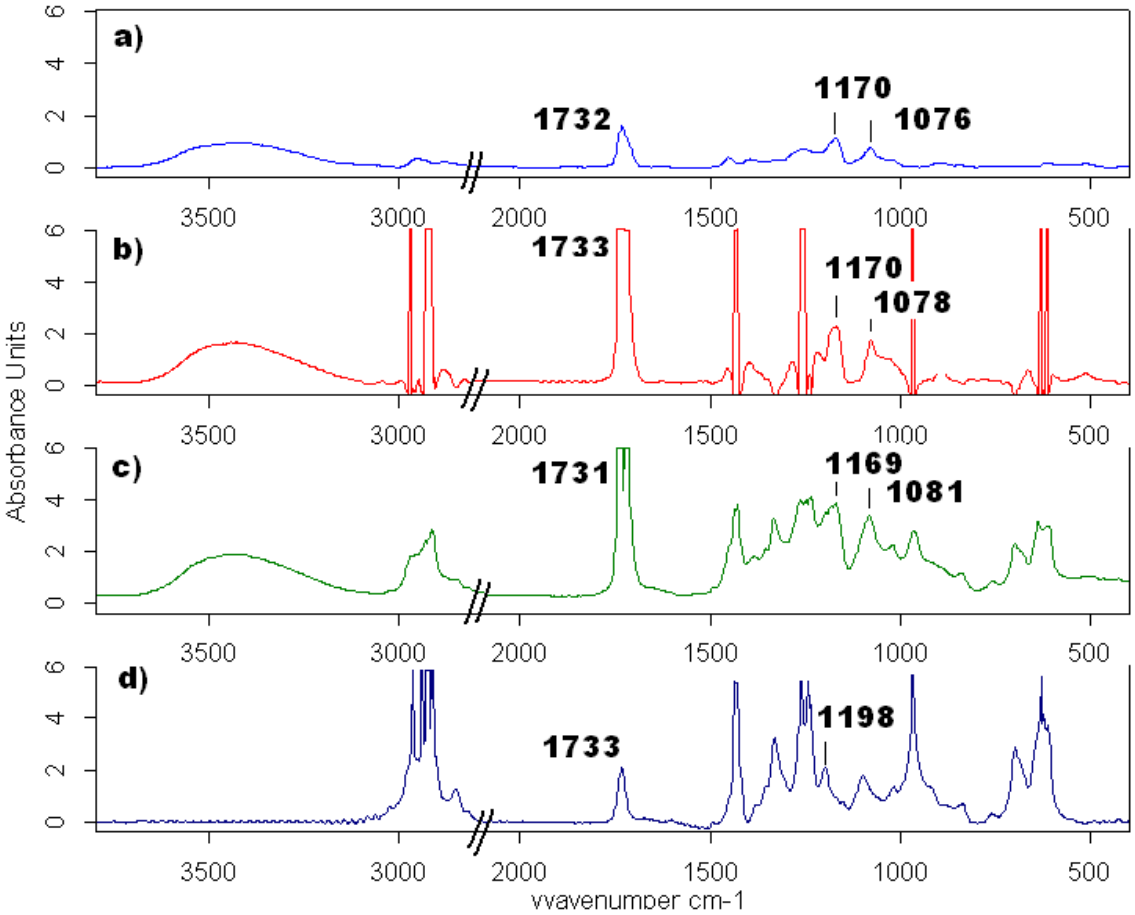

Figure 4.4. IR spectra of a) PHEA, b) PVC-*g*-PHEA (PVC background subtraction), c) PVC-*g*-PHEA, and d) PVC.

PHEA[67] is very similar in structure to PHEMA and therefore had analogous peaks for the carbonyl absorption, O-H bend and C-O stretch at 1170 and 1076 cm^{-1} for the free polymer, 1170 and 1078 cm^{-1} for the background subtraction of PVC and 1169 and 1081 cm^{-1} (along with absorptions for PVC) for the PVC-*g*-PHEA film (Figure 4.4).

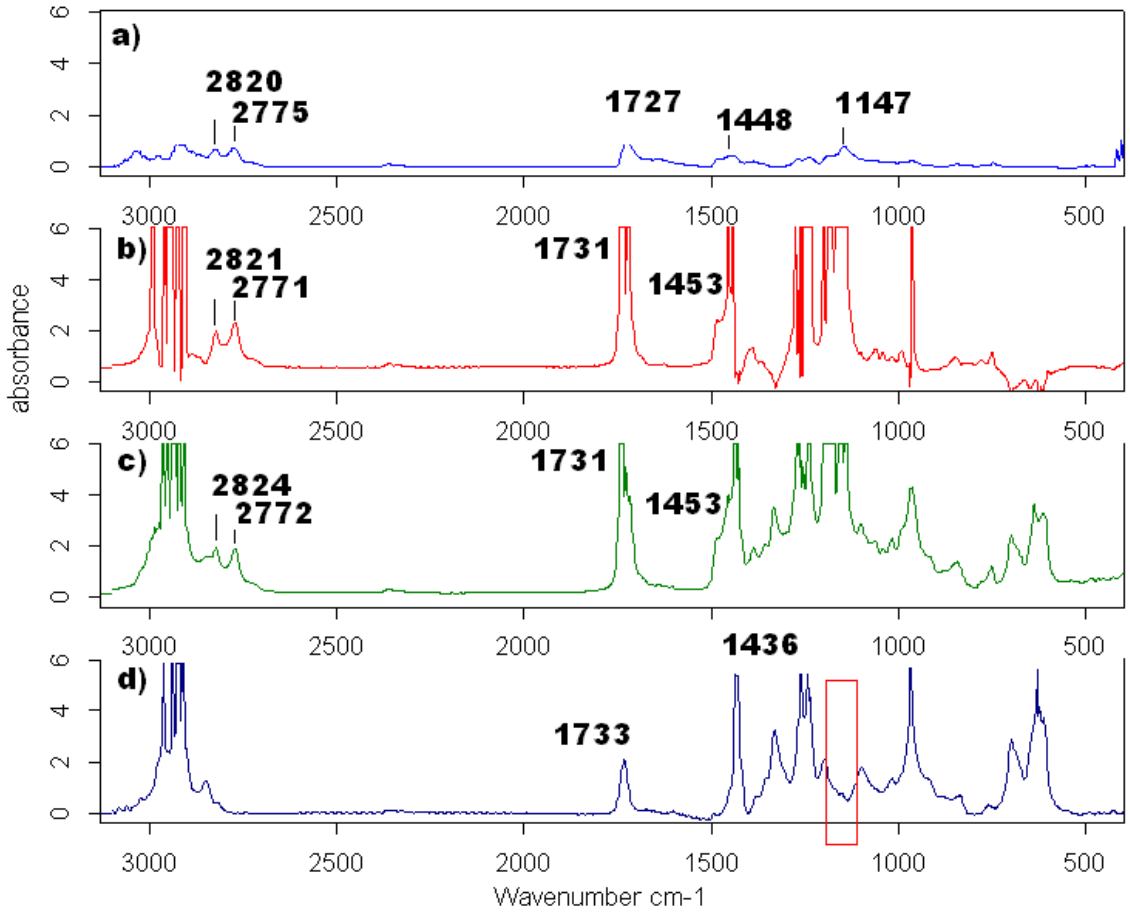

Figure 4.5. IR spectra of a) PDMAEMA, b) PVC-*g*-PDMAEMA (PVC background subtraction), c) PVC-*g*-PDMAEMA, and d) PVC.

PDMAEMA[68] has pendant methyl groups attached to tertiary nitrogens which gave unique C-H stretching and bending absorptions. Figure 4.5 exhibits two unique bands around 2820 and 2775 cm^{-1} for the C-H stretch of PDMAEMA (ν_s, CH_3) and one at 1448 cm^{-1} for the C-H asymmetric bend (δ_{as}, CH_3). The stretching bands are easily identifiable in the modified spectrum, and the bend appears as a shoulder to the asymmetric bend at 1436 cm^{-1} for PVC (δ_{as} CH_2). A C-N stretch was observed at 1147 cm^{-1} in the free polymer, background subtraction and modified film spectra while absent

in the PVC spectrum. Evidence of both PDMAEMA and PVC absorptions in the modified spectrum confirms that successful grafting has occurred.

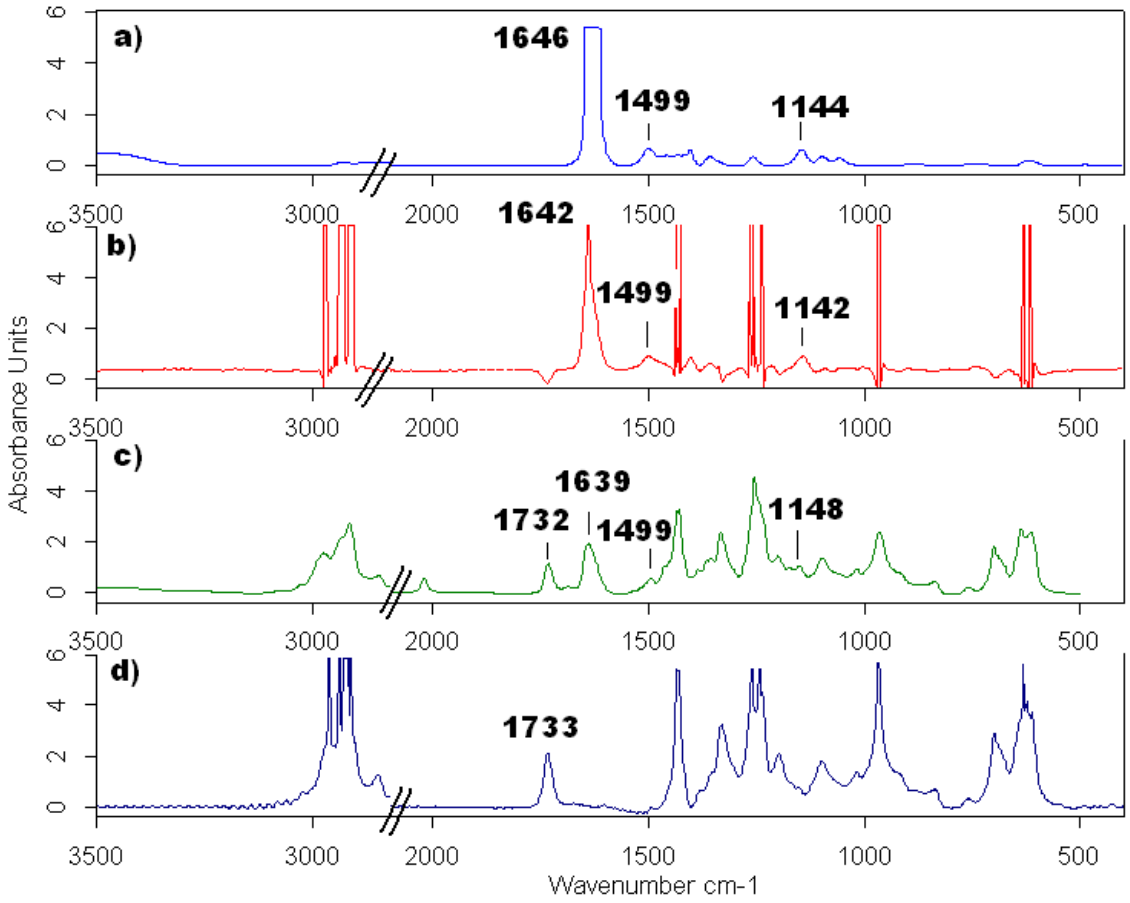

Figure 4.6. IR spectra of a) PDMA, b) PVC-*g*-PDMA (PVC background), c) PVC-*g*-PDMA, and d) PVC.

Figure 4.6 portrays an unique carbonyl absorption around 1640 cm^{-1} for free PDMA[69] and PVC-*g*-PDMA with and without background subtraction. A C-H bending absorption at 1499 cm^{-1} (δ_{as}, CH_3), indicative of the pendant methyl groups attached to tertiary nitrogen, was distinctive in the modified spectrum along with a C-N stretch at 1148 cm^{-1}. With the apparent plasticizer carbonyl absorption and C-Cl stretch in the modified spectrum, it is evident that successful grafting had occurred.

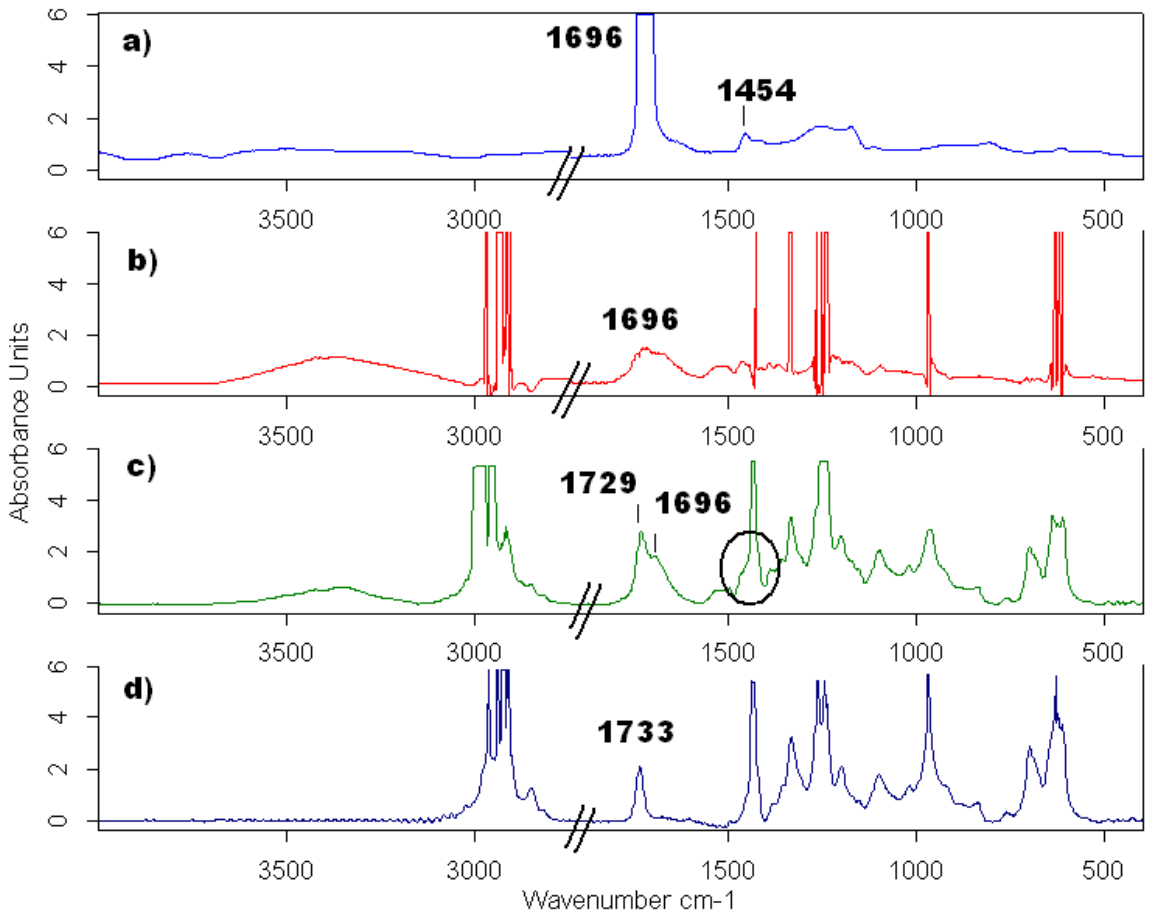

Figure 4.7. IR spectra of a) PAA, b) PVC-*g*-PAA with background subtraction of PVC, c) PVC-*g*-PAA, and PVC.

PAA[70] also demonstrated a unique carbonyl absorption at 1696 cm^{-1} as well as a broad O-H band at 3500 cm^{-1}(Figure 4.7). Asymmetric bending (1454 cm^{-1}) from the CH_2 backbone of PAA was also seen as a shoulder to the PVC C-H stretch in the PVC-*g*-PAA spectrum. Grafting was clearly successful with the presence of hydrophilic polymer and prominent plasticizer carbonyl and C-Cl absorptions in the modified spectrum.

The aromatic structure of P4VP[71] provided unique C-H and ring stretching absorptions above 3000 cm^{-1} and at 1593 cm^{-1} for the free polymer and the PVC-*g*-P4VP spectra with and without background subtraction. Presence of the plasticizer carbonyl

and C-Cl stretch in the modified spectrum provided evidence for effective grafting of P4VP to PVC (Figure 4.8).

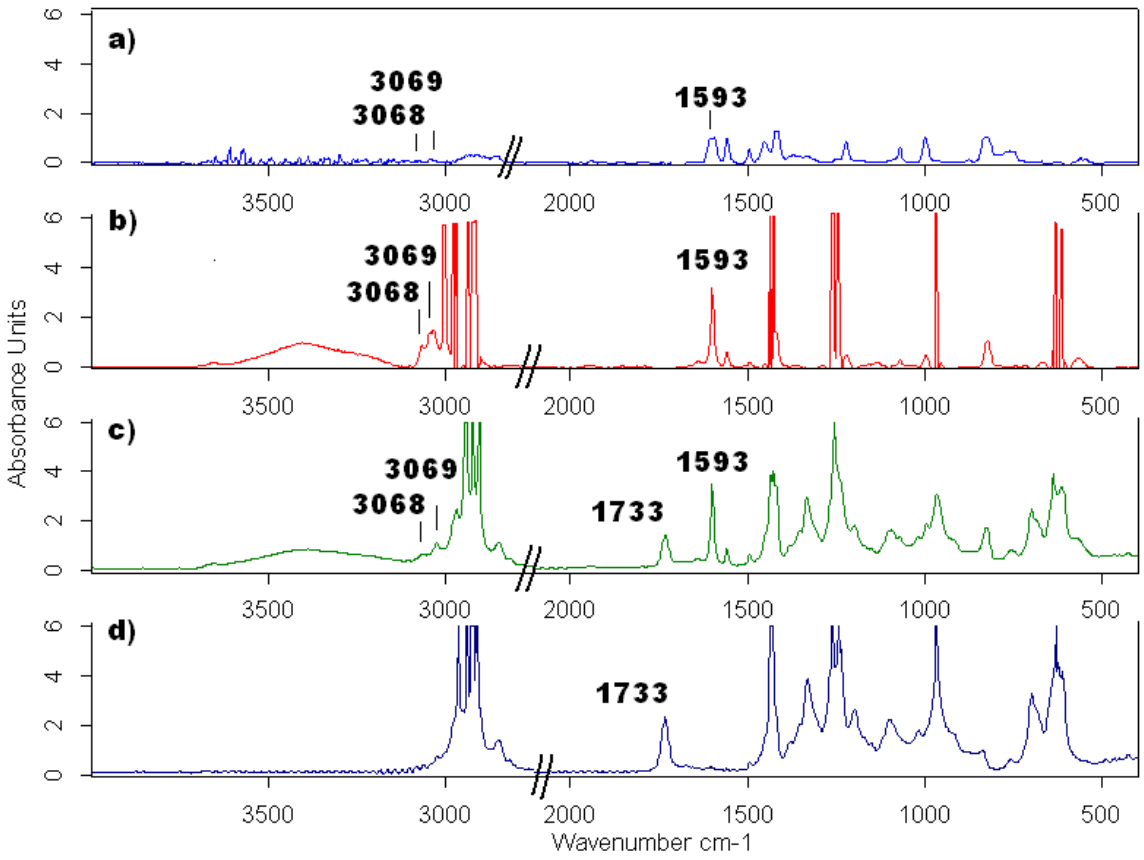

Figure 4.8. IR spectra of a) P4VP, b) PVC-*g*-P4VP with background subtraction of PVC, c) PVC-*g*-P4VP, and PVC.

An overlay spectrum (Figure 4.9) in the range of 1550-1800 cm^{-1} exhibits overlapping and unique carbonyl absorptions for all modified PVC films. In summary, PVC-*g*-PHEMA, PVC-*g*-PHEA and PVC-*g*-PDMAEMA carbonyl absorptions overlapped with the plasticizer carbonyl absorption. PVC-*g*-PAA, PVC-*g*-PDMA and PVC-*g*-P4VP had additional absorptions at 1687 cm^{-1}, 1640 cm^{-1} and 1600 cm^{-1}, respectively. The peak at 1600 cm^{-1} is assigned to an aromatic ring stretch. When PVC-

g-P4VP was quaternized with various alkylating agents, the aromatic ring stretch shifted to 1640 cm^{-1}; These systems are discussed in detail later.

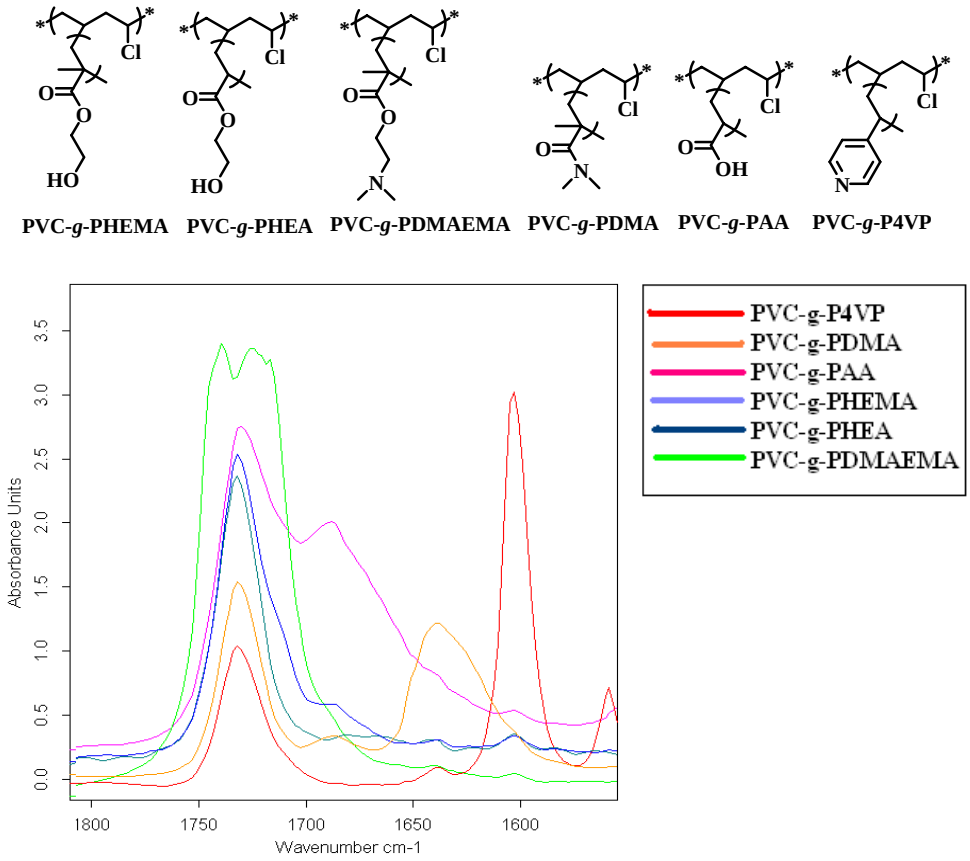

Figure 4.9. Transmission IR spectra of modified PVC films.

4.4 XPS Analysis

Surface characterization with XPS probed the elemental composition roughly 5 nm beyond the film surface with a 45 degree take-off angle. Table 4.2 contains the percentages of oxygen, nitrogen, carbon and chlorine found at 530, 400, 285 and 200 binding eV, respectively; the complete spectra are provided for each sample in Appendix A.

The neat PVC film was found to have the elements C, O and Cl at the surface. The presence of oxygen indicates the presence of plasticizer or oxidized PVC. In

comparison to all modified films, PVC should have a higher Cl percentage at the surface. This was true for PAA (1.9%), PDMA (4.6%), and PDMAEMA (4.4%). However, the presence of any chlorine on the surface implied a non-uniform grafting of hydrophilic polymers, or supported a grafted thickness thinner than the probe depth. In fact, some grafted polymer had higher chlorine surface percentages than PVC, such as PHEMA (6.8%), PHEA (8.5%) and P4VP (8.6%). These results cannot be explained. Regardless, the presence of other elements supports surface grafting.

Table 4.2. XPS data of PVC modified and unmodified films.

Sample Description	C1s %	O1s %	Cl2p %	N1s %	C/O	C/N
PVC	71.0	22.6	6.4	0	3.1	N/A
PVC-*g*-PHEMA	68.1	23.9	6.8	1.2	2.8	56.8
PVC-*g*-PHEA	66.4	23.5	8.5	1.6	2.8	41.5
PVC-*g*-PDMAEMA	73.0	16.4	4.4	0.7	4.5	104
PVC-*g*-PDMA	66.9	25.2	4.6	3.3	2.7	20.3
PVC-*g*-PAA	66.1	31.6	1.9	0.4	2.1	165
PVC-*g*-P4VP[a]	76.0	11.4	8.6	3.6	7.2	21.1

[a] PVC-g-P4VP based on average of Figure A.6 (Appendix A) and Bausch & Lomb data.

All modified films except PVC-*g*-P4VP and PVC-*g*-PDMAEMA showed higher oxygen percentages compared to PVC (22.6%). The most dramatic results obtained were that of PVC-*g*-PAA with an oxygen percent of 31.6, which is expected since other hydrophilic polymers such as PHEMA (23.9%), PHEA (23.5%), and PDMA (25.2%) are esters or amides instead of an acid. It is unknown why PVC-*g*-PDMAEMA (16.4%) has a lower oxygen percent than PVC, unlike for PVC-*g*-P4VP (11.4%) where it is expected due to absence of oxygen in the P4VP chemical structure.

The XPS spectrum of PVC did not contain a peak for nitrogen. However, all modified films displayed a peak at 400 eV which is attributed to AIBN decomposition products. PVC-*g*-PDMA (3.3%), PVC-*g*-P4VP (3.6%) and PVC-*g*-PDMAEMA (0.7%) all displayed higher nitrogen percentages which is expected based on their chemical structures. The major experimental discrepancy from expectation was the low nitrogen value for the PVC-*g*-PDMAEMA system, suggesting a low grafting coverage. The free polymer of PDMAEMA was examined by XPS to see if the same phenomenon occurred (Appendix A, Figure A.12). Unfortunately, the free polymer showed 6% nitrogen at the surface, meaning the grafted spectrum should not undergo conformational rearrangement to shield the nitrogen from the surface (which was one possible explanation).

Although is it difficult to compare the experimental results with theoretical percent calculations due to the unknown concentration of plasticizer or defects, the results support the successful attachment of hydrophilic monomers to PVC.

4.5 Measurement of Grafted Polymer Thickness

Three methods were used to determine thickness: IR calibration, gravimetric analysis and UV-Vis calibration.

4.5.1 IR Calibration Curve.

IR calibration curves were constructed via ellipsometry and transmission IR spectroscopy of hydrophilic polymer films on silicon wafers. The thickness values of the polymer coatings were plotted against the absorbance values obtained from transmission

IR spectroscopy using the Beer-Lambert law. Each polymer was spin cast 5-12 times to obtain sufficient data (Appendix B).

It was imperative to monitor an absorption peak from the hydrophilic polymer spectrum that was unique and not coincident with any PVC absorptions. Therefore, the C-O stretch was used for polymers that had overlapping carbonyl absorptions with PVC unless a background subtraction of PVC was performed on the modified film and the carbonyl peak was only attributed to the polymer graft. Figures 4.10 and 4.11 display a complete spectrum of the PHEMA coatings and an expanded spectrum of the carbonyl peaks of PHEA and PDMAEMA used in the construction of IR calibration curves.

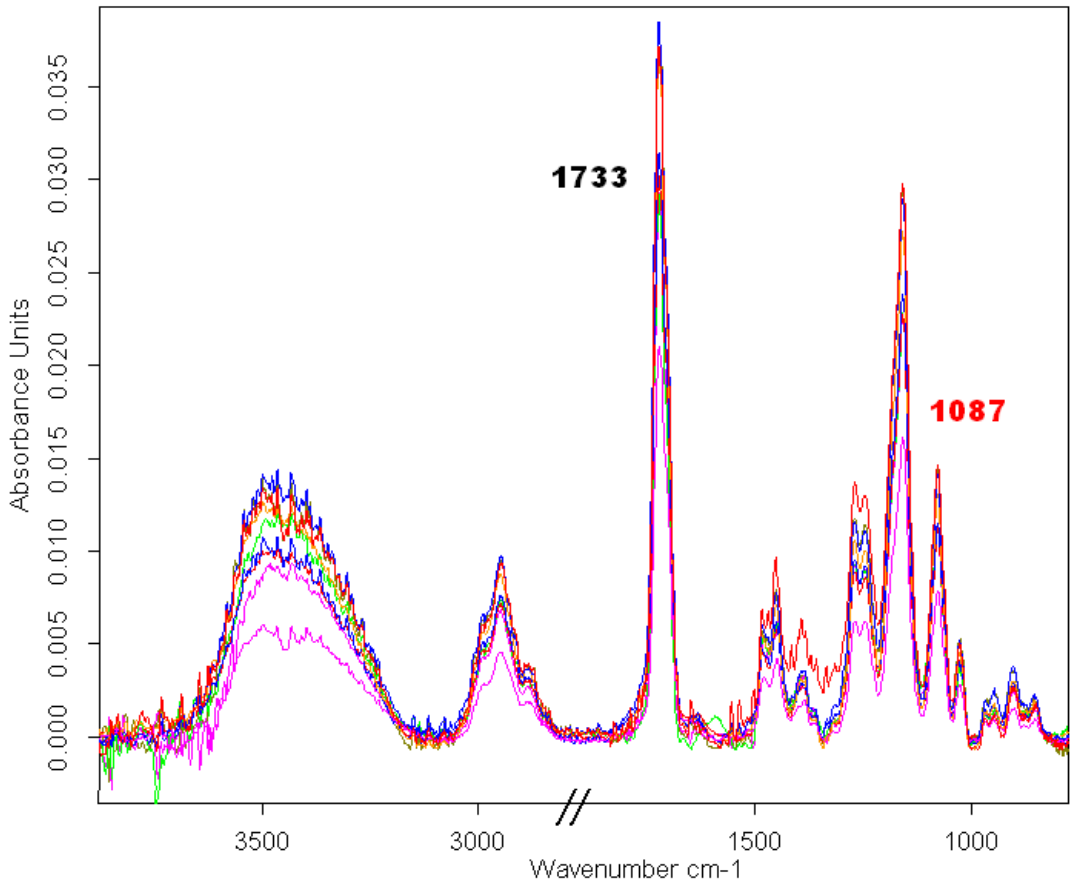

Figure 4.10. IR spectra of PHEMA coatings used in PHEMA IR calibration curve.

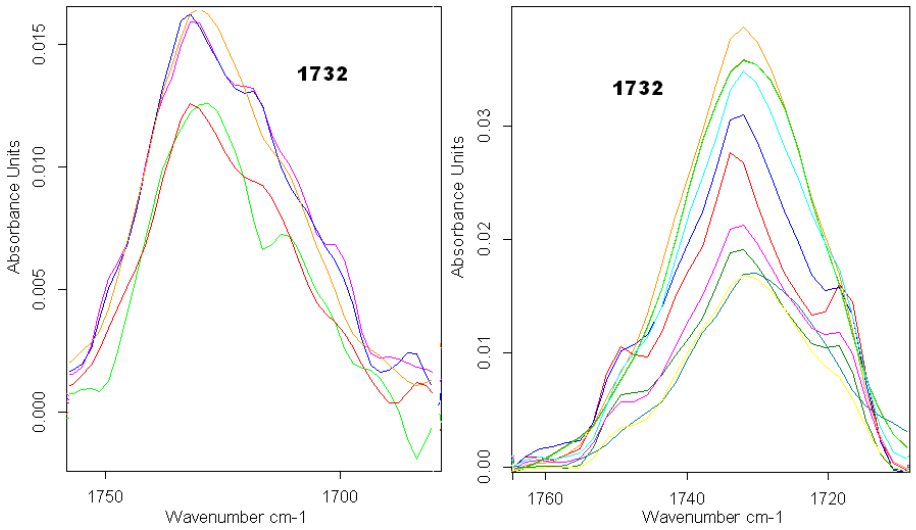

Figure 4.11. Transmission IR spectra of PHEA (left) and PDMAEMA (right) coatings.

Figures 4.12 and 4.13 illustrate two IR calibration curves for PHEMA and PHEA based on the C-O and C=O absorption values from the spectra of PHEMA and PHEA coatings. The equations of the lines were used to calculate thickness (x) of the grafted polymer layer when the absorbance (y) of the modified PVC film was known (Table 4.3). Unfortunately for both modified films, the carbonyl absorbance intensity in the IR spectra with a background subtraction of PVC exceeded the instrumental range. Thus, the C-O peaks at 1078 and 1167 cm^{-1} were used for PHEMA and PHEA calibration curves.

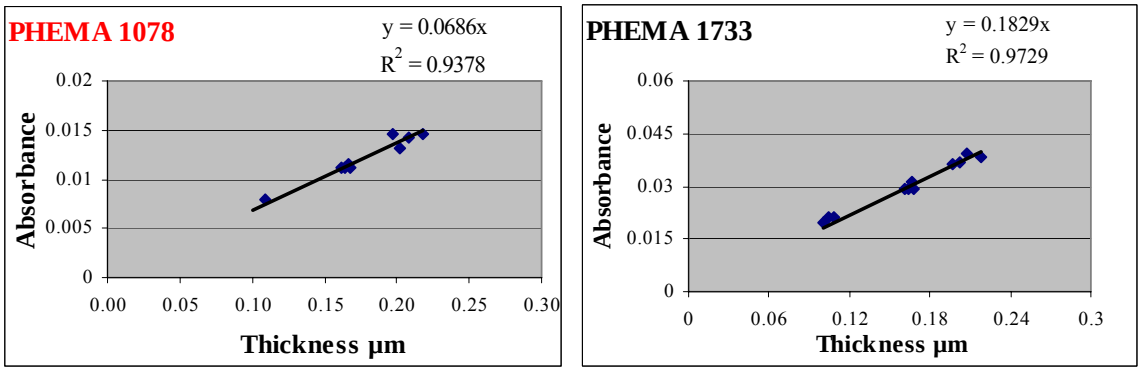

Figure 4.12. PHEMA calibration curves based on absorbance values at 1078, 1733 cm^{-1}.

Table 4.3. Thickness values for grafted layer on PVC as determined by FT-IR calibration.

Sample Description	Equation (μm)[a]	Thickness (μm)[b]
PVC-*g*-PHEMA	y = 0.0686x	28.1 ± 3.6
PVC-*g*-PHEA	y = 0.1363x	13.8 ± 6.1
PVC-*g*-PDMAEMA	y = 0.0863x	14.1 ± 5.0
PVC-g-PDMAEMA	y = 0.2322x	7.2 ± 2.0
PVC-*g*-PAA	y = 0.3887x	2.2 ± 2.5
PVC-*g*-PDMA	y = 0.3565x	1.3 ± 1.2
PVC-*g*-P4VP	y = 0.2852x	5.2 ± 2.7

[a] Equations were a linear regression of thickness (x) vs. absorption (y). [b]Calculation for error shown in Appendix C.

The modified PVC films displayed absorbance values of 3.85 and 3.75 for the C-O stretch of PHEMA and PHEA. The thickness values shown in Table 4.3 were calculated from the calibration curves. Half of this value accounted for the thickness of the hydrophilic graft, since both sides of the film were modified in the reaction. The calculated PHEMA and PHEA grafted thicknesses were 28.1 and 13.8 μm, respectively.

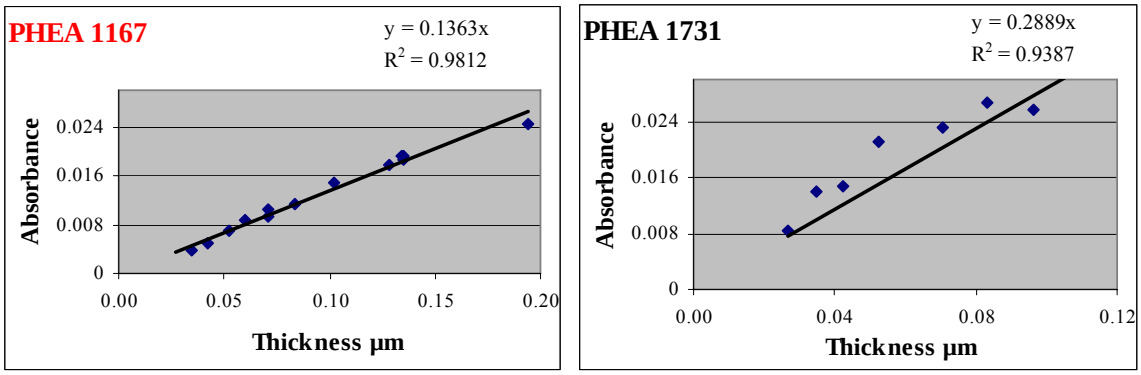

Figure 4.13. PHEA calibration curves based on absorbance values at 1167, 1731 cm^{-1}.

Two calibration curves for PVC-*g*-PDMAEMA were constructed based on the absorbances at 1733 and 1457 cm^{-1} (Figure 4.14). The grafted thickness of PDMAEMA was 7.2 µm for the carbonyl calibration and 14.1 µm for the C-H bend calibration.

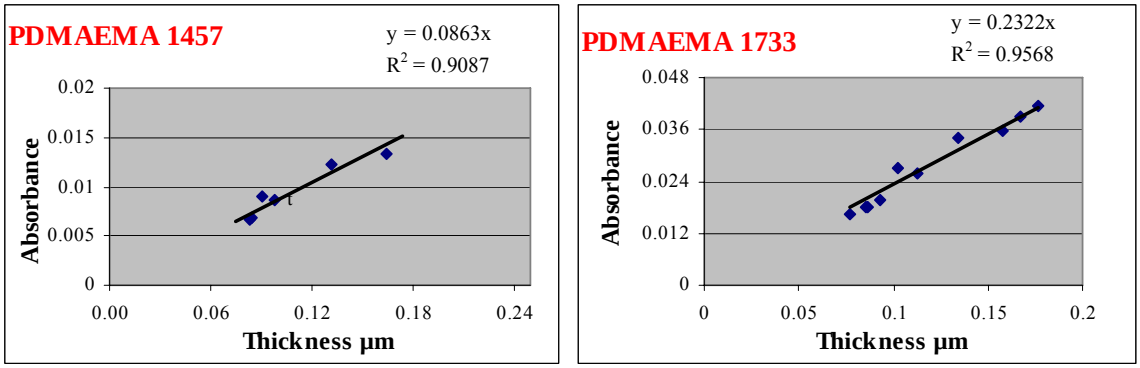

Figure 4.14. PDMAEMA calibration curves based on absorbance values at 1457 and 1733 cm^{-1}.

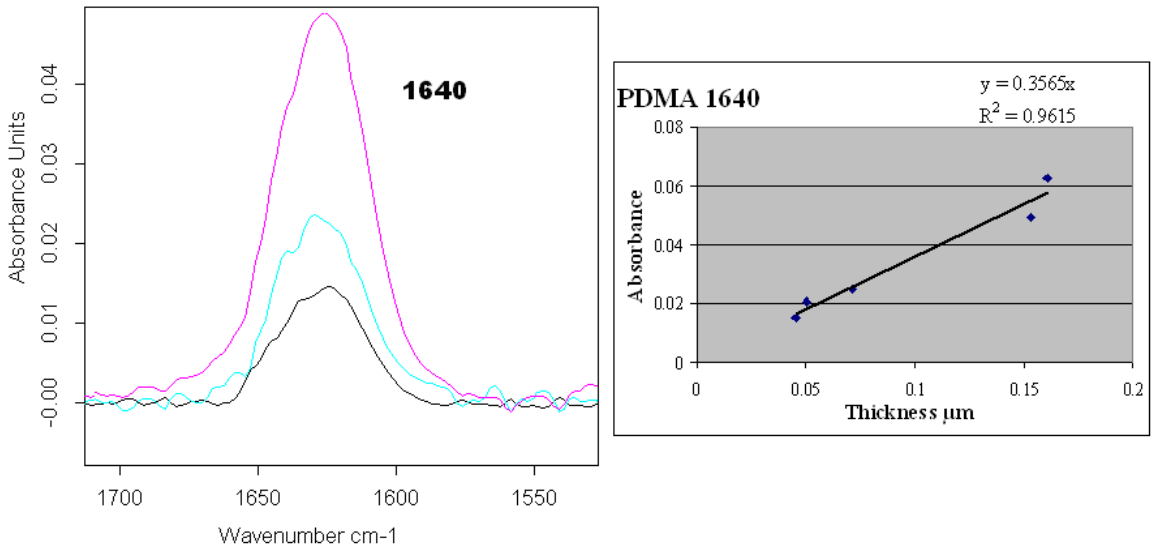

Figure 4.15. IR spectra of free PDMA coatings (left) and thickness vs. absorbance IR calibration curve.

The most unique absorbance of PDMA was the amide carbonyl absorption at 1640 cm^{-1}, which did not overlap with the 1733 cm^{-1} plasticizer absorption; the IR calibration curve for PDMA is shown in Figure 4.15. The carbonyl absorbance value for

PVC-*g*-PDMA was an average of 4 different films with an error of 0.41 AU. This error is rather dramatic since the absorbance value itself was only 0.90 AU. Consequently, the thickness calculated is actually 1.3 ± 1.2μm. We speculate that this large error can be attributed to the non-uniform surface grafting of the polymer.

The carbonyl absorbance for PAA and the aromatic ring stretch for P4VP were used to construct IR calibration curves seen in Figure 4.16. The average absorption for PVC-*g*-PAA at 1687 cm^{-1} was 1.68 ± 0.22 which gave a corresponding thickness of 2.2 ± 0.2 μm. The absorbance for PVC-*g*-P4VP (2.97) gave a calculated thickness of 5.2 μm.

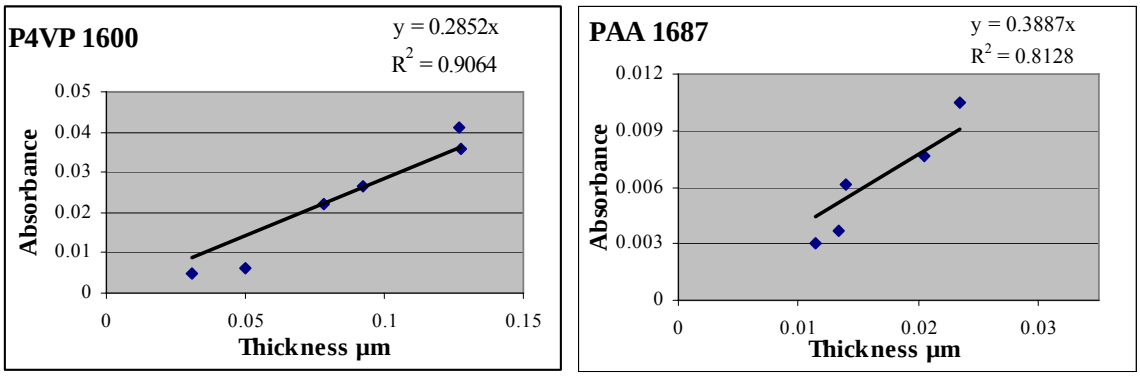

Figure 4.16. IR calibration curve for P4VP and PAA based on aromatic ring stretch and carbonyl absorbance values.

With this technique, grafted films were shown to have thickness values ranging from approximately 1-6 μm for PAA, PDMA, and P4VP and 7-29 μm for PDMAEMA, PHEA and PHEMA. The inaccuracy of this technique deals with changing variables, such as grafting uniformity, thickness of PVC and out of range absorbance values of the modified films in relation to the calibration curve.

4.5.2 Gravimetric Analysis

By determining the weight of the grafted layer, one can calculate the thickness of the grafted polymer since the area is known. Selective dissolution of the modified PVC film with a good solvent for PVC and a poor solvent for the hydrophilic polymer allowed collection of the hydrophilic grafted polymer.

For example, a film of PVC (78.5 cm^2) underwent the simple two step grafting polymerization with HEMA. The modified film was weighed (1.954 g) and placed into 150 mL of THF, where the PVC chains that were not covalently bonded to PHEMA dissolved while the PHEMA covalently grafted to PVC chains did not. The solids were collected upon centrifugation, dried and weighed (0.343 g). The thickness of the grafted PHEMA was then calculated from the following equation:

$$(W \times \rho^{-1} \times A^{-1}) /2 = H \quad (3)$$

where W = weight of PVC chains grafted to hydrophilic polymer, ρ = density of the hydrophilic polymer, A = area of film and H = thickness of hydrophilic graft. The factor of ½ is necessary because the weight is associated with the weight of grafted chains on both sides of the film.

Transmission IR spectroscopy was performed on the collected solution and the solid that were separated upon selective dissolution of the PVC-*g*-PHEMA film. The IR spectrum of the solution, which was thought to contain only PVC chains, and the spectrum of the PVC starting material are nearly identical as seen in Figure 4.17. This supports successful separation of the hydrophilic grafted layer. The collected solid was used to verify that PHEMA was present and grafted to PVC.

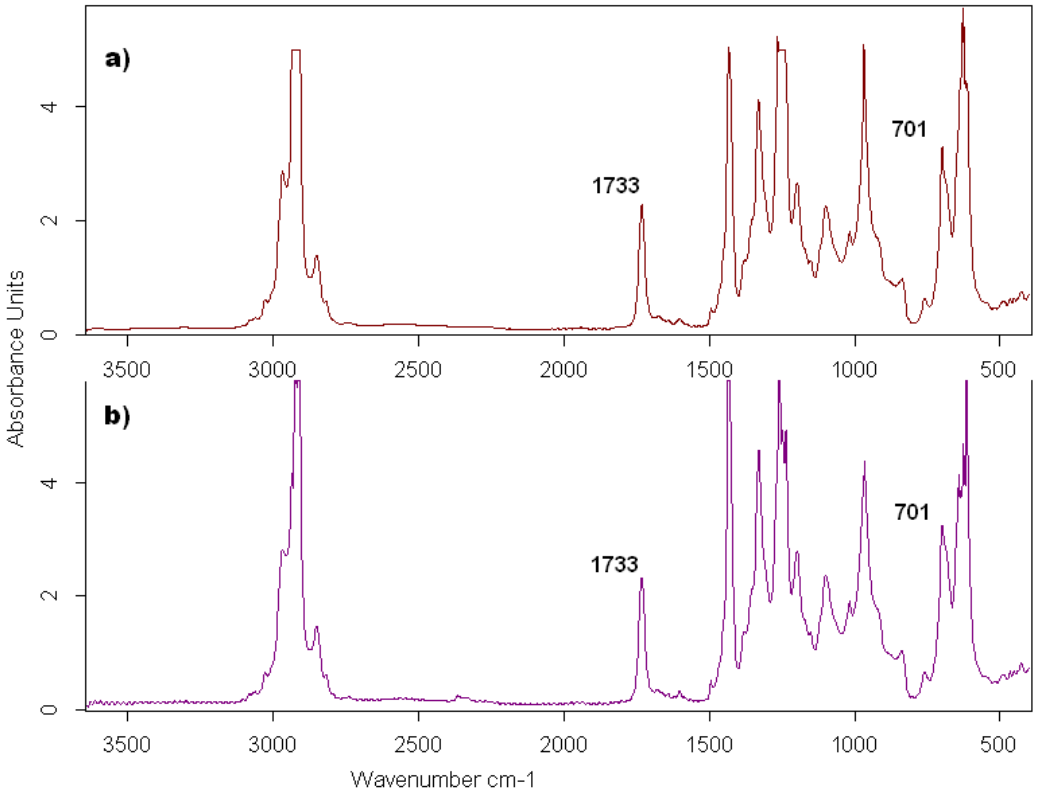

Figure 4.17. Comparison of IR spectra: a) the collected PVC from the selective dissolution of PVC-*g*-PHEMA, evaporated onto a salt plate and b) neat PVC film.

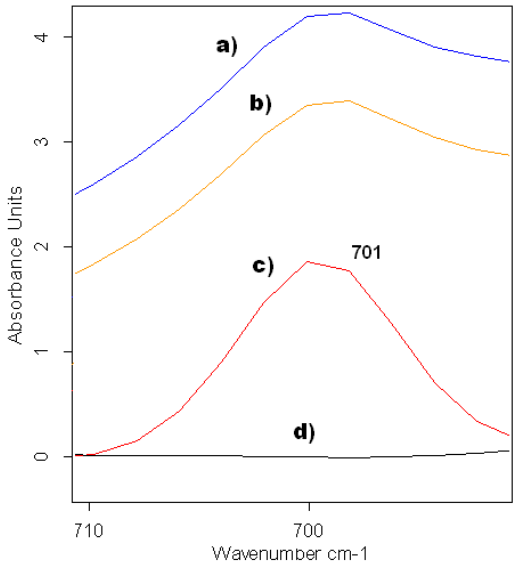

Figure 4.18. C-Cl IR absorption spectra for a) PVC-*g*-PHEMA, b) PVC from PVC-*g*-PHEMA selective dissolution, c) collected PHEMA-*g*-PHEMA grafted to PVC from selective dissolution and d) PHEMA from polymerization reaction.

Figure 4.18 exhibits three spectra that showed a C-Cl absorbance at 701 cm^{-1}, and one which didn't. Spectrum **a** represents the modified PVC-*g*-PHEMA film, spectrum **b** represents the PVC that was collected by selective dissolution and spectrum **d** displays PHEMA. PHEMA did not show an C-Cl absorption. Most importantly, spectrum **c** which represents the solid that was collected in dissolution does have an C-Cl absorption as well as peaks unique to PHEMA (not shown) thus providing evidence for the successful grafting of PHEMA to PVC.

Table 4.4 identifies the solvent used for selective dissolution, the area and weight of the grafted chains and the calculated thickness values. Even though the thickness value should be greater than the thickness value via IR spectroscopy (because this method includes the grafted PVC), they are comparable for the PHEMA, PHEA, PAA and P4VP systems.

Table 4.4. Thickness values for grafted layer as determined by gravimetric analysis.

Sample Description	Solvent[a]	Area (cm^2)[b]	Weight (g)[c]	H Gravimetric (μm)[d]	H IR (μm)
PVC-*g*-PHEMA	THF or MEK	92.09	0.34	16.2 ± 0.1	28.1
PVC-*g*-PHEA	MEK	63.57	0.13	8.7 ± 0.1	13.8
PVC-*g*-PAA	MEK	78.47	0.09	4.79 ± 0.07	2.2
PVC-*g*-PDMA	cyclohexanone	75.83	0.45	26.0 ± 0.2	1.3
PVC-*g*-P4VP	MEK	114.62	0.17	6.38 ± 0.07	5.2

[a]The solvent used for selective dissolution in gravimetric analysis. [b]The area of the modified film before gravimetric analysis. [c]The weight of the collected insoluble material upon selective dissolution. [d]Error calculated by propagation (Appendix B).

4.5.3 UV-Vis Calibration

The UV-Vis spectrum for P4VP exhibited an absorbance at 267 nm for the pyridine ring. Solutions ranging in concentration from 0 to 0.15 mg/mL were prepared. The calibration curve is shown in Figure 4.19. Based on an observed absorbance of 0.983, the calculated thickness for the grafted P4VP was 18.5 μm (Appendix C). The thickness of other modified PVC films could not be determined by this technique because the polymers absorb in the same range as the solvent.

Determination of the thickness of the grafted layer on PVC was challenging. While agreement between the IR spectroscopy and gravimetric methods was reasonable in all cases, the two methods indicate that a typical graft layer thickness is in the range of 1- 30 μm. The layer thicknesses for the PVC tubing are in the range of 23-100 μm (Section 4.9).

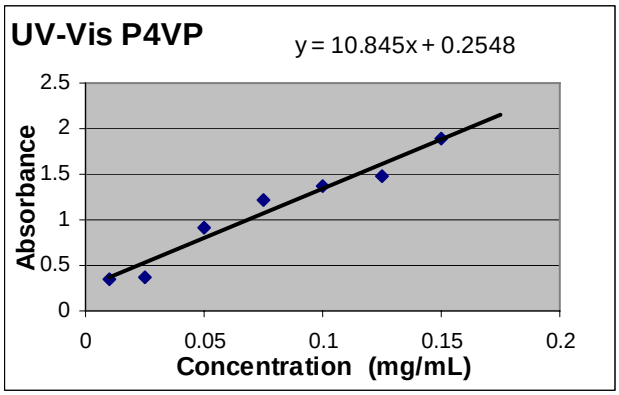

Figure 4.19. UV-Vis calibration curve for P4VP.

4.6 Coating of Hydrophilic Polymers to PVC

Because the thickness observed was not in the typical nanometer range of grafted polymers, a coating experiment was performed to verify that no free polymer had penetrated the surface of PVC accounting for the unexpectedly large results. PHEMA

and P4VP were added to a separate flask that contained a sample of PVC film and MeOH. The hydrophilic polymer dissolved as the mixture stirred at 70 °C under nitrogen overnight. Samples were subsequently cleaned by the same procedure as before.

Comparison of the IR spectra for the PVC film before and after the PHEMA coating experiment showed a discrepancy in the appearance of an O-H bend at 3300 cm^{-1} (not shown); however, this is attributed to the exposure to MeOH and insufficient drying since there was no C-O peak present at 1078 cm^{-1} after coating (Figure 4.20). Similarly, the P4VP coating experiment failed to show a discrepancy at 1600 cm^{-1} or above 3000 cm^{-1} (aromatic C-H stretching) as seen in the comparison of IR spectra for the potentially coated film, PVC and PVC-*g*-P4VP (Figure 4.21). The contact angle measurements after coating for PHEMA were 76± 2 (s), 79 ± 2(a), 67 ± 4(r) which correspond to uncoated PVC. Measurements confirm that these hydrophilic polymers do not adsorb onto PVC.

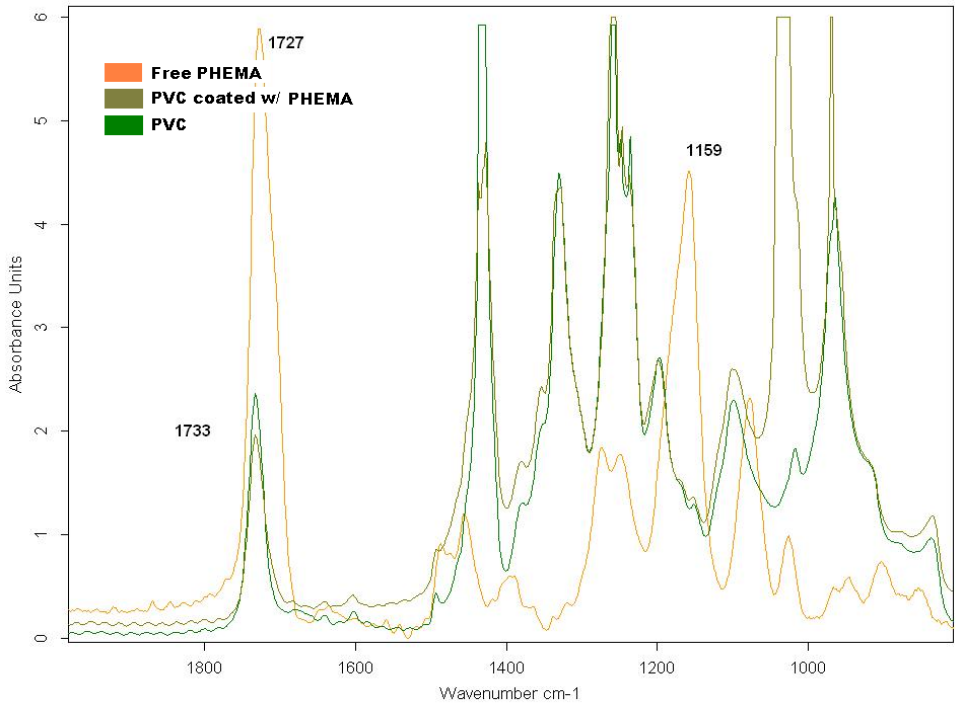

Figure 4.20. IR spectra of the PVC film after coating experiment with PHEMA (peach), PVC-*g*-PHEMA (brown) and PVC (green).

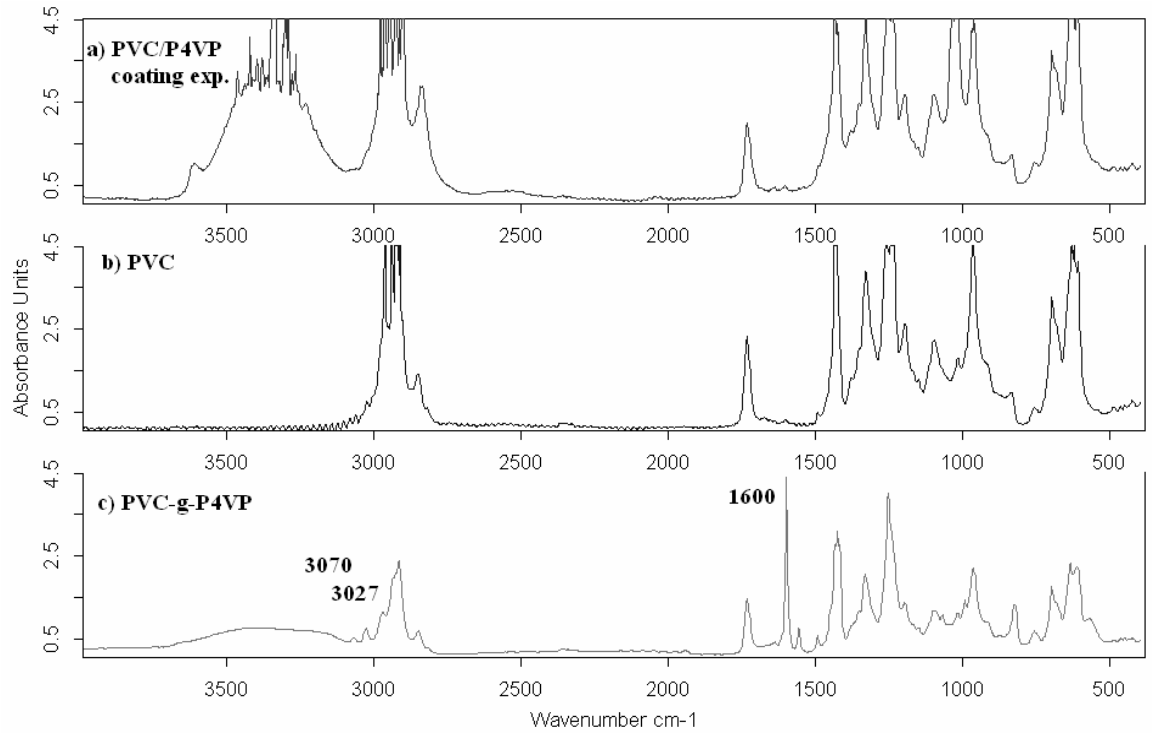

Figure 4.21. IR spectra of a) PVC after coating experiment with P4VP, b) PVC and c) PVC-*g*-P4VP.

4.7 Surface Roughness of PVC

Figure 4.22 displays the surface roughness between unmodified PVC and PVC-*g*-PHEA. We speculate that the small clusters account for the increased roughness. We attribute these clusters to grafted polymer. The rms roughness for the PVC-*g*-PHEA sample was 35 nm compared to 18 nm for untreated PVC.

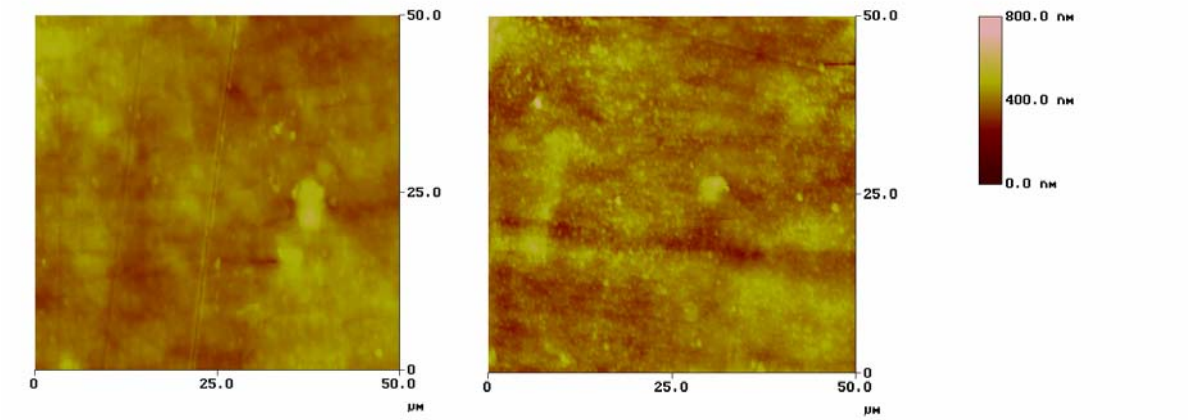

Figure 4.22. AFM images of untreated PVC (left) and PVC-*g*-PHEA (right).

4.8 Evidence for Covalent Attachment

Characterization methods used to prove covalent attachment were: transmission IR spectroscopy, GPC and elemental analysis. Transmission IR spectra were recorded on the starting materials, polymer and modified PVC films to substantiate covalent attachment by observation of key functional groups as seen in Chapter 4.3. GPC and elemental analysis were performed on the PVC-*g*-PHEMA sample collected during selective dissolution for gravimetric analysis. For the PHEMA modified system, bulk PVC chains were soluble in THF while the PVC-*g*-PHEMA chains remained insoluble. Also, the controlled radical experiment was consistent with radical generation at the surface of PVC.

4.8.1 Gel Permeation Chromatography

The chromatograms of PVC starting material, free PHEMA, free P4VP, PVC-*g*-PHEMA and PVC-*g*-P4VP were obtained. Figure 4.23 shows the chromatogram for the PVC sample in THF, M_n = 40,700 g/mol.

The PVC-*g*-PHEMA sample collected by selective dissolution was analyzed in DMF (Figure 4.24a) and compared with free PHEMA (Figure 4.24b). Both peaks have a broad distribution and a shoulder which is attributed to uncontrolled free radical polymerization. The M_n of free PHEMA was 23,000 g/mol while that of the PVC-*g*-PHEMA was 85,000 g/mol. The M_n of PVC-*g*-PHEMA should exceed the sum of the M_n for PVC and free PHEMA (63,700g/mol), assuming the molecular weight of free PHEMA is similar to that of the grafted PHEMA. The peak at 66 million g/mol for PVC-*g*-PHEMA far exceeds our expectations and at the time of this writing, we do not have a plausible explanation.

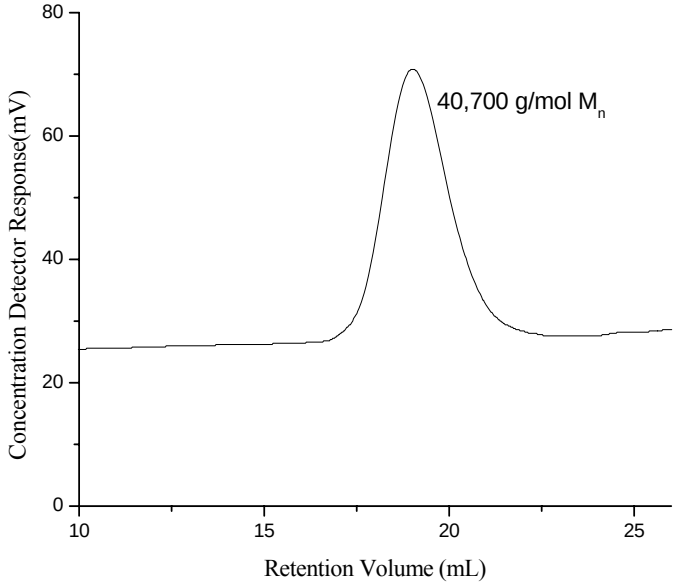

Figure 4.23. GPC chromatogram of unmodified PVC, M_n = 40,700 g/mol.

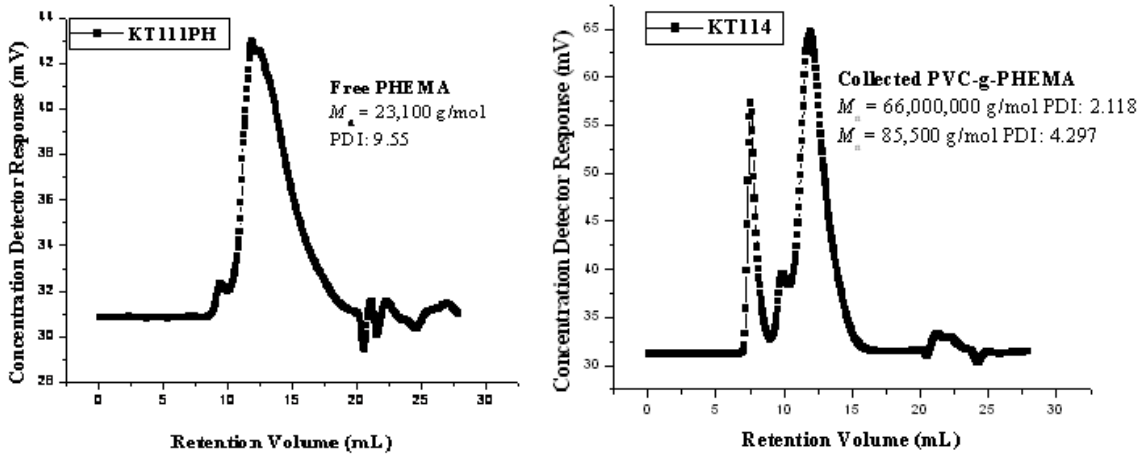

Figure 4.24. GPC chromatogram of a) free PHEMA and b) PVC-*g*-PHEMA collected by selective dissolution.

The sum of the M_n for free P4VP (13,800 g/mol) and PVC (40,700 g/mol) is 54,500 g/mol which is reasonably close to the actual M_n of PVC-*g*-PHEMA (59,500 g/mol). Abnormally high molecular weight peaks were also seen for free P4VP and collected PVC-*g*-P4VP (Figure 4.25) at 309,000,000 and 1,410,000 g/mol and 123,000,000 and 1,860,000 g/mol, respectively, which are not associated with the free polymer or grafted sample.

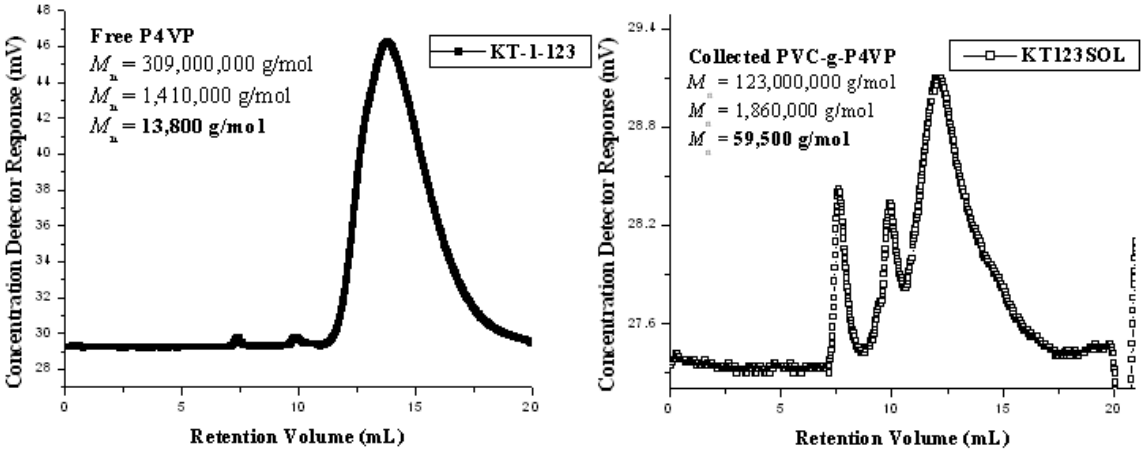

Figure 4.25. GPC chromatograms of free P4VP (left) and PVC-*g*-P4VP collected by selective dissolution (right).

The ambiguous high molecular weight peaks found in PVC-g-PHEMA, P4VP and PVC-g-P4VP are most likely artifacts of the particular analysis. Such high molecular weights with sharp peaks are usually attributed to crosslinked polymer. However, all samples were filtered before injection and the sample appeared to completely dissolve into solution. Also, since the P4VP and PVC-g-P4VP system had similar high molecular weights (at differenct concentrations) in both chromatograms, it is possible that the contaminants were coming from the column. Regardless, the GPC chromatograms offered additional support for covalent grafting of PVC, since in several examples, the M_n of the collected hydrophilic polymer was similar to the sum of the M_n of the free polymer and PVC starting material.

4.8.2 Elemental Analysis

The elemental analysis of the PVC-*g*-PHEMA collected by selective dissolution revealed 57.83% carbon, 8.00% hydrogen, <0.5% nitrogen, 29.76% oxygen and 1.67% chlorine. If the sample were PHEMA alone, the expected percentages would be 54.95% carbon, 8.45% hydrogen and 36% oxygen. The increase in carbon and chlorine percentages in addition to the decrease in oxygen and hydrogen percentages is consistent with both vinyl chloride and HEMA units being present in the isolated material.

4.9 Grafting Inside PVC Tubing

The graft polymerization of hydrophilic monomers HEMA, HEA, AA, DMA and 4VP from PVC tubing was conducted using a simple two step process: 1) physisorption

of a hydrophobic free radical initiator (AIBN) onto the surface of PVC, followed by 2) radical polymerization in hydrophilic media (Scheme 4.3).

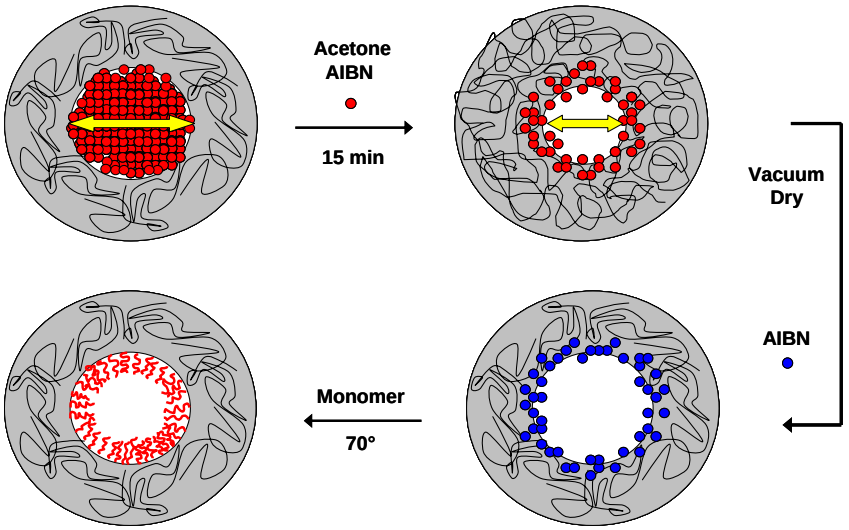

Scheme 4.3. Simple 2-step grafting of hydrophilic polymer to the interior of PVC tubing.

The interior of PVC tubing was first filled with initiator solution for 15 minutes. The inner diameter shrunk as PVC swelled in acetone and the chains expanded, increasing the free volume in the tubing. Upon drying, the initiator remained trapped at or near the surface. Next, the tubing was filled with a monomer solution and heated at 70 degrees for 24 hours with MeOH as solvent. As a result, hydrophilic polymer chains were grafted to the interior walls of the tubing. The modified PVC tubing was characterized by capillary rise and gravimetric analysis, since transmission IR spectroscopy of the tubing was not possible.

4.9.1 Capillary Rise

The Young-LaPlace equation below describes the phenomenon of capillary rise

$$\gamma = \Delta\rho \, g \, h \, r \, / \, 2 \cos \theta \qquad (4)$$

where θ is the contact angle, Δρ (g cm^{-3}) is the density difference of the liquid and air, g (cm s^{-2}) is the acceleration due to gravity, h (cm) is the rise of the liquid, r (cm) is the radius of the tube and γ (g s^{-2}) is the air-liquid surface tension. Ethylene glycol was used for unmodified PVC and PDMA, P4VP and PAA modified tubing. Water was used for PHEMA modified PVC tubing.

Table 4.5. Water contact angles and thickness values for modified PVC tubing.

Sample Description	Probe Fluid[a]	h (cm)[b]	θ°[c]	Thickness (μm)[d]
PVC-*g*-PHEMA	Deionized water	0.41	59	23 ± 1
PVC-*g*-PHEA	ethylene glycol	N/A	N/A	36.6 ± 0.7
PVC-*g*-PAA	ethylene glycol	0.68	52	58.6 ± 0.7
PVC-*g*-PDMA	ethylene glycol	0.70	50	99.8 ± 0.7
PVC-*g*-P4VP	ethylene glycol	0.80	43	59.4 ± 0.7
PVC	ethylene glycol	0.13	83	N/A

[a]The solvent used as the probe fluid with capillary rise. [b]The height at which the eluent rose measured from the liquid vapor surface to the meniscus. [c]The angle at which the solvent met the wall, calculated via the Young-LaPlace equation. [d]Propagation Error (Appendix B).

The decrease in contact angle (Table 4.5) of all modified PVC tubings relative to unmodified PVC indicates increased surface wettability that is comparable to modified flat PVC films. For example, the water contact angle of 59° for PVC-*g*-PHEMA tubing is relatively close to the film contact angle of 57°.

4.9.2 Gravimetric Analysis

Similar to the procedure of film gravimetric analysis, a piece of modified tubing was immersed in a specific solvent for selective dissolution of unmodified PVC chains.

The PVC chains that were covalently attached to the grafted polymer were collected by centrifugation, dried and weighed. The weight can be converted to volume and the volume of the grafted hydrophilic polymer is equivalent to:

$$V = \pi h [(r_{outer})^2 - (r_{inner})^2], \quad (5)$$

where r_{inner} is the radius of the modified PVC tube and r_{outer} is the radius of the initial unmodified PVC tube. Upon dissolving the PVC-*g*-PHEMA tube into THF, the bulk PVC chains went into solution while the PHEMA covalently bound to PVC chains did not. Figure 4.26 depicts the PVC-*g*-PHEMA tube after immediate immersion into THF. We speculate that the opaque inner surface represents the modified surface of the PVC tubing while the transparent part of the tubing, which dissolved completely after 5 minutes, represents bulk unmodified PVC chains. After dissolution, the solid sample was collected by centrifugation, dried and weighed. Film thickness values are listed in Table 4.5.

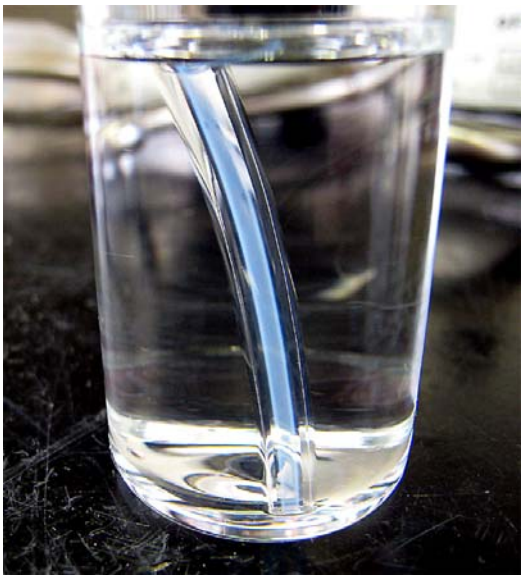

Figure 4.26. Picture of PVC-*g*-PHEMA tube in THF. The inside of the tube appears white because the PHEMA that is grafted to the interior chains is not soluble in THF.

The PVC-*g*-PDMA tubing gave a gravimetric thickness result for the grafted chains that was analogous to digital microscopic measurements. Without solvent, the PDMA graft appeared opaque in visible light, while the PVC tubing remained transparent. Figure 4.27 displays the same phenomenon of two distinct layers with different refractive indices for PVC-*g*-PDMA and PVC. The inner grafted layer (white) is slightly less than the scale bar measurement of 100 µm, similar to its gravimetric measurement of 99.8 µm.

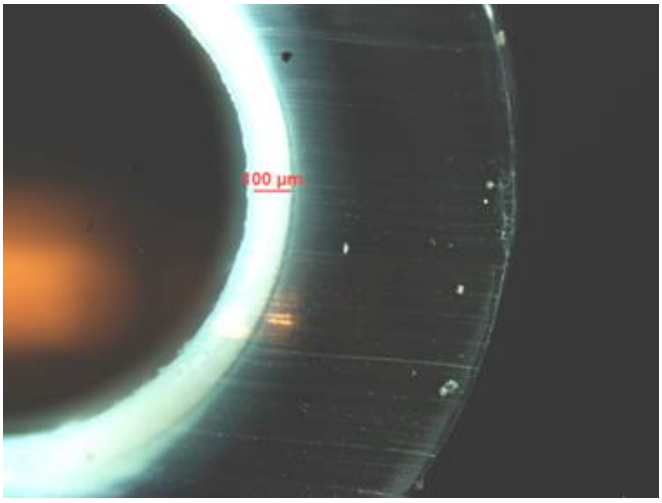

Figure 4.27. Digital microscopic image of PVC-*g*-PDMA in air; the inner white layer represents PDMA grafted chains with approximately 100 µm thickness.

4.10 Plasticizer Migration of Unmodified and Modified PVC films

Initially the migration of the plasticizer from the control was examined by directly immersing the unmodified PVC into hexanes and following the absorbance maximum at 278 nm with time. In only 3 days the absorbance was above an absorbance value (AU) of 3 (Figure 4.28). The control was compared to the amount of plasticizer detected from the PVC-*g*-PHEA, PVC-*g*-PHEMA, and PVC-*g*-PDMA samples which were all below 0.66 AU after one week, as seen in Table 4.6. The large difference is deceiving since it is probable that plasticizer was lost upon initiator deposition, where the 15 minutes swelling

time of the film in acetone prompted plasticizer mass transfer. Therefore, a more accurate comparison would require the use of a control that was exposed to acetone for the same amount of time as the modified films.

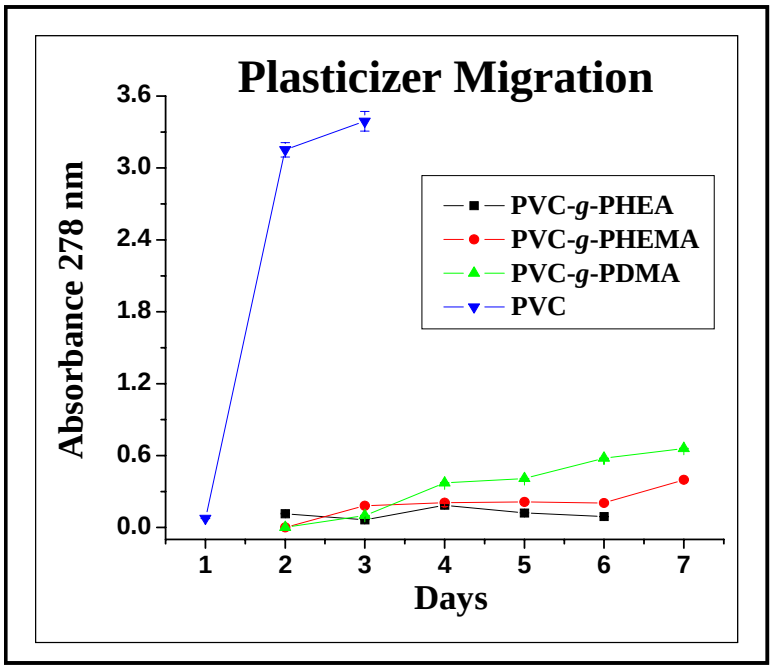

Figure 4.28. Plot of absorbance units at 278 nm for plasticizer extracted from PVC-*g*-PHEA, PVC-*g*-PHEMA, PVC-*g*-PDMA and PVC into hexanes at RT over 7 days.

Table 4.6. Absorbance (AU) data for plasticizer leaching from PVC and modified films.

Day	PVC	PVC-*g*-PHEA	PVC-*g*-PHEMA	PVC-*g*-PDMA
1	0.076 ± 0.001	0	0	0
2	3.152 ± 0.060	0.115 ± 0.003	0	0
3	3.389 ± 0.082	0.064 ± 0.001	0.183 ± 0.007	0.100 ± 0.002
4	N/A	0.187 ± 0.001	0.207 ± 0.002	0.372 ± 0.003
5	N/A	0.122 ± 0.001	0.213 ± 0.003	0.408 ± 0.001
6	N/A	0.091 ± 0.001	0.206 ± 0.001	0.578 ± 0.001
7	N/A	N/A	0.398 ± 0.004	0.659 ± 0.003

The next control was PVC that had been exposed to acetone for 15 minutes. This was a more accurate comparison to films that underwent initiator deposition for 15 minutes. We observed that most of the plasticizer was extracted from the PVC in 15

minutes (Figure 4.30), in part due to the extreme swelling of PVC in acetone (142%). This would in theory leave PVC two void areas of plasticizer sandwiching plasticized PVC. The time it takes for the plasticizer to pass through the void a distance d_L and reach the surface is t_L. Figure 4.29 demonstrates the theoretical picture of plasticized PVC after exposure to the initiator solution and the effect of exposure time on t_L. The film on the left represents exposure to the initiator solution for a longer time than the film on the right. It has more void area, as well as a larger d_L and t_L value.

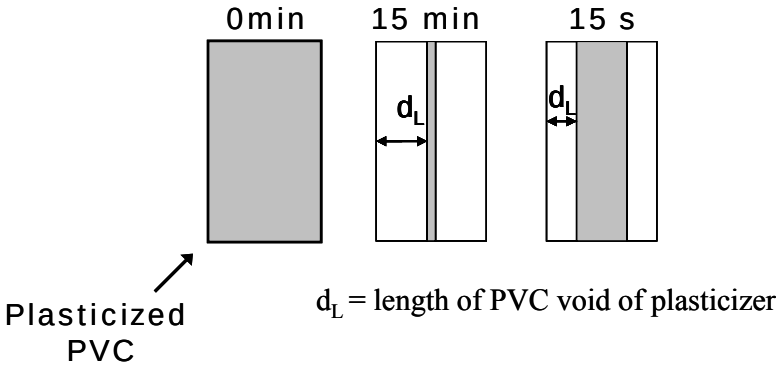

Figure 4.29. Plasticized PVC (grey) sandwiched by non-plasticized PVC (white); the film to the left was exposed longer to the initiator solution than the film to the right.

The extraction was continued for over 30 days to determine the effect of time on migration. It was speculated that after the lag time (t_L) the plasticizer absorbance value would drastically increase and eventually plateau which was observed for PVC.

Figure 4.30 displays a small jump in absorption from 0.031 (day 5) to 0.152 (day 8) which may be the critical time after t_L at which the majority of bulk plasticizer had diffused into the media. The absorbance of the plasticizer then reached a plateau after 31 days and never rose higher than 0.223 AU, meaning only 6.5 % of the plasticizer was left behind in the bulk PVC after being exposed to acetone for 15 minutes. This percentage was based on the absorbance of plasticizer extracted from unmodified and untreated PVC

(3.389 AU, Appendix B). Also, the observed absorbance units corresponding to extracted plasticizer were less for PVC than the modified samples, meaning more plasticizer was left behind in the PVC after acetone exposure and the grafted layer was not an effective barrier to plasticizer mass transfer.

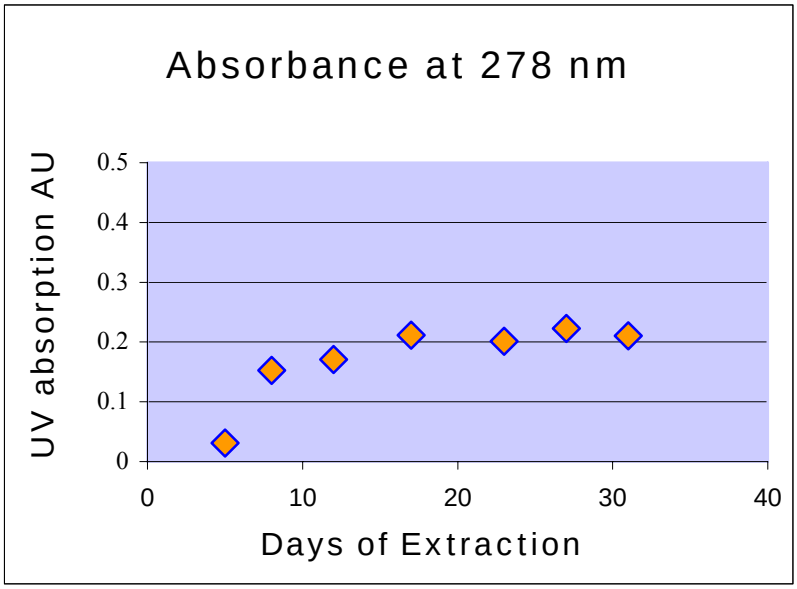

Figure 4.30. Plot of absorbance units of plasticizer at 278 nm for control PVC exposed to acetone for 15 minutes before extraction in hexanes at RT for 31 d in a closed cuvette.

Therefore, a new testing protocol was implemented. Because less than 7% plasticizer was retained in the PVC sample upon 15 minutes acetone immersion and polymerization, immersion times were reduced to 15 seconds to maximize the amount of residual plasticizer in the control and modified films. The plasticizer extracted with hexanes from this control gave an absorbance unit of 0.435, meaning only 12.7% of the plasticizer was retained in the sample after 15 seconds of immersion time in acetone (Figure 4.33). The percentage was again based on the plasticizer absorbance for unmodified and untreated PVC (3.389, Appendix B). This control was compared to samples modified with 15 seconds initiator deposition times.

Before the migration study was performed, characterization was necessary to prove that polymerization was effective after only 15 seconds initiation (fast dip) and that the grafted layer was of similar thickness to that of the modified films that underwent immersion in initiator solution for 15 minutes. The IR spectrum of the fast dip PVC-*g*-PDMA showed the presence of both PVC and PDMA absorptions (Figure 4.31). The peak at 1639 cm^{-1} gave an absorbance of 2.661 AU which corresponds to a thickness of 7.5 μm based on the IR calibration method discussed previously (Figure 4.15). This thickness value was close to that of the modified film that was exposed to the initiator solution for 15 minutes (1.3 μm, Table 4.3). Gravimetric analysis gave the weight of the grafted layer to be 0.3755 g which corresponds to a 38.8 μm thickness, a close value to the gravimetric thickness of the modified PVC-*g*-PDMA film that underwent immersion in initiator solution for 15 minutes (26 μm, Table 4.4).

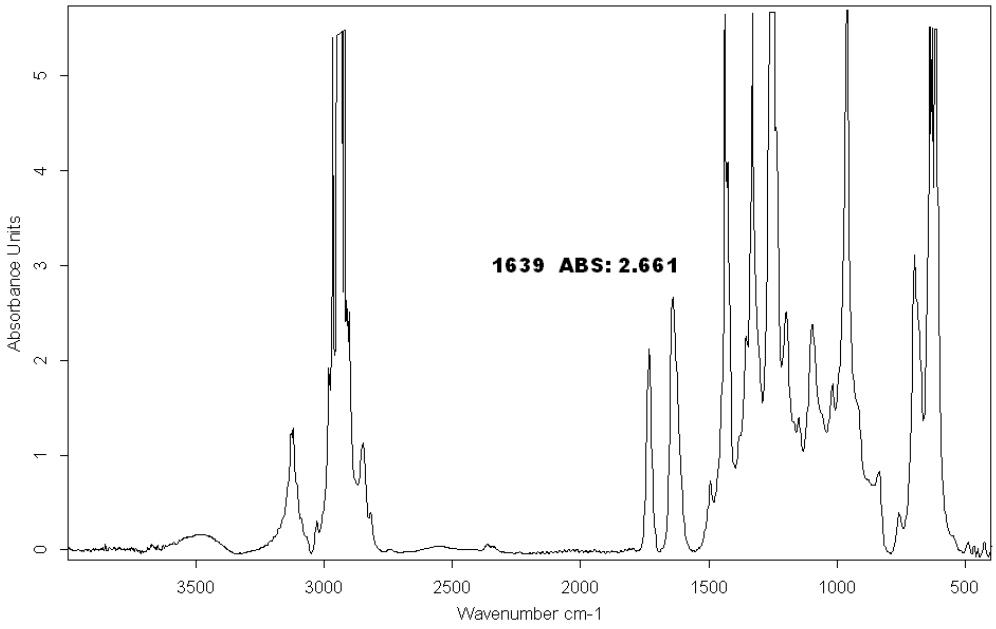

Figure 4.31. IR spectrum of PVC-*g*-PDMA with fast dip initiator deposition (15 s).

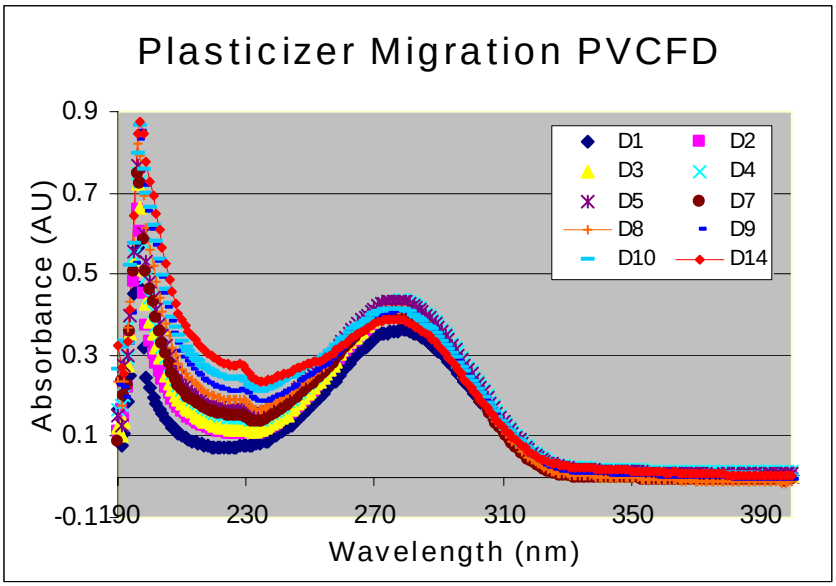

Figure 4.32. UV-Vis spectra of plasticizer extracted from PVC (FD acetone) in hexanes over two weeks in a closed cuvette. The letter D signifies days of extraction.

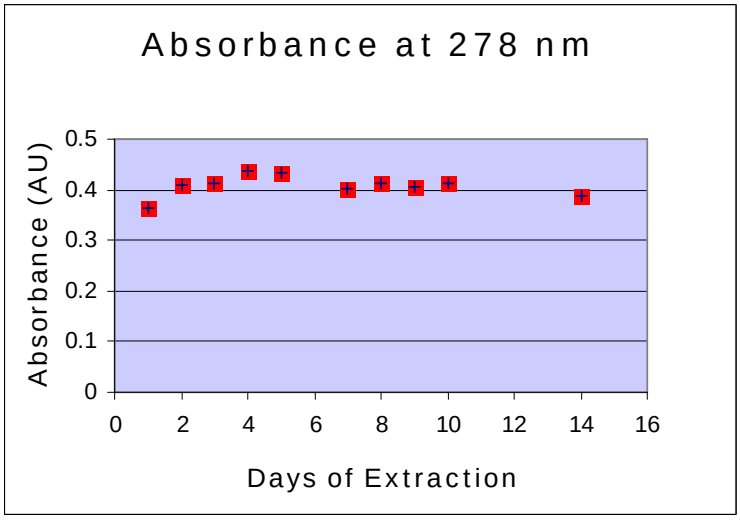

Days	AU (278 nm)
1	0.362
2	0.411
3	0.411
4	0.435
5	0.434
7	0.402
8	0.414
9	0.407
10	0.412
14	0.387

Figure 4.33. Plot of plasticizer AU at 278 nm vs. days of extraction in hexanes for the control PVC (15 seconds) over two weeks in a closed cuvette.

The migration study compared two systems that underwent fast dip (FD) immersion, PVC-*g*-PDMA and PVC-*g*-P4VP, with the control PVC fast dipped in acetone for 15 seconds. The control PVC, which was exposed to hexanes for 2 weeks, leached the most plasticizer in the first day, indicating a small t_L. Figure 4.32 displays

the UV-Vis spectra for the extraction media which gave an absorbance maximum at 278 nm representative of the plasticizer that leached from the control. The absorbance unit was 0.362 for day one and reached a plateau around 0.4 AU for the next 2 weeks as seen in Figure 4.33, the plot of AU at 278 nm vs. days of extraction.

Instead of a steady increase, the PVC-*g*-PDMA system showed fluctuations each day in the plasticizer AU due to systematic error. However, the AU never exceeded 0.034 after one month, indicating suppression of plasticizer migration through the grafted layer, because the equilibrium concentration of plasticizer in the hexanes was significantly less than the control (0.435 AU).

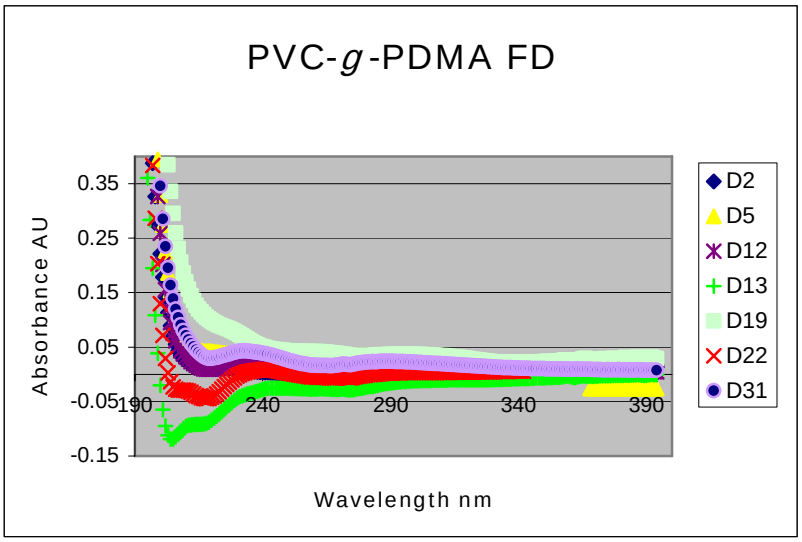

Figure 4.34. UV-Vis spectra of plasticizer extracted with hexanes from PVC-*g*-PDMA FD over 1 month in a closed cuvette.

Figure 4.34 displays the UV-Vis spectra for the extraction media for PVC-*g*-PDMA FD with hexanes over 1 month. In comparison to the control spectra (Figure 4.33) there is barely a peak visible at 278 nm. Figure 4.35, a plot of the AU vs. days for the PVC-*g*-PDMA FD system, exhibits an absorbance maximum in the range of ± 0.04 AU. Variation between days may be due to baseline or background error.

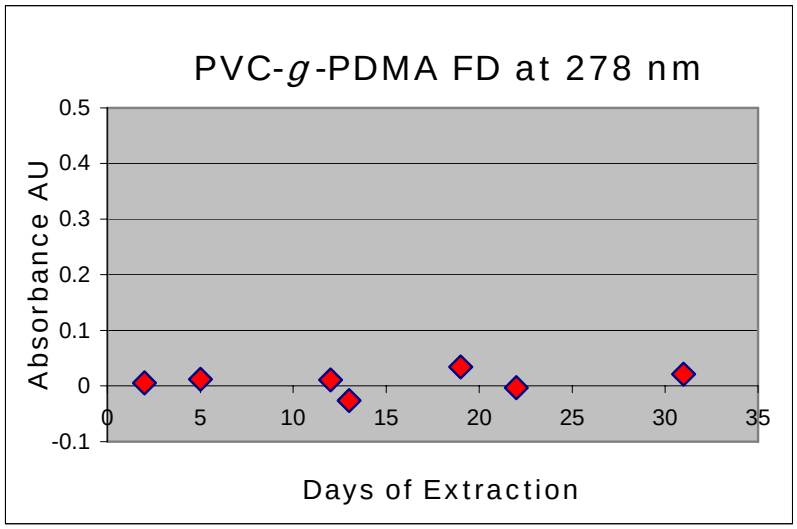

days	AU (278 nm)
2	0.005
5	0.012
12	0.011
13	-0.026
19	0.034
22	-0.003
31	0.021

Figure 4.35. Plot of plasticizer AU at 278 nm vs. days of extraction in hexanes for PVC-*g*-PDMA FD (1 month) in a closed cuvette.

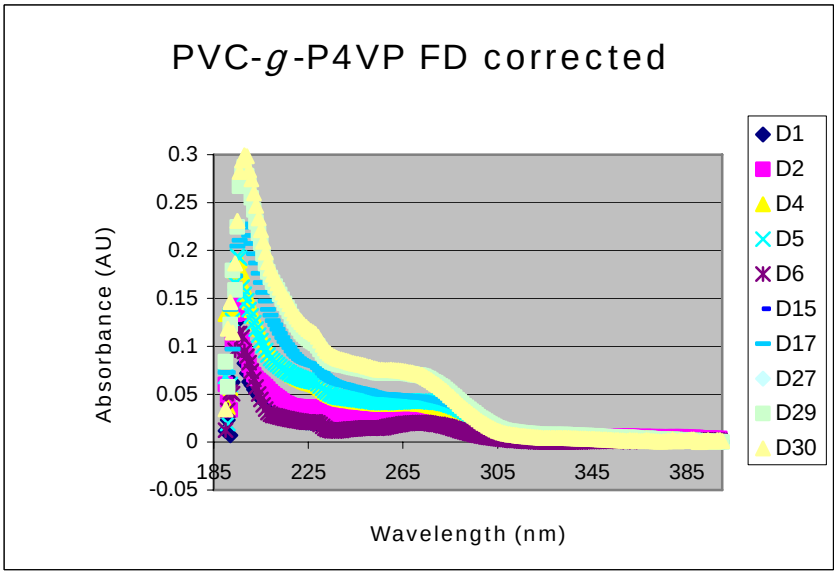

Figure 4.36. UV-Vis spectra of plasticizer extracted with hexanes from PVC-*g*-P4VP FD over 1 month in a closed cuvette. The letter D stands for days of extraction.

The PVC-*g*-P4VP FD system also significantly impeded the plasticizer migration. This maximum value of absorbance detected for the plasticizer (0.063 AU) for this system was substantially less than the maximum PVC control absorbance value of 0.435

AU. Figure 4.36 portrays the UV-vis spectra of the plasticizer absorbance maximum at 278 nm for the extraction media over 1 month. The plot of the AU at 278 nm over 1 month demonstrates an increasing trend in absorbance up to 0.063 AU, with the exception of days 6 and 27 (Figure 4.37). The variance of data points is likely due to systematic error. Regardless, both modified systems were effective in reducing plasticier migration.

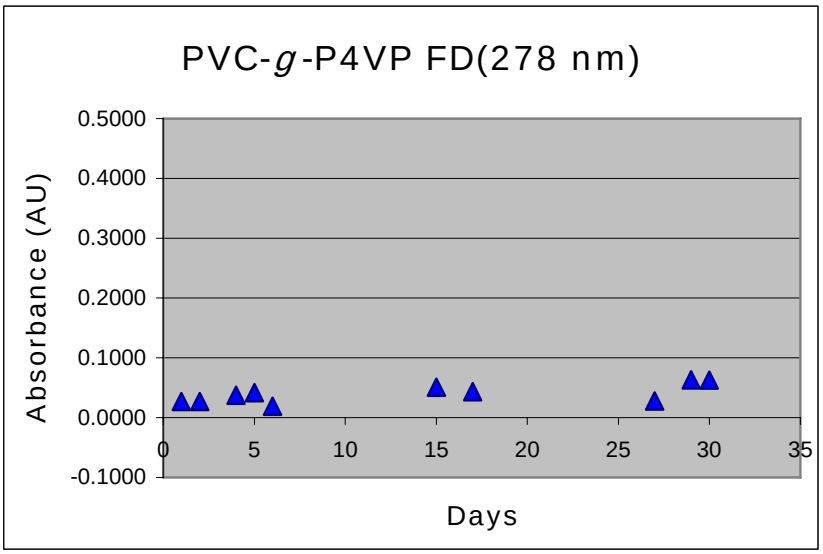

Days	AU (278 nm)
1	0.0267
2	0.0269
4	0.0373
5	0.0417
6	0.0187
15	0.0507
17	0.0433
27	0.0277
29	0.0630
30	0.0627

Figure 4.37. Plot of plasticizer AU at 278 nm vs. days of extraction in hexanes for PVC-*g*-P4VP FD (1 month) in a closed cuvette.

After the initial testing protocols failed to portray an accurate picture of the actual plasticizer migration, a new standard procedure was applied to the control and grafted films. Not only were the films exposed to the initiating solution for less time to retain the plasticizer in the bulk PVC film, but the segmented 10.5 cm^2 samples were placed at the bottom of a cuvette which was sealed with a screw top. This was superior to transferring the extraction media to a glass cuvette each day, done previously, because it minimized the potential error for solvent loss. The results demonstrate successful suppression of

plasticizer mass transfer for the modified PVC-*g*-PDMA and PVC-*g*-P4VP systems. Figure 4.38 shows a conclusive comparison plot of plasticizer absorbance units for fast dipped (15 seconds initiator deposition times) PVC-*g*-PDMA, PVC-*g*-P4VP and PVC control at 278 nm after extraction into hexanes over 31d.

The supplier of the PVC (Universal Plastics) refused to divulge the chemical nature of the plasticizer which was used as an additive to the PVC film. Therefore, the extraction media was evaporated and dissolved in $CDCl_3$ for ^1H NMR spectroscopic analysis. Typical phthalate ester chemical shifts were expected since the IR spectrum showed the carbonyl as a prominent functional group and the UV-Vis spectrum exhibited an absorbance maximum around 278 for DEHP. Unfortunately the ^1H NMR spectroscopic results were ambiguous for the film.

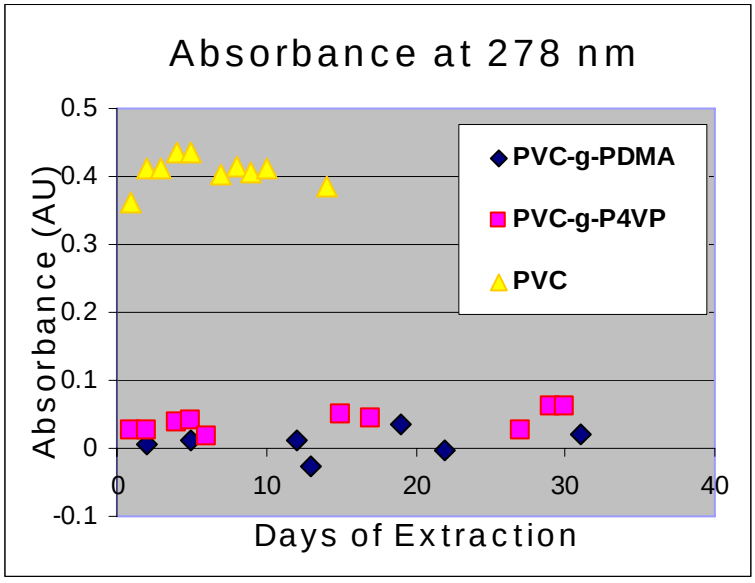

Figure 4.38. Plot of plasticizer AU at 278 nm vs. days of extraction in hexanes for PVC-*g*-PDMA FD (blue), PVC-*g*-P4VP FD (pink) and PVC FD (yellow) (1 month after FD with initiator solution (15 seconds)).

The tubing plasticizer was also extracted with hexanes, evaporated and dissolved into $CDCl_3$ for ^1H NMR analysis. In the case of the tubing, the ^1H NMR spectrum

(Figure 4.39) was consistent with the phthalate ester, DINP. The aromatic protons were observed as doublets around δ 7.7 and δ 7.5. The peak at δ 4.2 was indicative of the methyl group adjacent to the oxygen and the methine protons were found at δ 1.65. The remainder of the peaks was attributed to aliphatic groups, **e** (δ 1.25) and **f** (δ 0.85). The integration of the chemical shift at δ 1.25 was indicative of 10 methylene protons relative to two methine protons (**d**), which is consistent with the structure of DINP.

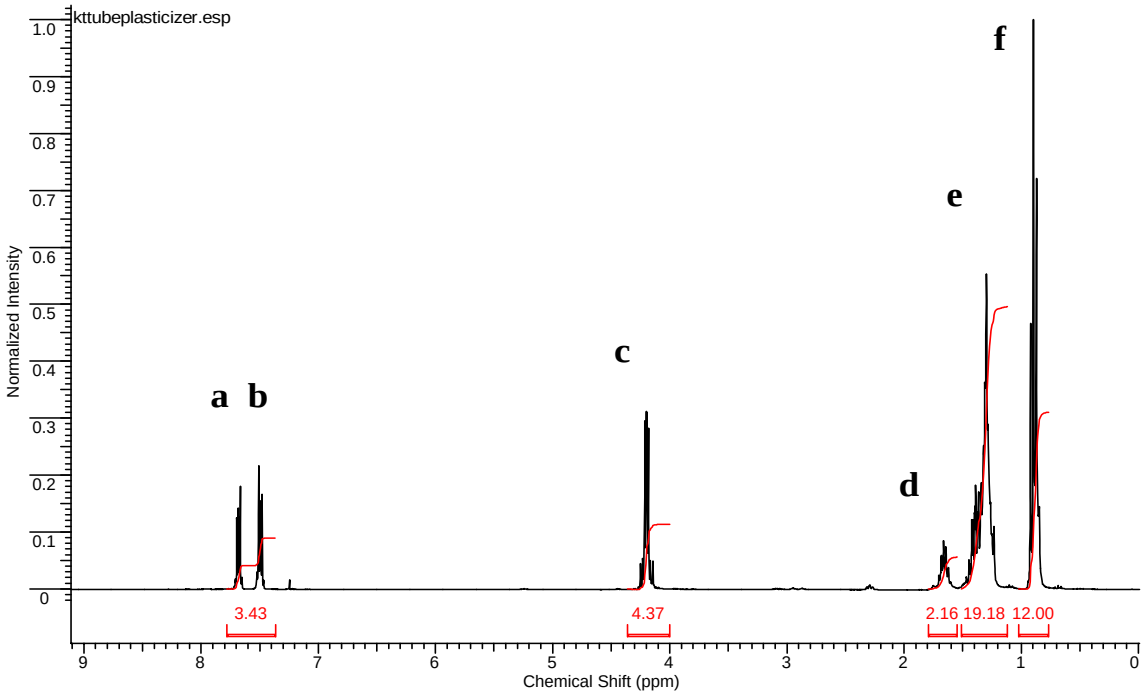

Figure 4.39. ^{1}H NMR spectrum of tubing plasticizer (DINP) extracted with hexanes.

4.11 Surface Modification of PVC for Antimicrobial Properties

Reagents that kill bacteria in solution, such as antibiotics, idodine, silver ions and quaternary ammonium compounds were only proven effective in solution. Tiller proved that P4VP quaternized with long alkyl chains killed bacteria in a dry environment. Therefore, PVC-*g*-P4VP was quaternized with 1-bromobutane, 1-bromohexane, 1-bromooctane, and 6-perfluorooctyl-1-bromohexane for reduced antimicrobial properties.

4.11.1 *N*-Alkylpyridinium Surfaces

The alkylation of PVC-*g*-P4VP proceeded by a S_N2 nucleophilic substitution of bromoalkanes with the pyridine nitrogen as depicted in Scheme 4.4. Upon reaction of the PVC-*g*-P4VP film with 1-bromooctane, **4c**, the IR spectra showed an increase in percent alkylation as reaction time increased. Qualitatively the films turned light brown to dark brown as depicted in Figure 4.40.

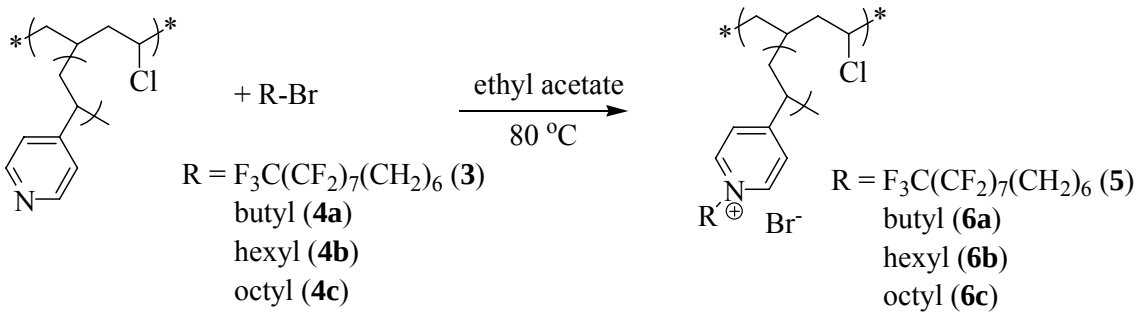

Scheme 4.4. Synthesis of N-alkypyridinium surfaces from PVC-*g*-P4VP.

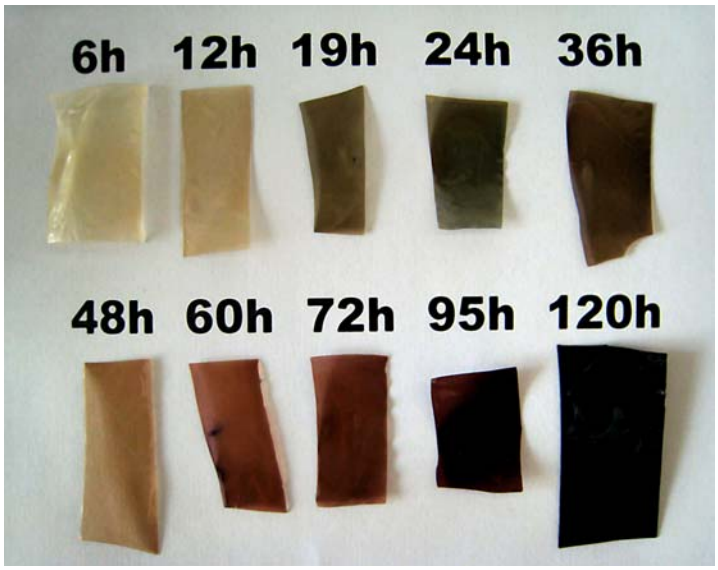

Figure 4.40. Image of PVC-*g*-P4VP films quaternized with 1-bromohexane in ethyl acetate at 80 °C for various reaction times.

IR spectroscopy of the *n*-octylpyridinium modified film (**6c**) was used to monitor the degree of quaternization with time. The aromatic ring stretch from pyridine shifted from 1600 to 1640 cm^{-1} upon alkylation of the nitrogen. As the reaction time proceeded, the 1600 cm^{-1} absorption diminished while the 1640 cm^{-1} absorption concurrently increased, indicating a higher degree of quaternization. Figure 4.41 demonstrates a similar trend for the absorption maximum intensity of PVC-*g*-P4VP films reacted with 1-bromooctane (**4c**) for various reaction times. The integration of the peak area for the quaternized (1640 cm^{-1}) and unquaternized (1600 cm^{-1}) peaks can be used to determine the conversion fraction which is plotted with time in Figure 4.42 for all alkylating agents. The conversion fraction is the percentage of pyridine units in the chains of the grafted P4VP that are quaternized by the aklylating agent. It is calculated by :

$$\text{Conversion fraction} = (\text{integration of } 1640\ cm^{-1}) / (\text{integration of } 1640\ cm^{-1} + \text{integration of } 1600\ cm^{-1} \quad (6)$$

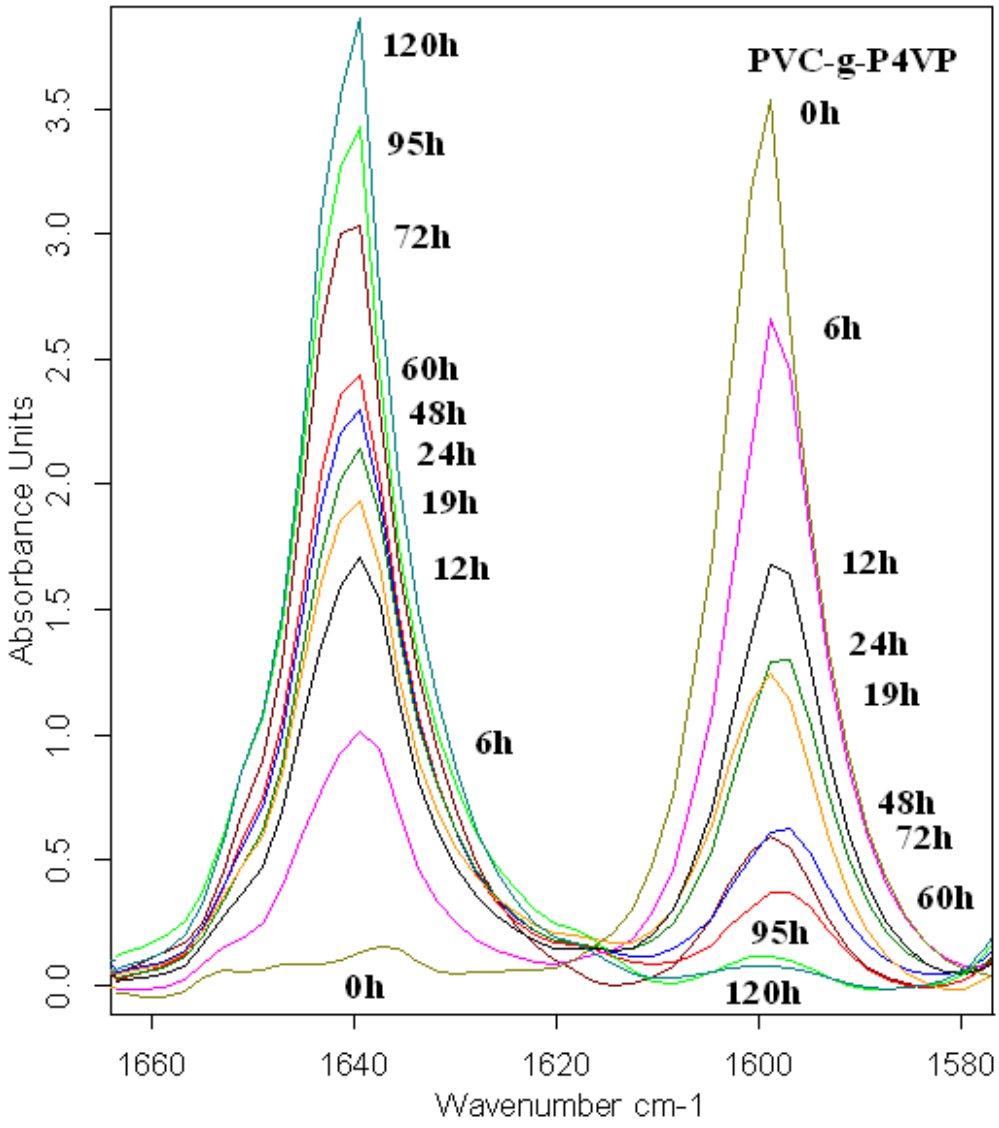

Figure 4.41. IR spectra of quaternization of PVC-*g*-P4VP films with 1-bromooctane in ethyl acetate at 80 °C for various times.

Figure 4.42 is a plot of conversion fraction version reaction time for **6c** and the fluorinated system (**3**) which will be discussed in detail later. The plot of the conversion for *n*-octylpyridinium films (**6c**) vs. reaction time indicates 50% conversion at 19 hours and almost complete conversion after 120 hours.

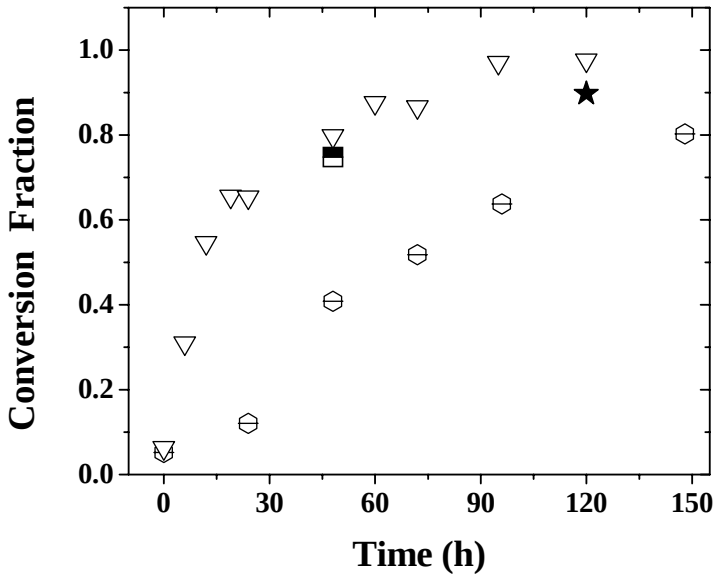

Figure 4.42. Conversion fraction of quaternized PVC-*g*-P4VP films with time (h) for samples reacted with 1-bromooctane (∇) or 6-perfluorooctyl-1-bromohexane (slashed hexagon) in ethyl acetate at 80 °C; additional conversion fractions are shown for films quaternized with 6-perfluorooctyl-1-bromohexane (**3**) for 24 h and 1-bromohexane (**4b**) for 24 h (half-filled box); 6-perfluorooctyl-1-bromohexane for 48 h and 1-bromohexane for 72 h (star).

The contact angles of the **6a**, **6b** and **6c** alkylated films all display significantly higher water contact angles than the PVC-*g*-P4VP film with the exception of the static and receding angles of **6a** as shown in Table 4.7. This discrepancy may be explained by the theory proposed by Tiller *et al.*[26] Nonalkylated P4VP chains are presumed to behave similar to P4VP chains quaternized with long alkyl moieties. Because of hydrophobic interactions, the chains experience an attractive van der Waals force. However, chains with short alkyl groups (**6a**) possess lower van der Waals forces that are insufficient to overcome the electrostatic repulsion from the polycation. The small discrepancy for **6a** may indicate a threshold number of carbon atoms necessary to significantly modify the surface energy of the film.

Table 4.7. Contact angle measurements of PVC, PVC-*g*-P4VP and quaternized films.

Sample Description	S°	A°	R°
PVC	74 ± 2	82 ± 2	67 ± 2
PVC-*g*-P4VP	62 ± 2	65 ± 2	53 ± 0
PVC-*g*-P4VP4C[a] **(6a)**	60 ± 4	69 ± 2	53 ± 2
PVC-*g*-P4VP6C[a] **(6b)**	78 ± 5	83 ± 6	68 ± 5
PVC-*g*-P4VP8C[a] **(6c)**	80 ± 3	83 ± 4	69 ± 2
PVC-*g*-P4VP$(CH_2)_6(CF_2)_8F$[b] **(5)**	91 ± 7	98 ± 5	75 ± 4

[a]Samples were reacted with the appropriate alkylating agent for 120 h at 80 °C in ethyl acetate. [b]Sample was reacted with 6-perfluorooctyl-1-bromohexane for 148 h at 80 °C.

The **6b** and **6c** polymers displayed higher advancing water contact angles than PVC-*g*-P4VP, making these alkylated surfaces similar in wettability to the starting PVC film. A more hydrophobic surface was observed for the fluorinated film (**5**) with a high water contact angle of 98 °C.

The thicknesses of the alkylated films were calculated using IR calibration curves of absorption vs. thickness as discussed previously (Figure 4.16). The PVC-*g*-P4VP used for quaternization had a thickness of 6.2 μm for the grafted P4VP layer while **6c** was found to be 6.8 μm thick. The increase in thickness is attributed to the increase in molecular weight of the grafted repeat unit from 105 g/mol for P4VP to 271 g/mol for P4VP8C with *n*-octyl chains and the bromine counteranion.

The control PVC-*g*-P4VP film was placed in ethyl acetate, in the absence of alkylating agent, at 80 °C for 120 hours to observe possible intramolecular quaternization between the chlorinated PVC backbone and the pyridine ring. The presence of the peak at 1640 cm^{-1}, with an absorption unit of 0.147, confirmed the occurrence of this side reaction during polymerization of poly(4-vinylpyridine). While this experiment confirms this reaction, we are not able to assess its rate relative to the intermolecular alkylation with haloalkanes.

4.11.2 Synthesis of 6-Perfluorooctyl-1-bromohexane (**3**)

As explained earlier, Ober *et al.*[29] discovered an alkylating agent which had superior performance against *staphylococcus aureus* than the bromoalkanes just discussed. PS-*b*-P4VP was quaternized with 6-perfluorooctyl-1-bromohexane (**3**) for increased antimicrobial properties. The longer, more hydrophobic chain was presumed to disrupt the cytoplasmic membrane of the phospholipids bilayer more because of the higher charge density and stronger electrostatic interactions. Therefore, this compound was of interest to this research and was synthesized.

The experimental procedure was based on a method reported in literature.[49] First 6-perfluorooctyl-1-hexanol (**2**) was synthesized as shown in Scheme 4.5. The fluorinated alcohol was characterized by ^{1}H NMR analysis and compared favorably with the literature values. The aliphatic absorptions which integrated to 4 protons each were found at δ 1.43 (**b**) and δ 1.60 (**c**) in Figure 4.44. Other aliphatic absorptions with integration of 2 protons, representative of **d** and **a**, were displayed at δ 2.08 and δ 3.67, respectively.[49] An expansion of the spectrum in Figure 4.45 shows integration and splitting.

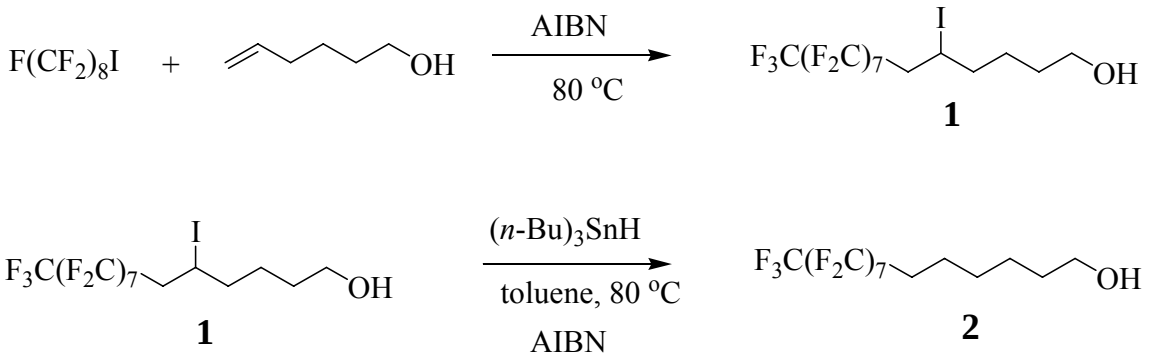

Scheme 4.5. Synthesis of 6-perfluorooctyl-1-hexanol (**2**).

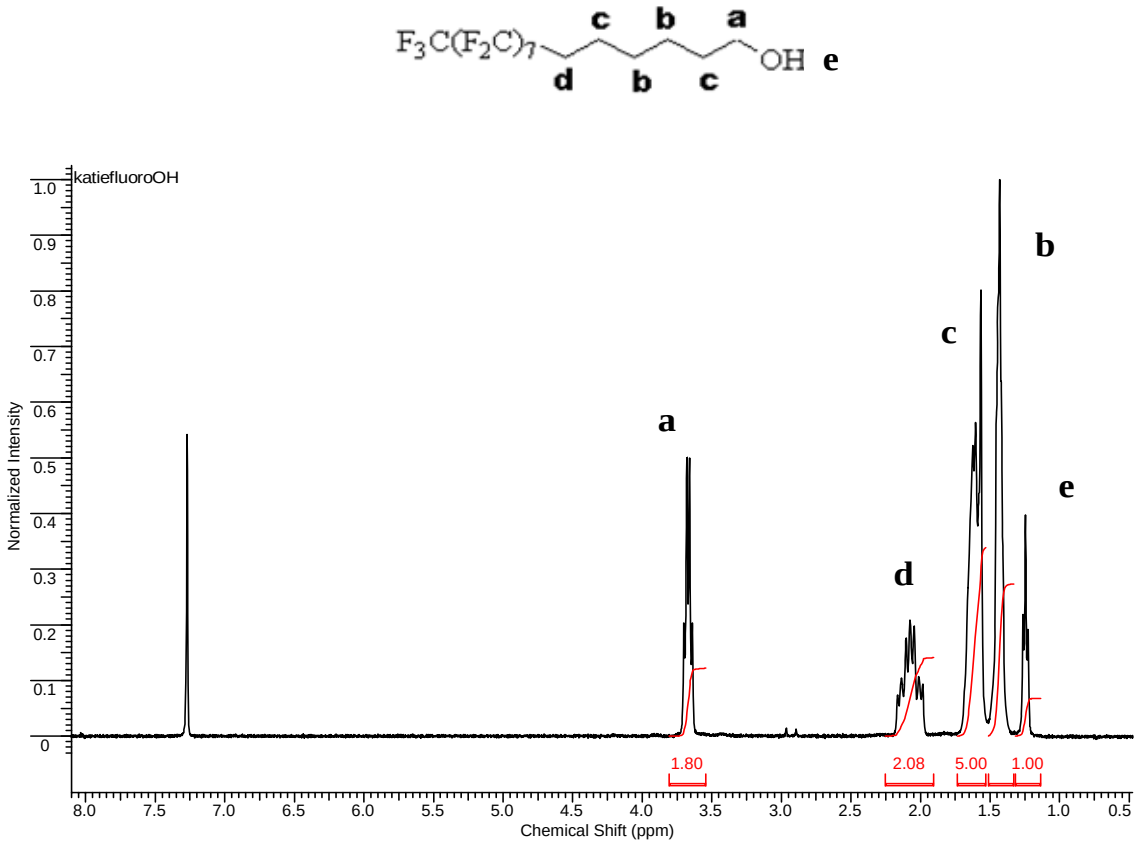

Figure 4.43. ^{1}H NMR spectrum of 6-perfluorooctyl-1-hexanol (**2**).

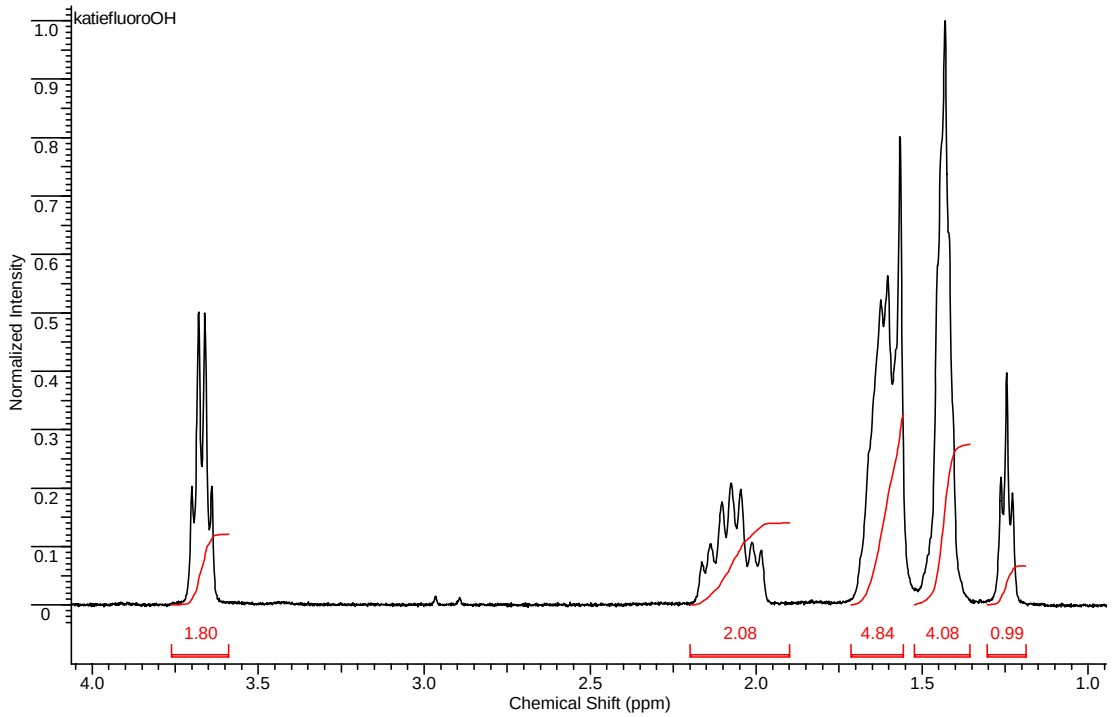

Figure 4.44. Expanded ^{1}H NMR spectrum of **2:** peak splitting and integration.

The synthesis of the brominated fluoroalkane **3** was based on the literature (Scheme 4.6).[50] Successful characterization by ^{1}H NMR analysis of the brominated fluoroalkane was only possible after column chromatographic purification to remove the triphenylphosphine oxide; small traces are still observed near δ 7 after purification (Figure 4.47).

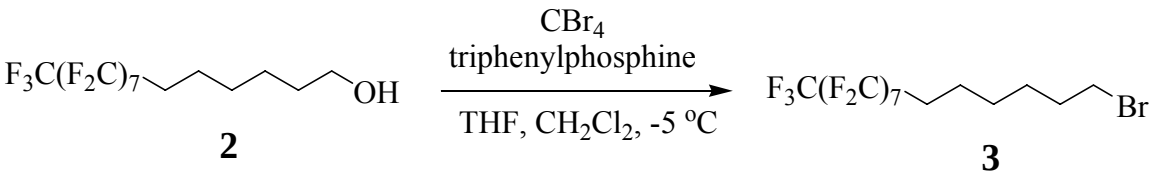

Scheme 4.6. Synthesis of 6-perfluorooctyl-1-bromohexane (**3**).

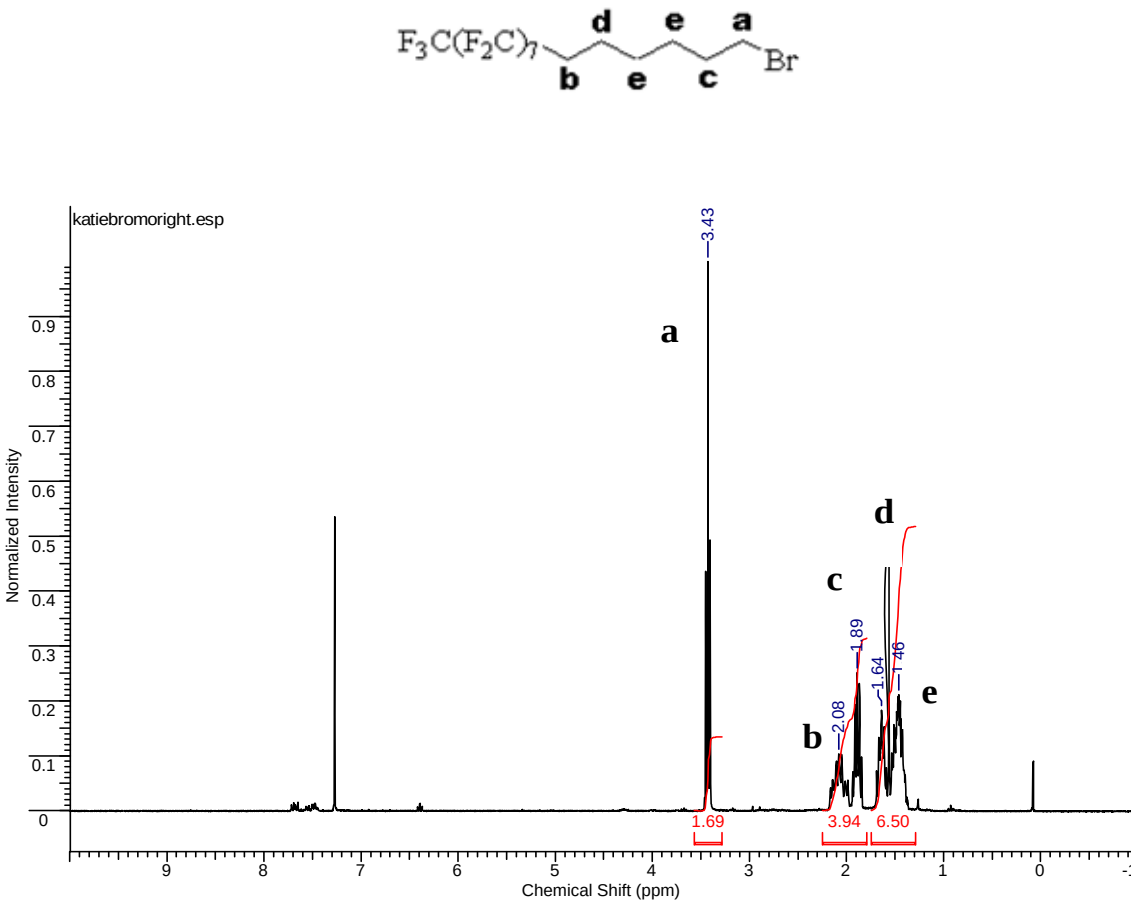

Figure 4.45. ^{1}H NMR spectrum of 6-perfluorooctyl-1-bromohexane (**3**).

Expansion of the ^{1}H NMR spectrum in Figure 4.46 displays the entire aliphatic region which gave integration in the ratio close to 2:4 for absorptions represented by **a** vs. absorptions represented by both **b** and **c**. The ratio of **a** to both **e** and **d** was close to 2: 6. The peak splitting for **b** is due to the expected F-H coupling.[50]

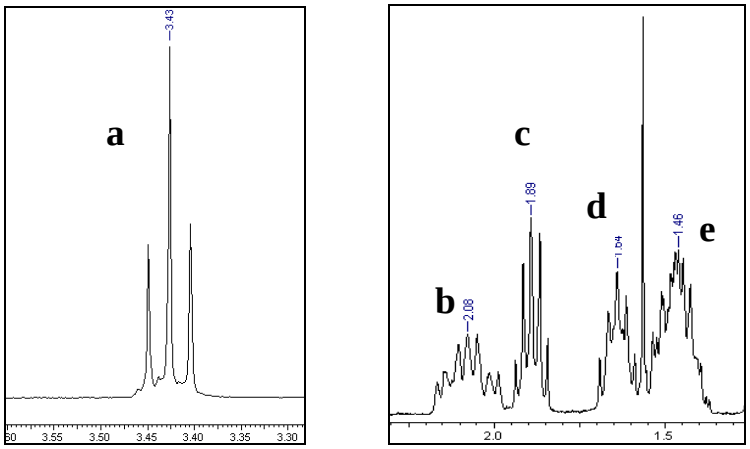

Figure 4.46. Expanded ^{1}H NMR spectrum of **3:** δ 3.43 and δ 1- 2.2.

4.11.3 *N*-Fluoroalkylpyridinium Surfaces

We speculated that films quaternized with 6-perfluorooctyl-1-bromohexane (**3**) would have a higher surface charge density attributed to a higher percentage of polycations at the surface. P4VP cations are brought to the surface by the extension of hydrophobic C_8F_{17} groups into air. The localization of CF_3 groups at the surface also creates a low surface tension measured by water contact angle. PVC-*g*-P4VP was reacted with the fluorinated alkylating agent (**3**) for 148 hours in ethyl acetate at 80 °C (Scheme 4.4) to afford PVC-g-P4VP$(CH_2)_6(CF_2)_8F$ (**5**). The product has advancing and receding contact angles of 98° and 75° (Table 4.7), indicating a considerably lower surface energy relative to PVC-*g*-P4VP as well as the nonfluorinated *N*-alkypyridinium surfaces.

The fluorinated film was not completely quaternized as shown by the IR spectrum in Figure 4.48. Therefore, for specified fluorinated films, the unreacted pyridine groups were subsequently quaternized with 1-bromohexane (**4b**) to achieve higher conversion with shorter reaction time (Scheme 4.7).

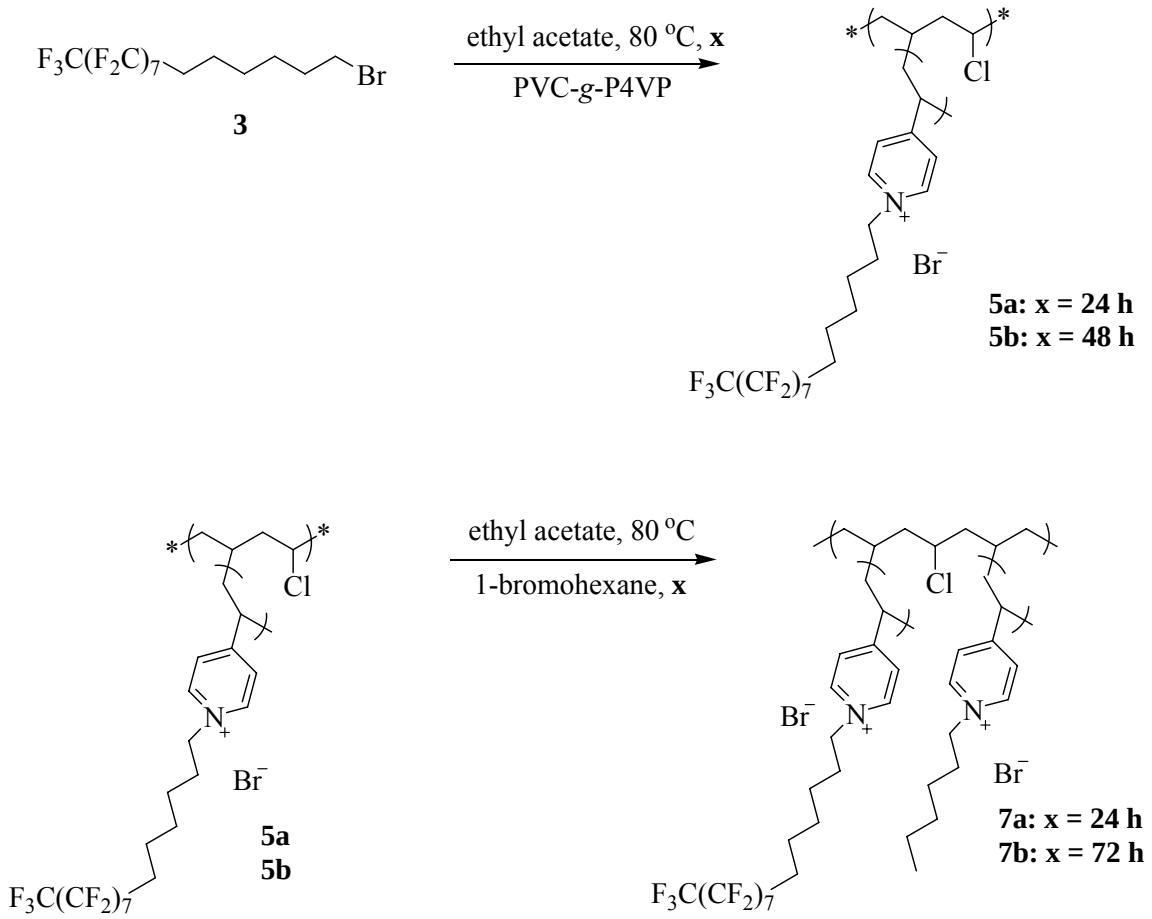

Scheme 4.7. Quaternization of PVC-*g*-P4VP with **3** for 24 h (**5a**) and 48 h (**5b**) along with subsequent reaction with 1-bromohexane for 24 h (**7a**) and 72 h (**7b**).

The observed trend in Figure 4.48 mimics the previously mentioned alkylated spectra. As the peak at 1600 cm^{-1} (unquaternized ring stretching) diminishes with reaction time, the peak at 1640 cm^{-1} (quaternized ring stretching) grows in intensity. Two fluorinated films were further reacted with **4b** for 24 and 48 hours. The 24 hour (**5a**) and

48 hour (**5b**) specimens were additionally reacted with 1-bromohexane for 24 hours and 72 hours, respectively (Scheme 4.7). The mixed sample, **7a**, which reacted for a total of 48 hours with both reagents had a product absorption intensity far greater than the sample only reacted with the fluorinated reagent for 48 hours (**5**). This trend was duplicated by the mixed sample which was reacted with both reagents for a total of 120 hours, **7b**. This sample did not reach complete conversion but was quaternized to a greater extent than PVC-*g*-P4VP reacted with the fluorinated reagent for 148 hours.

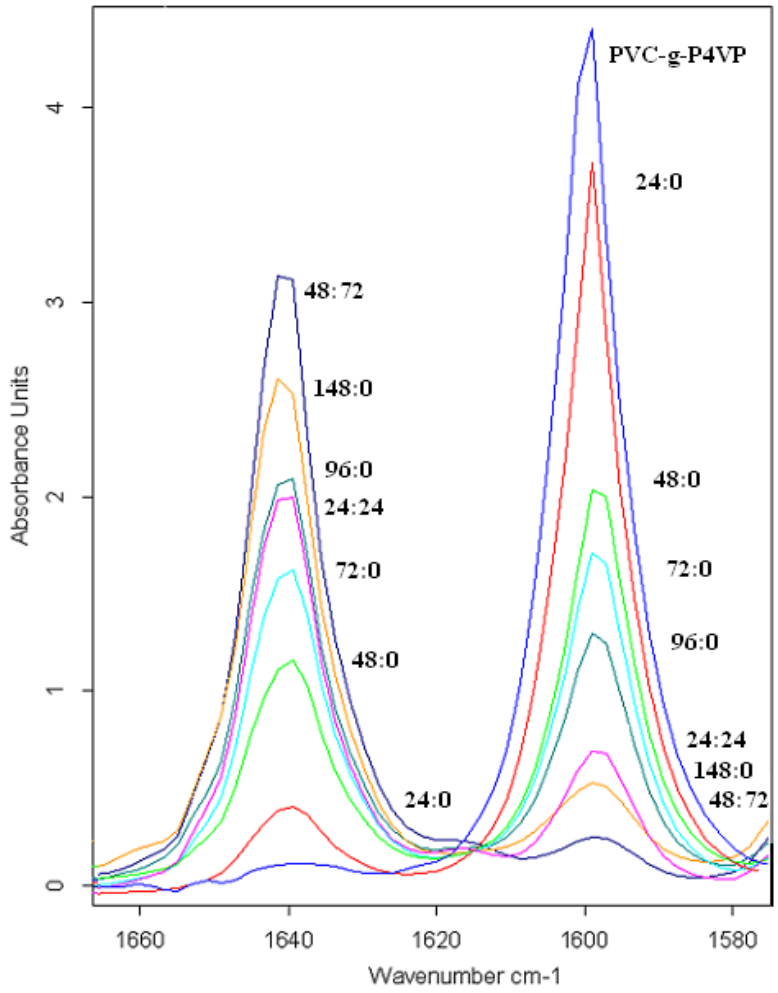

Figure 4.47. IR spectra of the formation of quaternized PVC-*g*-P4VP films by reaction with 6-perfluorooctyl-1-bromohexane (**3**) followed by 1-bromohexane (**4b**). The time of reaction with each alkylating agent is noted in hours next to the spectrum (**3**:**4b).**

Figure 4.42 exhibits the extent of reaction vs. the reaction time for all polycations. The scattered plot for the fluorinated films (**5, 5a, 5b**) illustrates 50% conversion at 72 hours and 80% conversion after 148 hours. Further quaternization of the fluorinated films was obtained by subsequent reaction with **4b**. The film that was quaternized with **3** and **4b** for 24 hours each (half-filled box) gave 80% conversion while the film quaternized with **3** for 48 hours and **4b** for 72 hours (star) showed almost 90% conversion.

In comparison to the *n*-octylpyridinium film (**6c**), the fluorinated films appear to have a slower conversion time during the S_N2 nucelphilic substitution reaction. To explain this phenomenon, the rate constant was quantified for both reactions. By plotting ln (1-p) vs. time for both reactions (Figure 4.43), we can extrapolate the rate constants. The rate constants for quaternization with **4c** and **3** were 0.0633 and 0.0693 L mol^{-1} s^{-1}, respectively. Because the rate constants are close, the difference in conversion has to be attributed to the starting concentration of reagent. The concentration of 6-perfluorooctyl-1-bromohexane (**3**) was 0.154 mol/L, whereas the concentration of **4c** was 0.579 mol/L. This difference is why **4c** reacted faster than **3** along with possible diffusion problems.

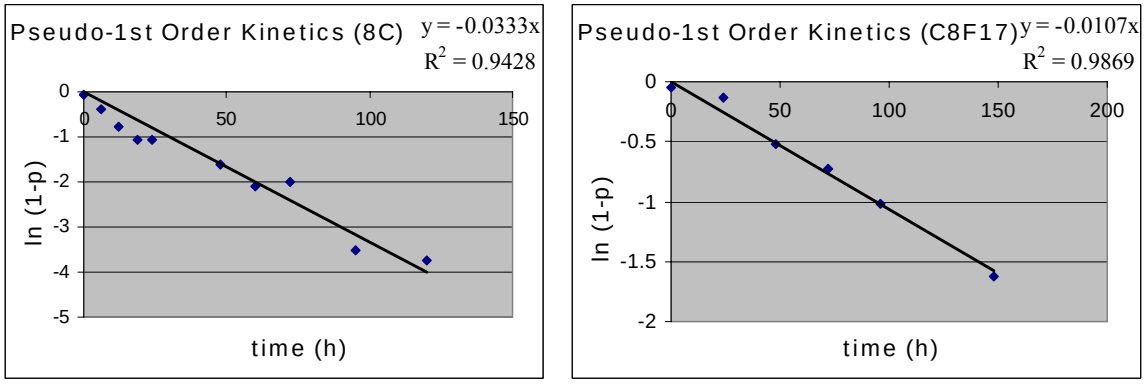

Figure 4.48. Pseudo-1st order kinetic plots of ln(1-p) vs. time (h) for the quaternization of 1-bromooctane (left) and 6-perfluorooctyl-1-bromohexane (right).

4.11.4 XPS Analysis of Quaternized Surfaces

XPS of the control PVC-*g*-P4VP was performed at Bausch and Lomb and Case Western Reserve University; all other samples were examined only at Case Western Reserve University. All quaternized samples were analyzed to within 20 eV of the specific binding energies of the spectrum.

The most interesting peak noted for all quaternized samples was the shoulder or double peak found for Nitrogen at 401 and 399 eV (Appendix A). The unquaternized PVC-*g*-P4VP (Appendix A, Figure A.6) system displayed a nitrogen peak at 399 eV which shifted to 401 upon quaternization with 1-bromobutane (Appendix A, Figure A.7) and 1-bromohexane (Appendix A, Figure A.8). The relative intensity of the two peaks could be correlated with the extent of quaternization if there was better resolution. The sample quaternized with 1-bromooctane, **6c** (PVC-g-P4VP8C, Appendix A, Figure A.9), showed more of a shoulder effect as well as the sample quaternized with 6-perfluorooctyl-1-bromohexane for 148 hours, **5** (PVC-*g*-P4VP148F, Appendix A, Figure A.10). However, when PVC-*g*-P4VP was quaternized with 6-perfluorooctyl-1-bromohexane for 48 hours and subsequently quaternized with 1-bromohexane for 72 hours, **7b** (PVC-g-P4VPF/6C, Appendix A, Figure A.11), the quaternization was more complete and the nitrogen peak was found at 401 eV.

Table 4.8 displays the increasing trend for the percent carbon at the surface which followed: PVC-*g*-P4VP8C > PVC-*g*-P4VP6C > PVC-*g*-P4VP4C and PVC-*g*-P4VP (Bausch & Lomb results). Inversely, the decreasing trend for the percent oxygen at the surface followed the reverse order. The percent nitrogen of the alkylated samples was also slightly less than the PVC-*g*-P4VP sample, which is expected based on the addition

of more carbon via the alkylation. The **6a**, **6b** and **6c** samples were all around 2-3% nitrogen while the control PVC-*g*-P4VP was 4.8%. As expected, the percentage of nitrogen for **5** and **7b** were significantly less, 0.1% and 2.1%, respectively, while the percent fluorine increased to 5.5% and 7.3%, respectively.

Table 4.8. XPS data for PVC-*g*-P4VP and PVC-*g*-P4VP quaternized samples.

Sample Description	C1s	O1s	N1s	Cl2p	Si2p	F1s	C/O	C/N	O/N
PVC-*g*-P4VP[a]	77.4	10.7	1.4	6.8	3.7	N/A	7.2	55.3	7.6
PVC-*g*-P4VP[b]	73.7	9.5	4.8	11.2	N/A	N/A	7.8	15.4	2.0
PVC-*g*-P4VP4C (**6a**)	72.4	8.7	2.2	13.3	3.5	N/A	8.3	32.9	4.0
PVC-*g*-P4VP6C (**6b**)	72.9	7.4	2.2	13.8	3.7	N/A	9.9	33.1	3.4
PVC-*g*-P4VP8C (**6c**)	83.4	5.9	2.8	6.3	1.5	N/A	14.1	29.8	2.1
PVC-*g*-P4VP148hF (**5**)	82.9	11.4	0.1	0.1	N/A	5.5	7.3	829	114
PVC-*g*-P4VPF/6C (**7b**)	74	2.4	2.1	14.3	N/A	7.3	30.8	35.2	1.1

[a]This film (Case Western Reserve) was used in the quaternization of **5** and **7b**
[b]This film (Bausch & Lomb) was used in the quaternization of **6a**, **6b** and **6c**

The 3-D histogram below (Figure 4.49) describes all the trends for N, O, and C percentages of PVC-*g*-P4VP, PVC-*g*-P4VP4C (**6a**), PVC-*g*-P4VP6C (**6b**), and PVC-*g*-P4VP8C (**6c**). The C% increased with length while the N% and O% inversely decreased.

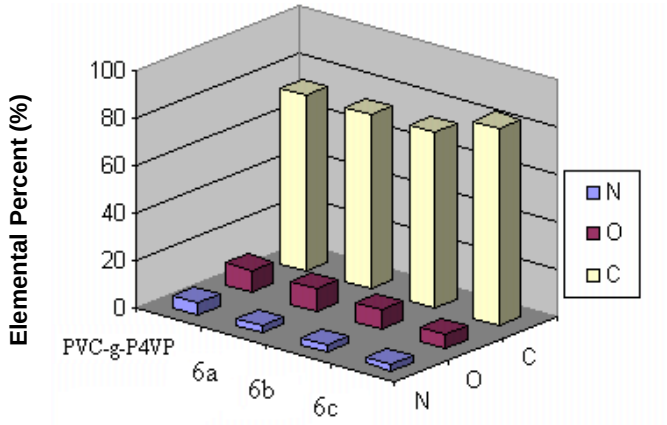

Figure 4.49. XPS elemental percentages of N, O, and C for polymer film samples: PVC-*g*-P4VP, PVC-*g*-P4VP4C (6a), PVC-*g*-P4VP6C (6b), and PVC-*g*-P4VP8C (6c).

4.11.5 Bacterial Inhibition Studies

As revealed by Tiller *et al.*[26] and Ober *et al.*,[29] polycations with long alkyl or fluorinated substituents proved effective in killing airborne bacteria. Even though their initial systems were different, neat P4VP and PS-*g*-P4VP, we believed our quaternized PVC-*g*-P4VP systems would be just as effective.

To test for antimicrobial properties, four strains of bacteria in concentrations of 10^2, 10^3 or 10^4 colony-forming units (CFU) per mL were applied in increments of 10 μL to the surface of two controls (PVC and PVC-*g*-P4VP) and the *N*-alkylpyridinium quaternized films (**5**, **6b**, **6c**). For the vitality of bacteria, films were covered with commercial agar. Incubation at 35 °C increased the rate of bacteria colony growth which was monitored after 1 day. Selected films were observed over a 2 day incubation. All results of bacteria growth are listed in Table 4.9.

There are over 30 strains of staphylococcal species divided into coagulase negative and coagulase positive strains. *Staphylococcus epidermis*, the most common human pathogen, is coagulase negative while *staphylococcus aureus* is coagulase positive. PVC-*g*-P4VP controls that were exposed to different concentrations of *coagulase negative staphyloccocus* all showed bacterial colony growth after 1 day incubation at 35 °C that intensified over 24 hours. Figures 4.50 and 4.51 are digital photos with 2.5 magnification of the infested area of the PVC-*g*-P4VP film exposed to the bacteria in concentrations of 10^2, 10^3 and 10^4 CFU/mL for 1-2 days incubation. The number of bacteria colonies multiplied with increasing concentration. The PVC control had strong colony growth that coalesced after 1 day for 10^2 and 10^4 CFU/mL *coagulase negative staphylococcus*. (Figure 4.52). The **6b** and **6c** films were resistant to the

bacteria, as the pictures showed absolutely no growth of the 10^4 CFU/mL *coagulase negative staphylococcus* (Figure 4.53). Films appeared red due to their discoloration upon quaternization.

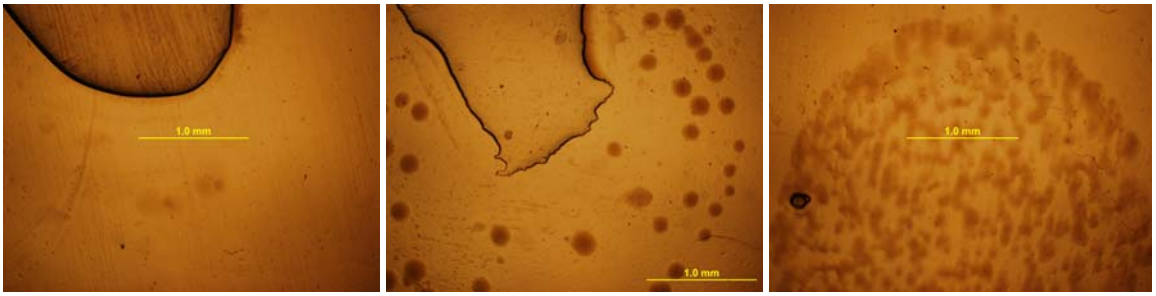

Figure 4.50. PVC-*g*-P4VP control incubated 1 day with 10^2 (left) 10^3 (middle) and 10^4 (right) CFU/mL Coag. Staph.

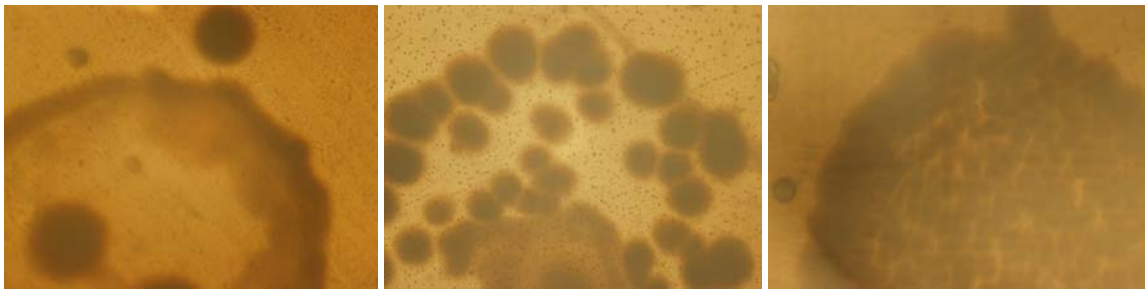

Figure 4.51. PVC-*g*-P4VP control incubated 2 days with 10^2 (left) 10^3 (middle) and 10^4 (right) CFU/mL Coag. Staph.

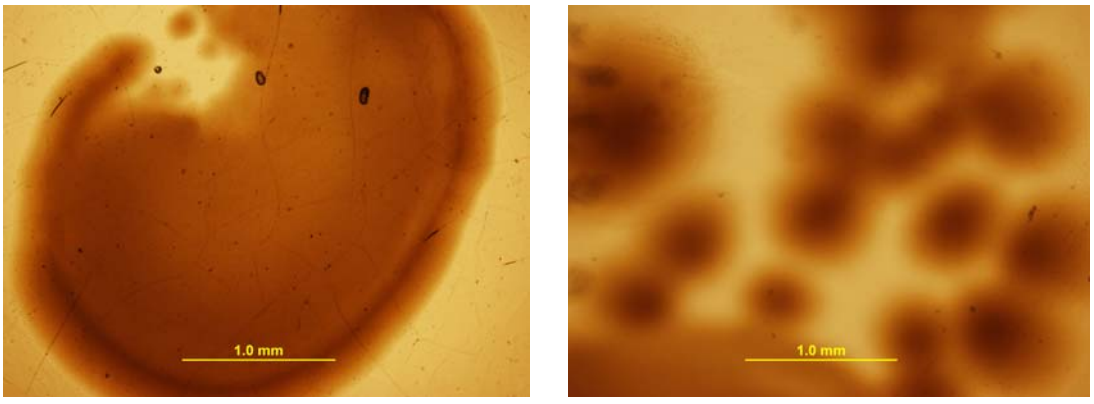

Figure 4.52. PVC control incubated for 1 day with 10^2 (left) and 10^4 (right) CFU/mL Coag. Staph.

Table 4.9. Bacteria growth on PVC and modified PVC films over 2 days incubation.

Sample		Coag. Staph[a]			S.A[b]	
	(D[e])	10^2 CFU/ mL	10^3 CFU/ mL	10^4 CFU/ mL	10^3 CFU/ mL	10^4 CFU/ mL
PVC	1	heavy	N/A	heavy	Light	moderate
PVC-*g*-P4VP	1	light	moderate	heavy	moderate	heavy
PVC-*g*-P4VPC6	1	none	none	none	None	none
PVC-*g*-P4VPC8	1	none	none	none	None	none
PVC	2	heavy	N/A	heavy	moderate	heavy
PVC-*g*-P4VP	2	moderate	heavy	heavy	heavy	heavy
PVC-*g*-P4VPC6	2	none	none	none	Light	moderate
PVC-*g*-P4VPC8	2	none	none	none	None	none

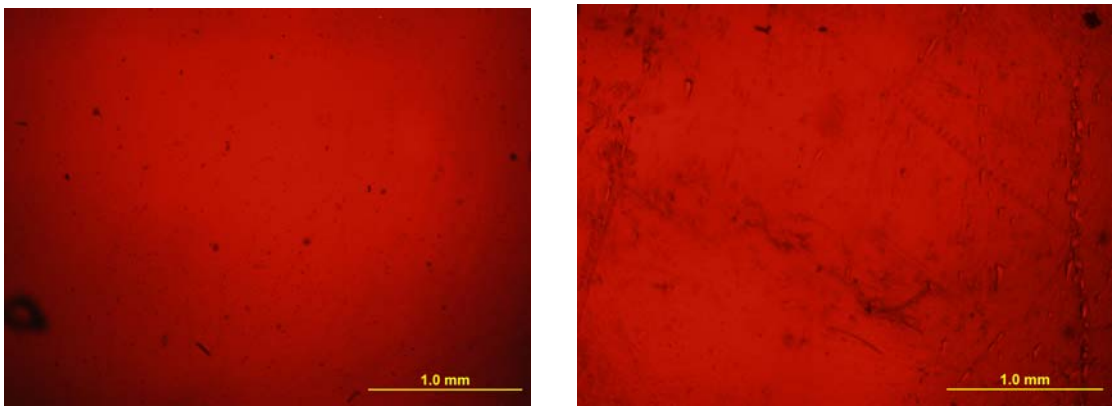

Figure 4.53. PVC-*g*-P4VPC6 (left) and PVC-*g*-P4VPC8 (right) incubated 1 day with 10^4 CFU/mL Coag. Staph.

The colony growth of 10^3 CFU/mL *staphylococcus aureus* (S.A.) on PVC-*g*-P4VP and PVC controls was well defined for the first day of incubation while the 10^4 CFU/mL colonies were coalesced (Figure 4.54 and 4.56). After day two the 10^3 CFU/mL S.A. colonies began to fuse together on the PVC-*g*-P4VP film (Figure 4.55).

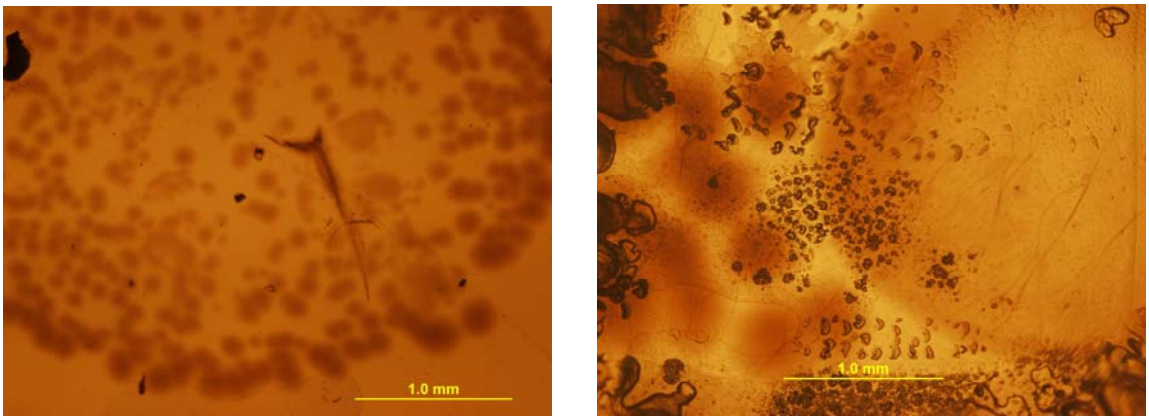

Figure 4.54. PCV-*g*-P4VP control incubated for 1 day with 10^3 (left) and 10^4 (right) CFU/mL S. A.

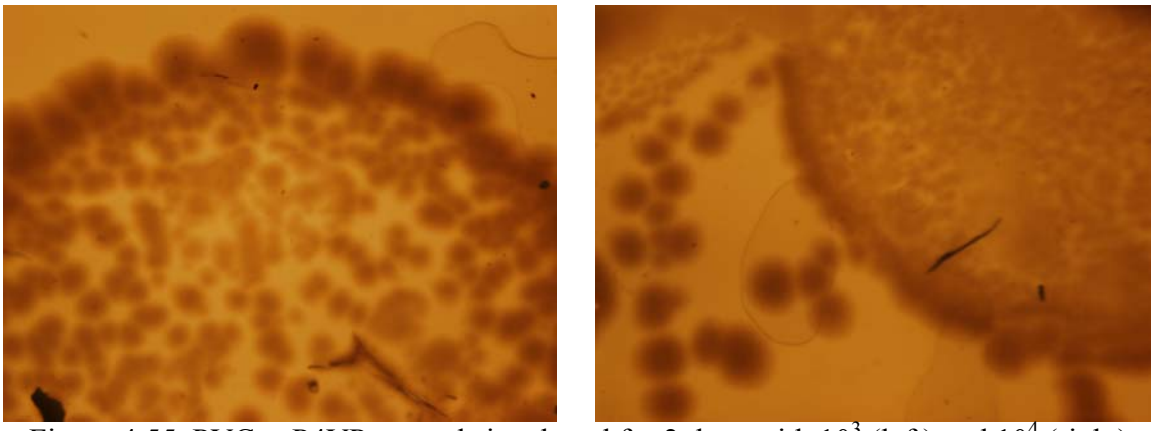

Figure 4.55. PVC-*g*-P4VP controls incubated for 2 days with 10^3 (left) and 10^4 (right) CFU/mL S.A.

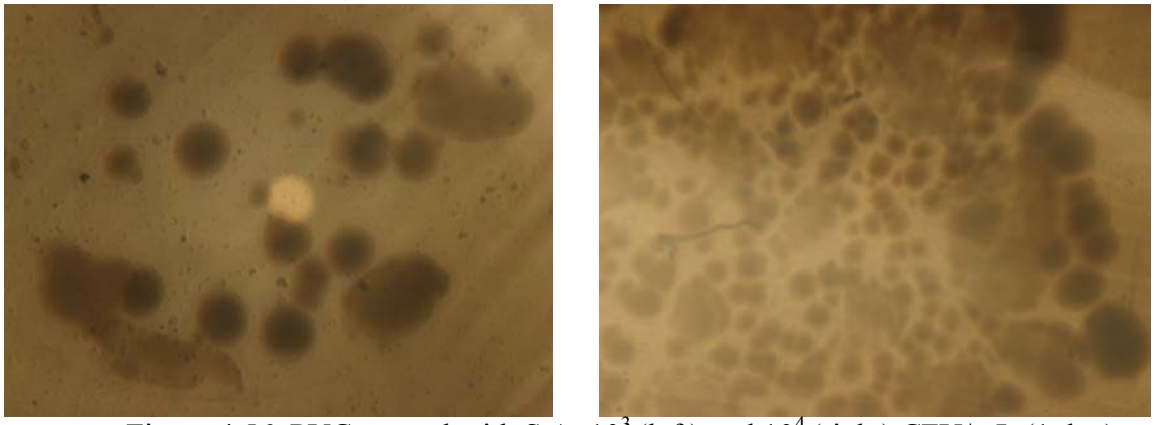

Figure 4.56. PVC control with S.A. 10^3 (left) and 10^4 (right) CFU/mL (1 day).

Again, the **6b** and **6c** films repressed the growth of bacteria. Figures 4.57 and 4.58 do not exhibit any sign of colony formation for 10^3 and 10^4 CFU/mL S.A. after 1 day incubation. The **6c** films continued to remain free of bacterial growth after the second day of incubation (not shown) while **6b** displayed a moderate number of S.A. colonies for both 10^3 and 10^4 CFU/mL (Figure 4.59). It was observed that after a few days the films would slightly detach and curve away from the glass substrate due to the moisture of the agar. It is uncertain whether 1) the growth that occurred after the second day of incubation was a result of the film losing contact with the bacteria which grew in the layer of agar, thus promoting growth or 2) the film no longer killing bacteria.

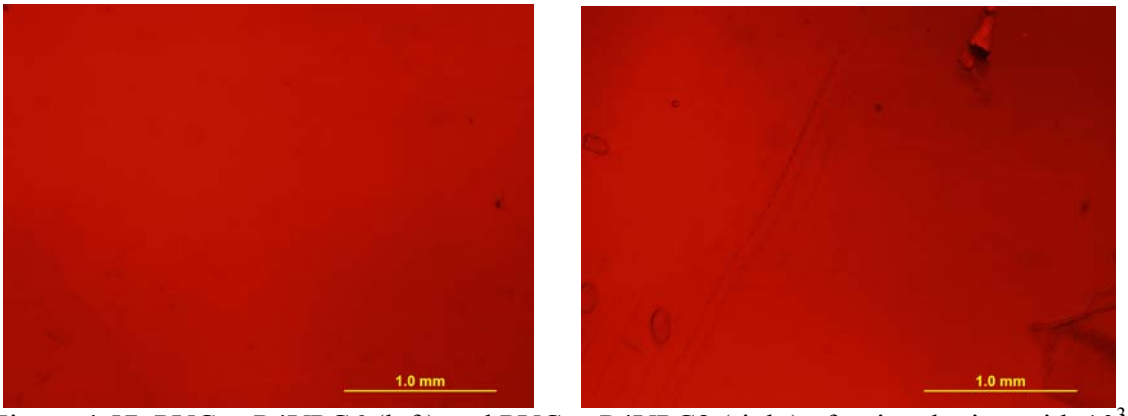

Figure 4.57. PVC-*g*-P4VPC6 (left) and PVC-*g*-P4VPC8 (right) after incubation with 10^3 CFU/mL S.A. for 1 day.

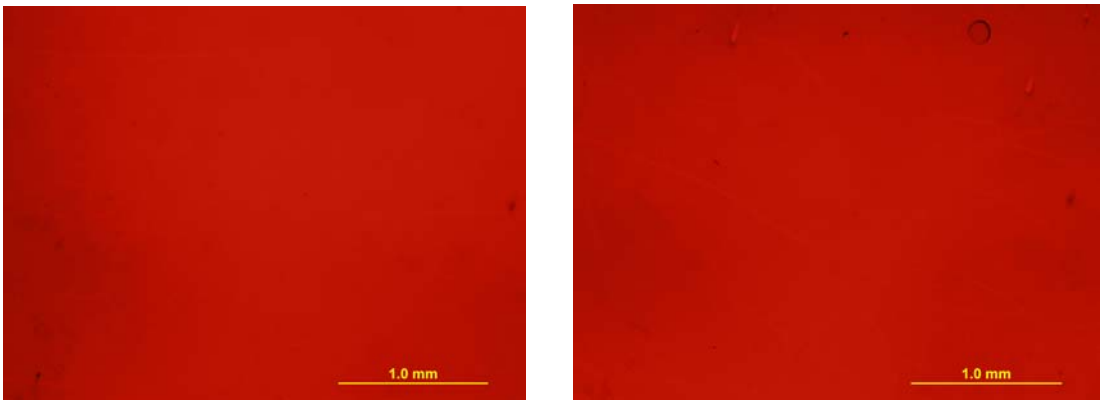

Figure 4.58. PVC-*g*-P4VPC6 (left) and PVC-*g*-P4VPC8 (right) after incubation with 10^4 CFU/mL S.A. for 1 day.

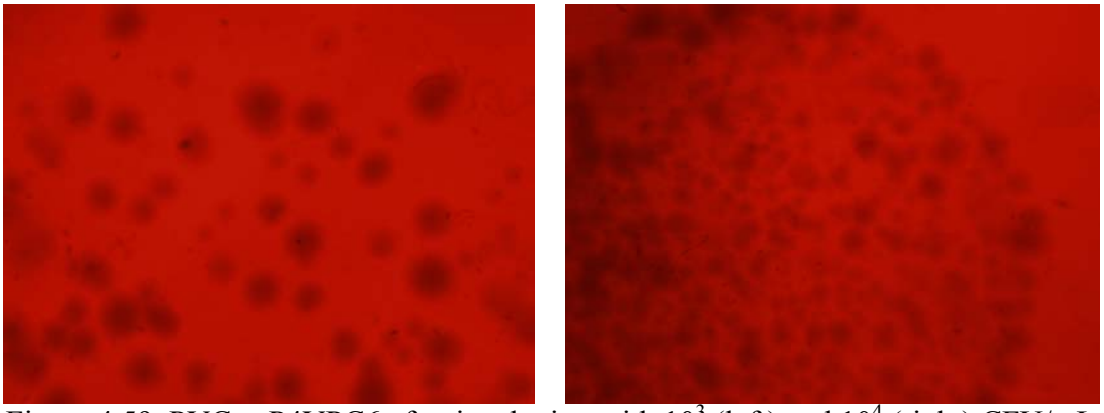

Figure 4.59. PVC-*g*-P4VPC6 after incubation with 10^3 (left) and 10^4 (right) CFU/mL S.A. for 2 days.

For the other strains of bacteria, *escherichia coli* (E. Coli) and *psuedomonas aueruginosa* (P.A.), colony formation was thwarted for the **6b** and **6c** films and the controls (PVC, PVC-*g*-P4VP). The only visible change was the air bubbles formed between the control film's surface and the agar for E. Coli in Figures 4.60 and 4.61, which has no significance. The controls exposed to P.A. (Figure 4.60 and 4.61) and the 6b film (Figure 4.62) show no change. Because the controls were unable to grow colonies, the comparison to antibacterial films was irrelevant.

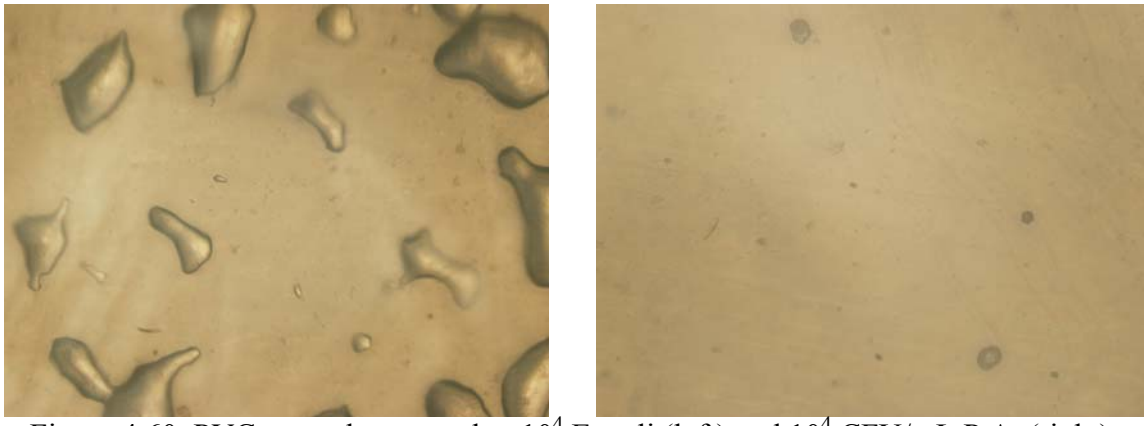

Figure 4.60. PVC controls exposed to 10^4 E. coli (left) and 10^4 CFU/mL P.A. (right).

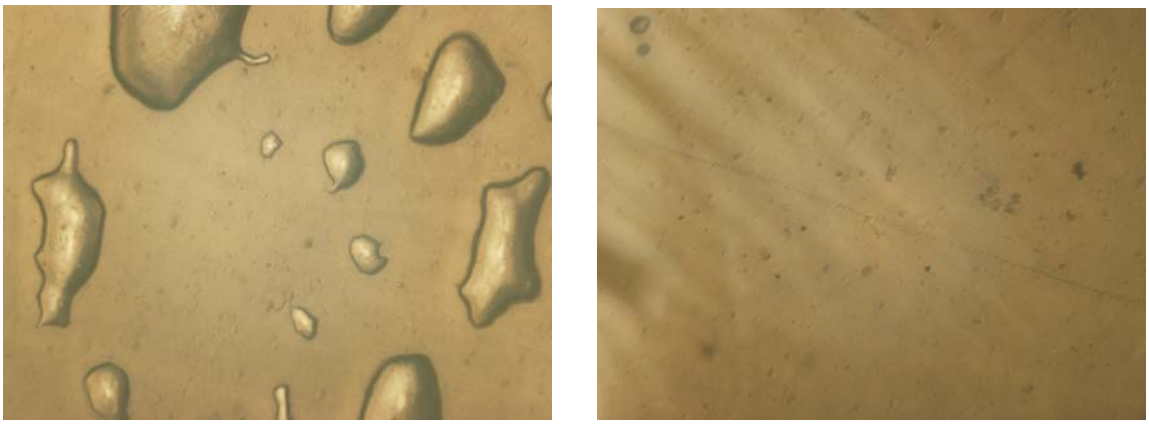

Figure 4.61. PVC-*g*-P4VP controls exposed to E. Coli (left) and P.A. (right).

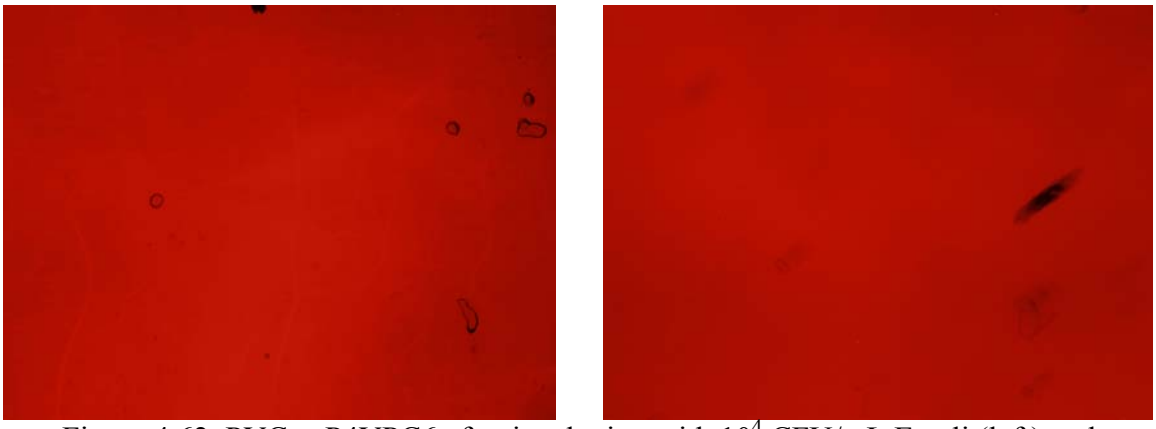

Figure 4.62. PVC-*g*-P4VPC6 after incubation with 10^4 CFU/mL E.coli (left) and P.A.(right).

The main difference between the two strains of staphyloccoci and E. Coli and P.A is the structure of the cytoplasmic membrane cell wall. Coag. Staph. and S. A. are gram positive, meaning their cell wall is 15-80 nm thick, consisting of multiple layers of peptidoglycan (Scheme 4.8).[51] E.coli and P.A. are gram negative bacteria with a thin (10 nm) cell wall composed of only one layer of peptidoglycan surrounded by an outer lipopolysaccharide membrane.[52]

The mechanism for cell disruption for gram positive bacteria involves the lysozyme cleavage of the beta 1, 4-glycoside bond.[53] It is apparent that the **6b** and **6c**

films provide lysozyme cleavage with both strains of Staph while PVC and PVC-*g*-P4VP do not. For gram negative bacteria, the cell disrupts by the plausible mechanisms suggested earlier which involve either 1) the hydrophobic insertion of the hydrophobic polycation tail after the electrostatic interaction between the negatively charged phosphates and the positively charged cation[54] or 2) the displacement of Mg^{2+} or Ca^{2+} with the polycations which then again allow proximity for hydrophobic insertion.[29]

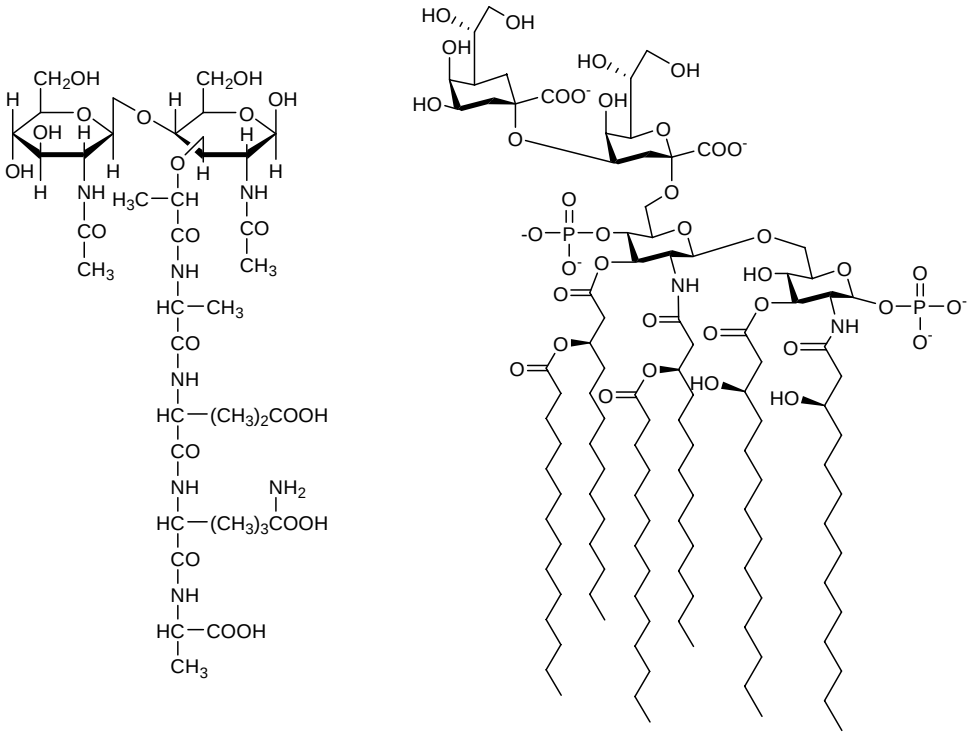

Scheme 4.8. Structure of E. coli peptoglycan (left) and lipopolysaccharide wall (right). [52]

The **6b** and **6c** films presumably operated with one of these mechanisms to effectively kill all bacteria. Unfortunately, the PVC and PVC-*g*-P4VP control films also killed the gram negative bacteria. It is probable that E. coli and P.A. were more

susceptible to disruption when in contact with the controls because their thin cell membrane only had one layer of peptidoglycan, where as S.A and S.E. strains had multiple layers. Therefore, it is only realistic to report the success of our antibacterial films against the S.A.and Coag. Staph. for potential PVC medical device applications.

Consequently, the fluorinated modified films (**5**) were only subjected to the S.A. bacteria strain. As previously mentioned, PS-*b*-P4VP quaternized with **3** gave superior inhibition to S.A. in comparison to the PS-*b*-P4VP surface quaternized with **4b**. Therefore, it is expected that **5** will be more effective in comparison to PVC-*g*-P4VP6C (**6b**) or PVC-*g*-P4VP8C (**6c**).

Figure 4.63 displays a samples of **5** incubated with S.A. (10^4 CFU/mL) for one day. As predicted, the surface was effective in killing the bacteria. Both the fluorinated films (**5**) and **6c** had superior performance against S.A than **6b**. More over, all films were exceptionally sufficient when compared to the control PVC and PVC-*g*-P4VP unmodified films.

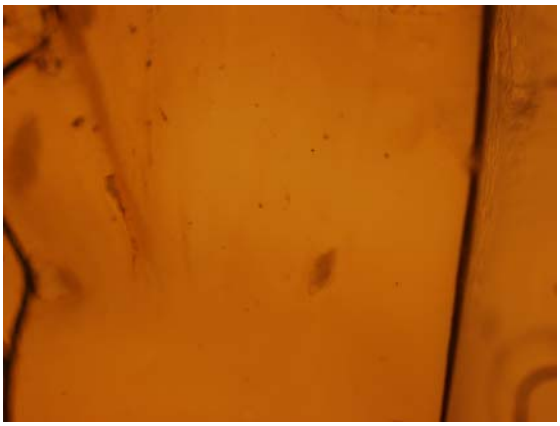

Figure 4.63. A sample of PVC-*g*-P4VPF (**5)** incubated with S.A. for 1 day.

CHAPTER V

SUMMARY

Poly(vinyl chloride) (PVC) bears several disadvantages, such as the toxicity of the common plasticizer additive (DEHP) and its hydrophobic surface which promotes protein, platelet and cell adhesion. Extensive research on surface crosslinking and surface coating have solved some of the problems of plasticizer migration or biocompatibility. A promising technology that addresses both issues is the surface grafting of hydrophilic polymers.

Analogous to the surface modification of PDMS,[25] we have covalently attached hydrophilic monomers onto the hydrophobic PVC polymer surface by an experimentally simple polymerization technique which involves the following steps: (1) physisorbtion of AIBN onto the surface of PVC, followed by (2) radical graft polymerization of the hydrophilic monomers onto the polymer surfaces. By exploiting the polarity disparity between the substrate and polymerization media, we hypothesize that radicals were formed on the PVC surface by chlorine abstraction. Radical polymerization with hydrophilic monomers (acrylic acid (AA), *N*,*N*-dimethylacrylamide (DMA), 2-hydroxyethyl acrylate (HEA), *N,N*-dimethylaminoethyl methacrylate (DMAEMA), 2-hydroxyethyl methacrylate (HEMA) and 4-vinylpyridine (4VP)) altered the surface of PVC films and tubing.

Surface characterization by water contact angle measurements and capillary rise exhibited static, advancing and receding angles similar to literature values for each hydrophilic polymer. X-ray photoelectron spectroscopy showed the presence of hydrophilic polymer as well as chlorine in the surface composition of the modified film. Atomic force microscopy suggested a non-uniform surface modification.

The thickness of the grafted polymer layer was established by gravimetric analysis and the construction of IR and UV-Vis calibration curves. The hydrophilic grafts ranged in thickness from 1-28 μm (film) and 22-100 μm (tubing). IR spectroscopic analysis was also used to confirm the presence of grafted polymer on the surface.

Selective dissolution was used for the gravimetric analysis. Comparison of the GPC of the free polymer and the insoluble material collected by gravimetric analysis supported covalent attachment of PHEMA and P4VP to PVC. The molecular weights of PVC-*g*-PHEMA and PVC-*g*-P4VP were close to the summation of the free polymer and PVC molecular weights. Elemental analysis of the insoluble material also confirmed the presence of chlorine in the grafted sample. Transmission IR spectra of the modified films displayed absorbance values from functional groups unique to both the free polymer and PVC starting material.

The plasticizer migration was followed with UV-Vis over several days using hexanes as the extracting solvent. The control sample which was exposed to acetone for 15 seconds was compared to samples modified with only 15 seconds initiator deposition times. The UV-Vis absorbance unit corresponding to the plasticizer was less than 0.1 over 30 days for the extraction of plasticizer from PVC-*g*-PDMA and PVC-*g*-P4VP. The

absorbance unit of the control was above 0.4, proving that the hydrophilic graft does reduce the migration of plasticizer from the sample.

PVC was grafted with P4VP for potential antimicrobial properties. Upon quaternization with 1-bromobutane, 1-bromohexane, 1-bromooctane and 6-perfluorooctyl-1-bromohexane, PVC-*g*-P4VP became discolored and less transparent with reaction time. There was no bacterial colony growth after 1 day incubation with *staphylococcus aureus*, meaning these films were adequate for killing bacteria on contact.

Overall, PVC was modified with several hydrophilic polymers by a simple procedure without the use of harsh chemicals or costly equipment. The hydrophilic graft proved effective at reducing the plasticizer migration and the long hydrophobic substituents of the polycations rendered the surface of PVC antimicrobial. These modifications would be useful in the application of PVC for medical products, but would require extensive forethought before entering the market. Things to be considered are: degradation upon autoclaving, uniformity of grafting, dimensional reproducibility, cleansing of antimicrobial films and transparency of quaternized films.

REFERENCES

1) Rahman, M.; Brazel, C. S. *Prog. Polym. Sci.* **2004**, *29(12)*, 1223-1226.

2) Manojkumar, V.; Padmakumaran Nair, K. G.; Santhosh, A.; Deepadevi, K. V.; Arun, P.; Lakshmi, L. R.; Kurup, P. A. *Vox Sang.* **1998**, *75*(2), 139-144.

3) Hill, S. S.; Shaw, B. R.; Wu, A. H. *Biomed. Chromatogr.* **2003**, *17*(4), 250-262.

4) Currie, E. P.; Norde, W.; Cohen, M. A. *Adv. Colloid Interface Sci.* **2003**, *100*, 205-265.

5) Breme, F.; Buttstaedt, J.; Emig, G. *Thin solid Films* **2000**, *377-378*, 755-579.

6) Messori, M.; Toselli, M.; Pilati, F.; Fabbri, E.; Pasquali, L.; Nannarone, S. *Polymer* **2004**, *45*, 805-813.

7) Balazs, D. J.; Hollenstein, C.; Mathieu, H. J. *Plasma Process. Polym.* **2005**, *2*, 104-111.

8) Balazs, D. J.; Triandafillu, K.; Wood, P.; Chevolot, Y.; Van Delden, C.; Harms, H.; Hollenstein ,C.; Mathieu, H. J. *Biomaterials* **2004**, *25*, 2139-2151.

9) Tan, Q. G.; Ji, J.; Zhao, F.; Fan, D. Z.; Sun, F. Y.; Shen, J. C. *J. Mater. Sci.: Mater. in Medicine* **2005**, *16(7)*, 687-692.

10) Yoshizaki, T.; Tabuchi, N.; Van Oeveren, W.; Shimbamiya, A.; Koyama, T.; Sunamori, M. *Int. J. Artif Organs* **2005**, *28(8)*, 834-40.

11) Zhang, W.; Chu, P. K; Ji, J.; Zhange, Y.; Liu, X.; Fu, R. K. Y.; Ha, P. C. T.; Yan, Q. *Biomaterials* **2006**, *27(1)*, 44-51.

12) Audic, J. L.; Poncin-Epaillard, F.; Reyx, D.; Brosse, J. C. *Journal of Applied Polymer Science* **2000**, *79(8)*, 1384.

13) Ito, R.; Seshimo, F.; Haishima, Y.; Hasegawa, C.; Isama, K.; Yagami, T.; Nakahashi, K.; Yamazaki, H.; Inoue, K.; Yoshimura, Y.; Saito, K.; Tsuchiya, T.; Nakazawa, H. *International Journal of Pharmaceutics* **2005**, *303*, 104.

14) Jayakrishnan, A.; Sunny, M. C. *Polymer* **1996**, *37(23)*, 5213.

15) Lakshmi S.; Jayakrishnan, A. *Polymer* **1998**, 3*9(1)*, 151.

16) Lakshmi S.; Jayakrishnan, A. *J Biomed Mater Res Part B: Appl Biomater* **2003**, *65B*, 204.

17) Lakshmi S.; Jayakrishnan, A. *Biomaterials* **2002**, *23*, 4855.

18) Bergbreiter, D. E.; Xu, G. F. *Polymer* **1996**, *37(12)*, 2345-2352.

19) Lee, W. F.; Hwong, G. Y. *Eur Polym J* **1997**, *33(9)*, 1499-1504.

20) Sreenivasan, K. *J Appl Polym Sci* **1999**, *74*, 113-118.

21) Lakshmi, S.; Jayakrishnan, A. *Artificial Organs* **1998**, *22(3)*, 222-229.

22) Balakrishnan, B.; Kumar, D. S.; Yoshida, Y.; Jayakrishnan, A. *Biomaterials* **2005**, 2*6*, 3495-3502.

23) Balakrishnan, B.; James, N. R.; Jayakrishnan, *A Polym Int* **2005**, *54*, 1304-1309.

24) Zhao, B.; Brittain, W. J. *Prog. Polym. Sci.* **2000**, *25(5)*, 677-710.

25) Hu, S. W.; Brittain, W. J. *Macromolecules* **2005**, *38*, 3263-3270.

26) Klibanov, A. M.; Lewis, K.; Tiller, J. C.; Liao, C. J. *Proc. Natl. Acad. Sci.* **2001**, *98(11)*, 5981-5985.

27) Gao, B.; Lv Y.; Jui, H. *Polym. Int.* **2003**, *52*, 1468-1473.

28) Gao, B.; He, S.; Guo, J.; Wang, R. J. *Appl. Polym. Sci.* **2005**, *100*, 1531-1537.

29) Ober, C. K.; Krishnan, S.; Ward, R. J.; Hexemer, A.; Sohn, K. E.; Lee, K. L.; Angert, E. R.; Fischer, D. A.; Kramer, E. J. *Langmuir* **2006**, *22*, 11255-11266.

30) *PVC Handbook*; Wilkes C. E., Summers J. W., Daniels C. A., Ed.; Munich: Cincinnati, Ohio, 2005; p 1-19.

31) Cox, S. S.; Hodgens, A. T.; Little, J. C. *Journal of the Air & Waste Management Association* **2001**, April, 1-23.

32) Su, C. S.; Patterson, D.; Schreiber, H. P. *J. of App. Polym. Sci.* **1976**, *20*, 1025-1034.

33) Stevens, M. P. *Polymer Chemistry*, 3rd ed.; New York: McGraw Hill; 1994.

34) Dictionary.com, http://dictionary.reference.com/browse/lubricity, accessed November 11, 2008.

35) Tickner J. A.; Rossi M.; Haiama N.; Lappe M.; Hunt P. The use of di(2-ethylhexyl) phthalate in PVC medical devices: exposure, toxicity and alternatives Center for Sustainable Production. Lowell. MA: 1999 http://www.sustainableproduction.org/downloads/DEHP%20Full%20Text.pdf

36) Kambia, K.; Dine, T.; Gressier, B.; Bah, S.; Germe, A. F.; Luyckx, M.; Brunet, C.; Michaud, L.; Gottrand, F. *Int. J. Pharm.* **2003**, *262(1-2)*, 83.

37) Kambia, K.; Dine, T.; Gressier, B.; Bah, S.; Germe, A. F.; Luyckx, M.; Brunet, C.; Michaud, L.; Gottrand, F. *Int. J. Pharm.* **2003**, *262(1-2)*, 83.

38) Hileman, B. *Chem. Eng. News* **2002**, *80(37)*, 6.

39) Fugit, J. L.; Taverdet, J. L.; Gauvrit, J. Y.; Lanteri, P. *Polym. Int.* **2003**, *52*, 670-675.

40) Matyjaszewski, K.; Russell, A. J.; Lee, S. B.; Koepsel, R. R.; Morley, S. W.; Sun, Y. *Biomacromolecules* **2004**; *5*: 877-882.

41) Brittain, W. J; Boyes, S. G.; Granville, A. M.; Baum, M.; Akgun, B.; Mirous, B. *Surface Sciences* **2004**; *570*: 1-12.

42) Hawker, C.; Russell, T. P.; Mansky, P.; Liu, Y.; Huang, E. *Science* 1997; 275(7): 1458-1460.

43) *Anionic Polymerization*; Quirk, R. P.; Hsieh, H. L.; Hudgin, D. E., Ed.; Marcel Dekker, Inc.: New York, New York 1996.

44) *Principles of Polymerization*; Odian, G.; Hodgkin, J., Ed.; John Wiley & Sons, Inc.: Hoboken, NJ 2004.

45) Seçkin, T.; Önal, Y.; Yesilada, Ö.; Gültek, A. *J. Mater. Sci.* **1997**, *32*, 5993-5999.

46) Rühe, J.; Biesalski, M. *Macromolecules* **1999**, *32*, 2309-2316.

47) Klibanov, A. M.; Lewis, K.; Lin, J.; Tiller, J. C.; Lee, S. B.; Lewis, K. Biotechnology Letters **2002**, *24*, 801-805.

48) Gao, B.; He S.; Guo, J.; Wang, R. J. *Materials Letters* **2007**, *61*, 877-883.

49) Höpken, J.; Möller, M.; Boileau, S. *New Polymeric Mater.* **1991**, *2(4)*, 339-356.

50) Ober, C. K.; Wang, J. *Macromolecules* **1997**, *30*, 7560-7567.

51) Bacteria, accessed Oct. 28th, 2008, http://users.rcn.com/jkimball.ma.ultranet/BiologyPages/E/Eubacteria.html

52) MicrobiologyBytes, accessed Oct. 28th, 2008, http://microbiologybytes.wordpress.com/2008/02/25/peptidoglycan-the-strength-and-weakness-of-bacteria/

53) Today's Online Textbook of Bacteriology, accessed Oct. 28th, 2008, http://www.textbookofbacteriology.net/BSRP.html

54) Ivanov, I.; Klein, M. L.; McCammon, J. A.; Vemparala, S.; Phphristic, V.; Kuroda, K.; DeGrado, W. F. *J. Am. Chem. Soc.* **2006**, *128*, 1778-1779.

55) Cho, J.; Hong, J.; Char, K.; Caruso, F. *J. Am. Chem. Soc.* **2006**, *128(30)*, 9935-9942.

56) TexLoc Refractive Index of Polymers, accessed Oct. 28th, 2008, http://www.texloc.com/closet/cl_refractiveindex.html

57) Onciu, M.; Onen, A.; Yagci, Y. Polymeric N-Allyl Vinylpyridinium Salts as Addittion Fragmentation Type Initiators for Cationic Polymerization, http://www.ehb.itu.edu.tr/~yusuf/paperWords/78.doc, accessed November 10, 2008.

58) *Advanced Organic Chemistry*; March, J., Ed.; John Wiley & Sons, Inc.: New York, New York, **1992**; 4th Ed.

59) *The Aldrich Library of 13C and 1H FTNMR Spectra*; Pouchert, Behnke, Ed.; Aldrich Chemical Co. Inc.: Milwaulkee, WI, **1993**; 1st Ed.

60) Lim, H.; Lee, Y.; Han, S.; Cho, J.; Kim, K. *J. Vac. Sci. Technol. A.* **2001**; *19(4)*: 1490-1496.

61) Martins, M. C. L.; Wang, D.; Ji, J.; Feng, L.; Barbosa, M. A. *Biomaterials* **2003**; *24(12)*: 2067.

62) Xu, C.; Wu, T.; Batteas, J.; Drain, C. M.; Beers, K. L.; Fasolka, M. J. *Appl. Surface Sci.* **2006**; *252(7)*: 2529.

63) Shyh-Dar, L.; Ging-Ho, H.; Chang, P. C. T.; Chen-Yu, K. *Biomaterials* **1996**; *17(16)*: 1599.

64) Baum, M.; Brittain, W. J. *Macromolecules* **2002**; *35*: 610-615.

65) Sangribsub, S.; Tangboriboonrat, P.; Pith, T.; Decher, G. *Eur. Polym. J.* **2005**; *41(7)*: 1531

66) Xu, J. W.; Bulter, I.; Gilson, D. Vibrational Spectroscopic Investigation of 2-Hydroxyethyl Methacrylate (HEMA) and Poly-2-hydroxyethylmethacrylate (PHEMA),http://iadr.confex.com/iadr/china04/preliminaryprogram/abstract_49544.htm, accessed November 9, 2008.

67) Kim, J. H.; Sim, S. J.; Lee, D. H.; Kim, D.; Lee, K. Y.; Chung, D. J.; Kim, J. *Polym. J.* **2004**; *36*:943-948.

68) Zhu, S.; Yang, N.; Zhang, D. *Materials Chemistry and Physics* **2008**; in press.

69) Tamaki, R.; Naka, K.; Chujo, Y. *Polym. J.* **1998**; *30*: 60-65.

70) Moharram, M. A.; Allam, M. A. *J. App. Polym. Sci.* **2007**; *105*: 3228-3234.

71) Panov, V. P.; Kazarin, L. A.; Dubrovin, V. I.; Gusev, V. V.; Kirsh, Y. É. *Journal of Applied Spectroscopy* **1974**; *21(5)*: 1504-1510.

APPENDICES

APPENDIX A.

XPS SPECTRA

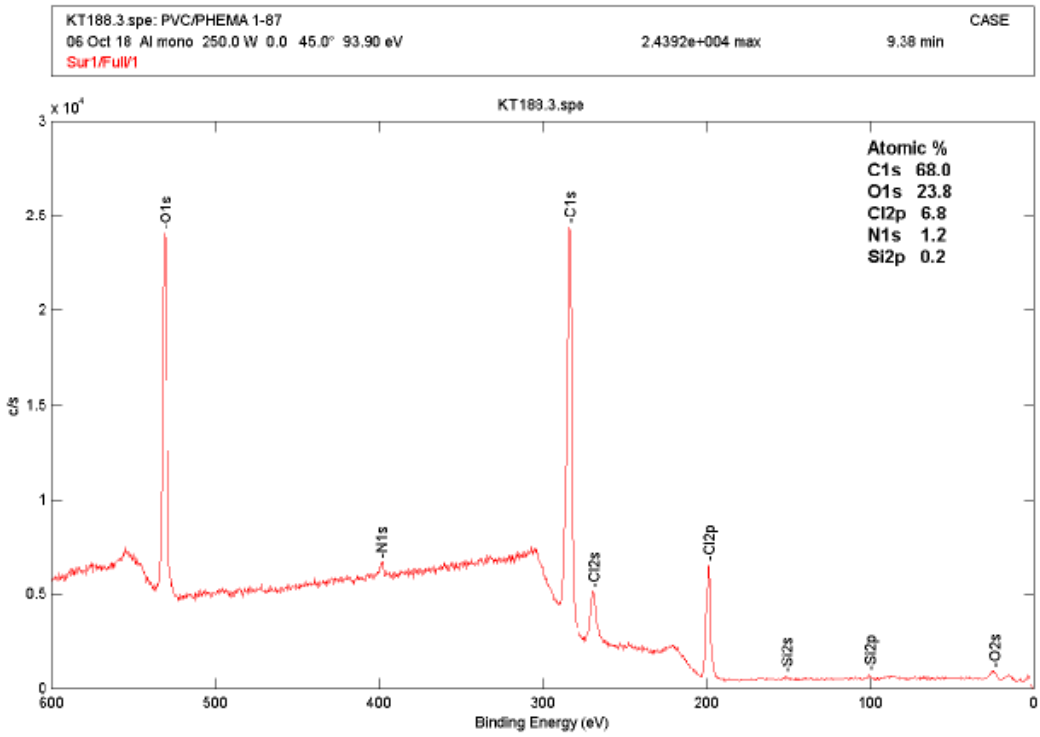

Figure A.1. XPS spectrum for PVC-*g*-PHEMA.

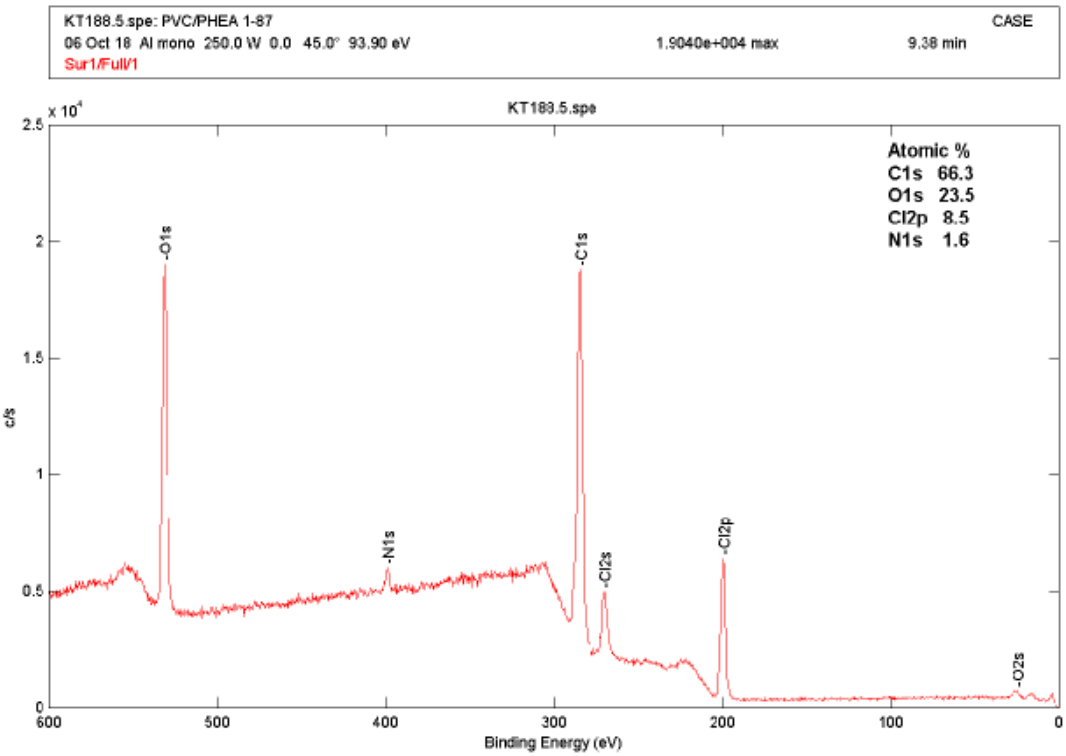

Figure A.2. XPS spectrum for PVC-*g*-PHEA.

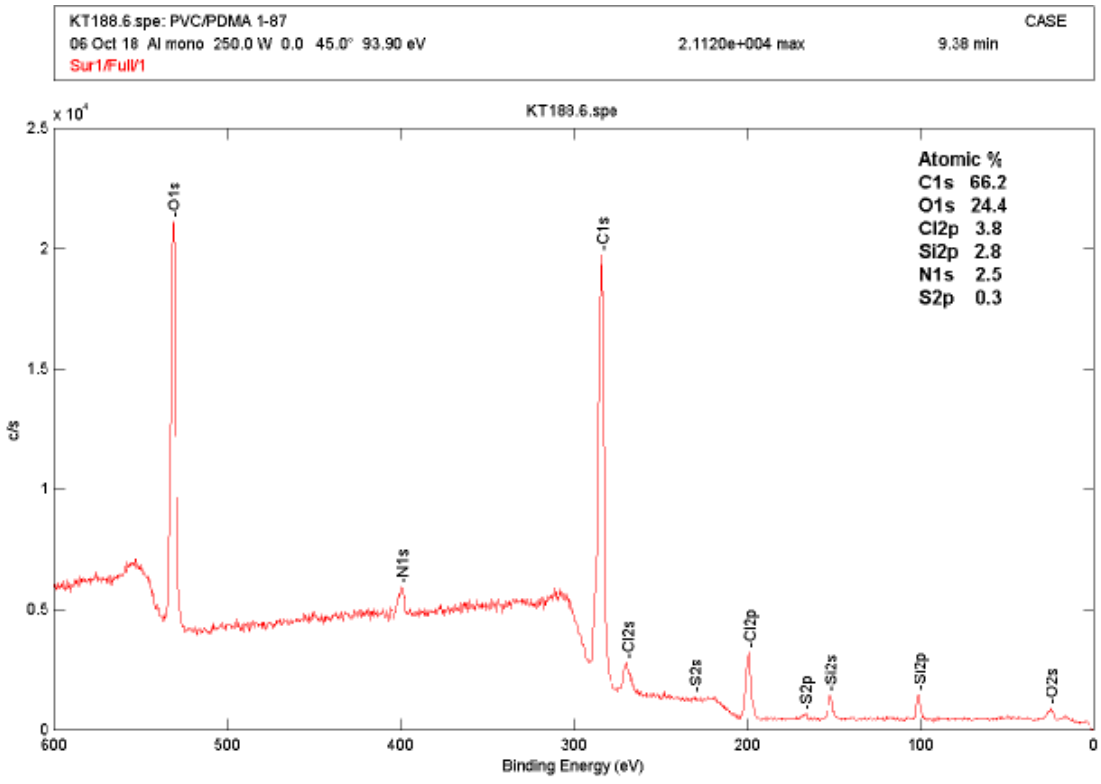

Figure A.3. XPS spectrum of PVC-*g*-PDMA.

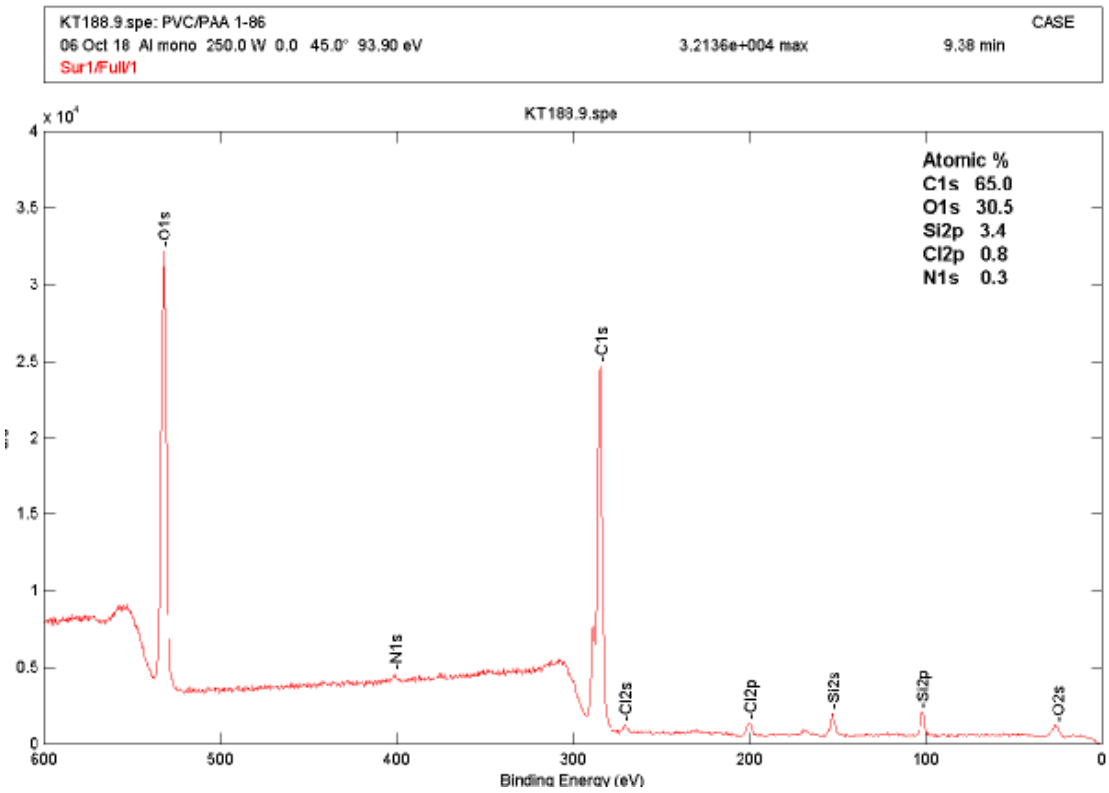

Figure A.4. XPS spectrum of PVC-*g*-PAA.

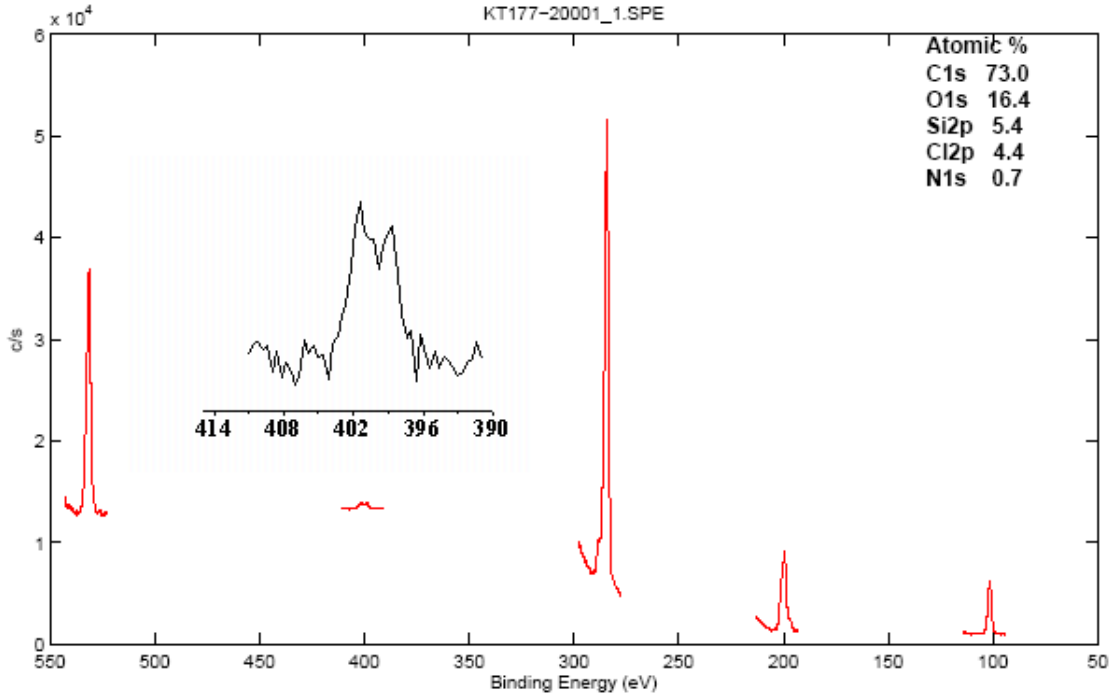

Figure A.5. XPS spectrum for PVC-*g*-PDMAEMA. Elements were probed within 20 eV of their specific binding energies for O (530), N (398.6, 401), C (284), Cl (199) and Si (101).

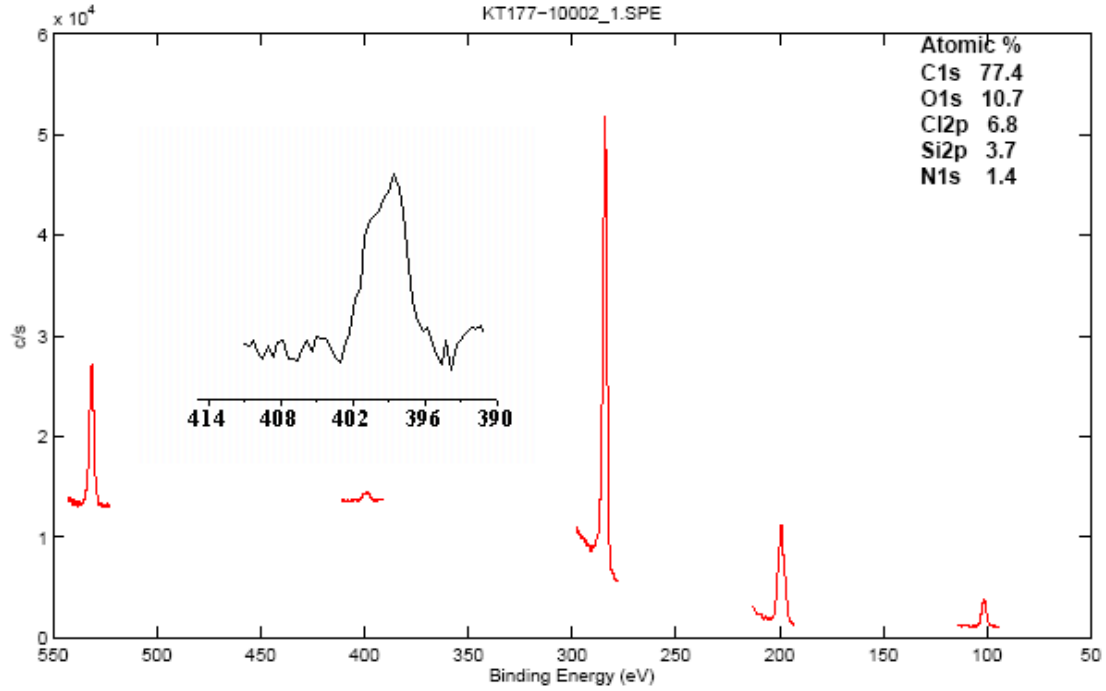

Figure A.6. XPS spectrum for PVC-*g*-P4VP. Elements were probed within 20 eV of their specific binding energies for O (530), N (398, 401), C (284), Cl (199) and Si (101).

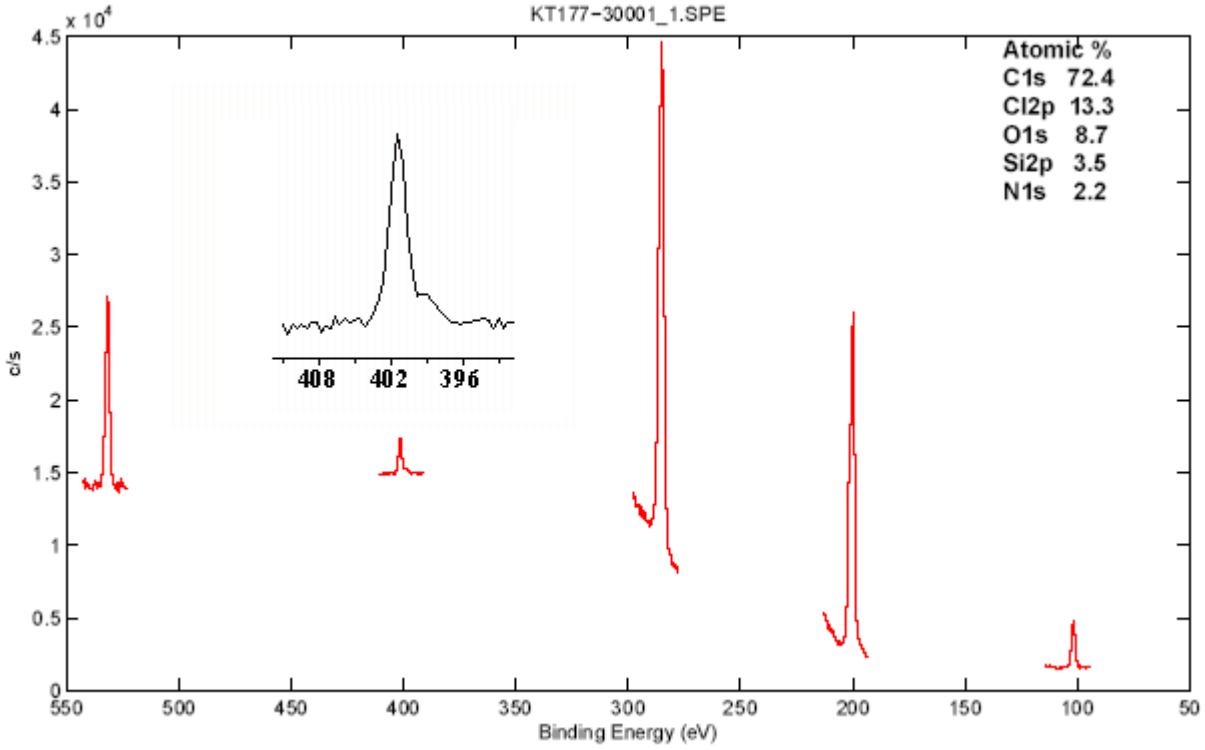

Figure A.7. XPS spectrum for PVC-*g*-P4VP4C film. Elements were probed 20 eV of their specific binding energies for O (530), N (399, 401.4), C (284), Cl (199) and Si (101).

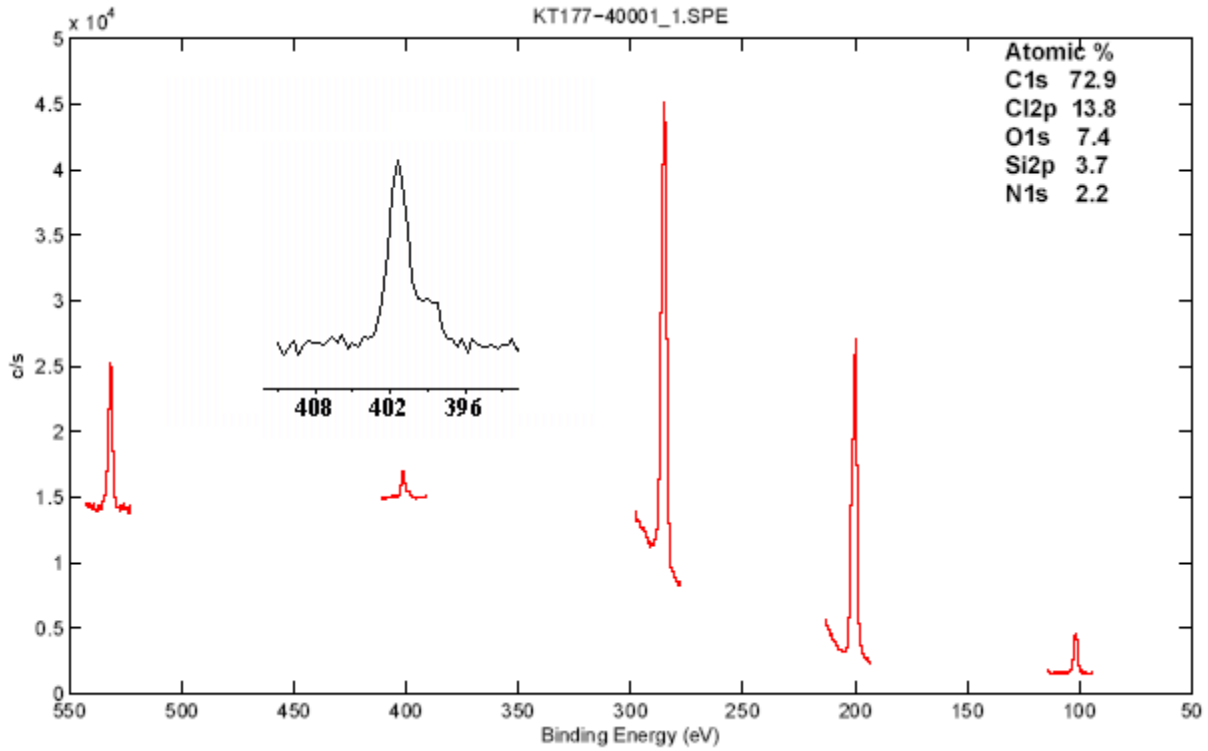

Figure A.8. XPS spectrum for PVC-*g*-P4VP6C film. Elements were probed 20 eV of their specific binding energies for O (530), N (398.6, 401.4), C (284), Cl (199) and Si (101).

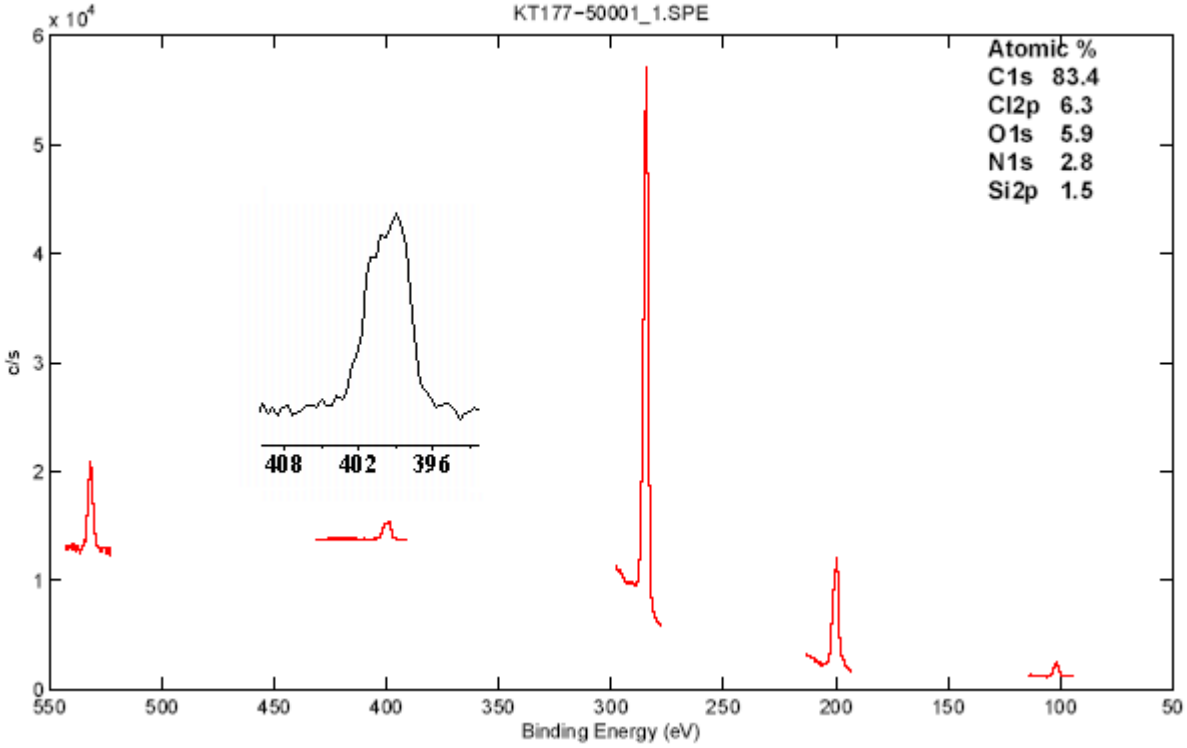

Figure A.9. XPS spectrum for PVC-*g*-P4VP8C film. Elements were probed 20 eV of their specific binding energies for O (530), N (399, 400), C (284), Cl (199) and Si (101).

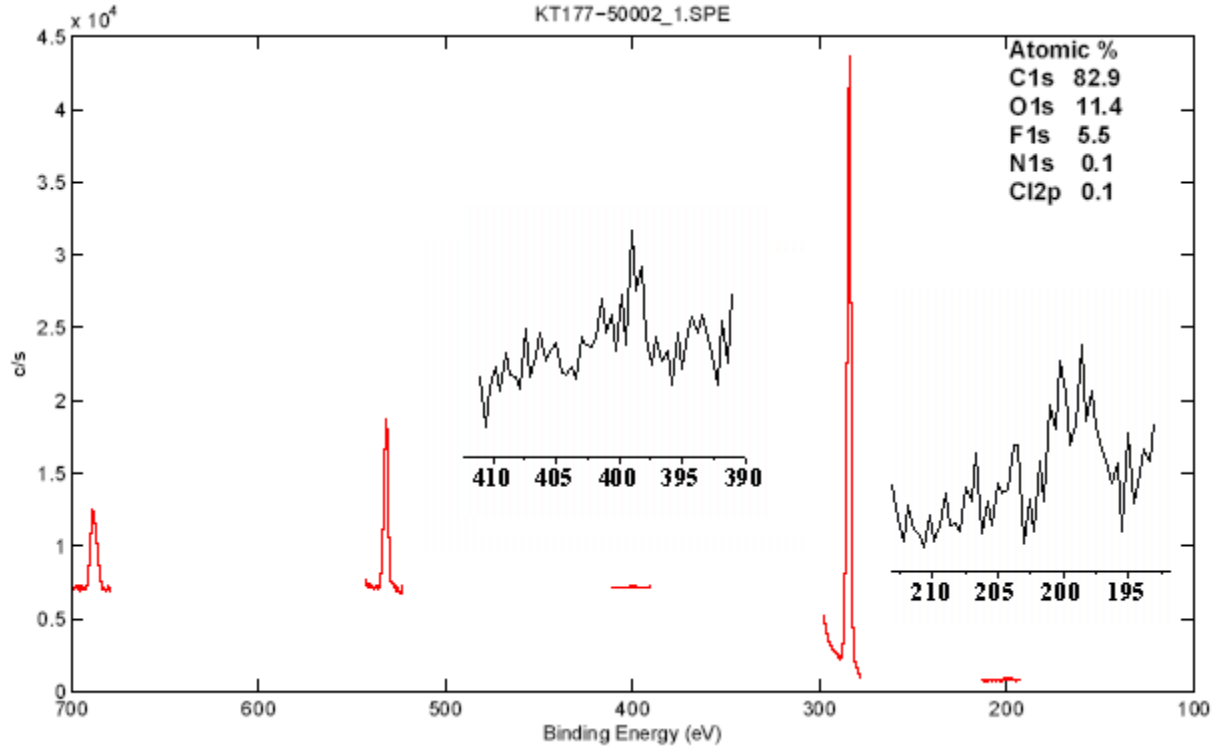

Figure A.10. XPS spectrum for PVC-*g*-P4VP148hF film. Elements were probed 20 eV of their specific binding energies for F (688), O (530), N (399), C (284), and Cl (199).

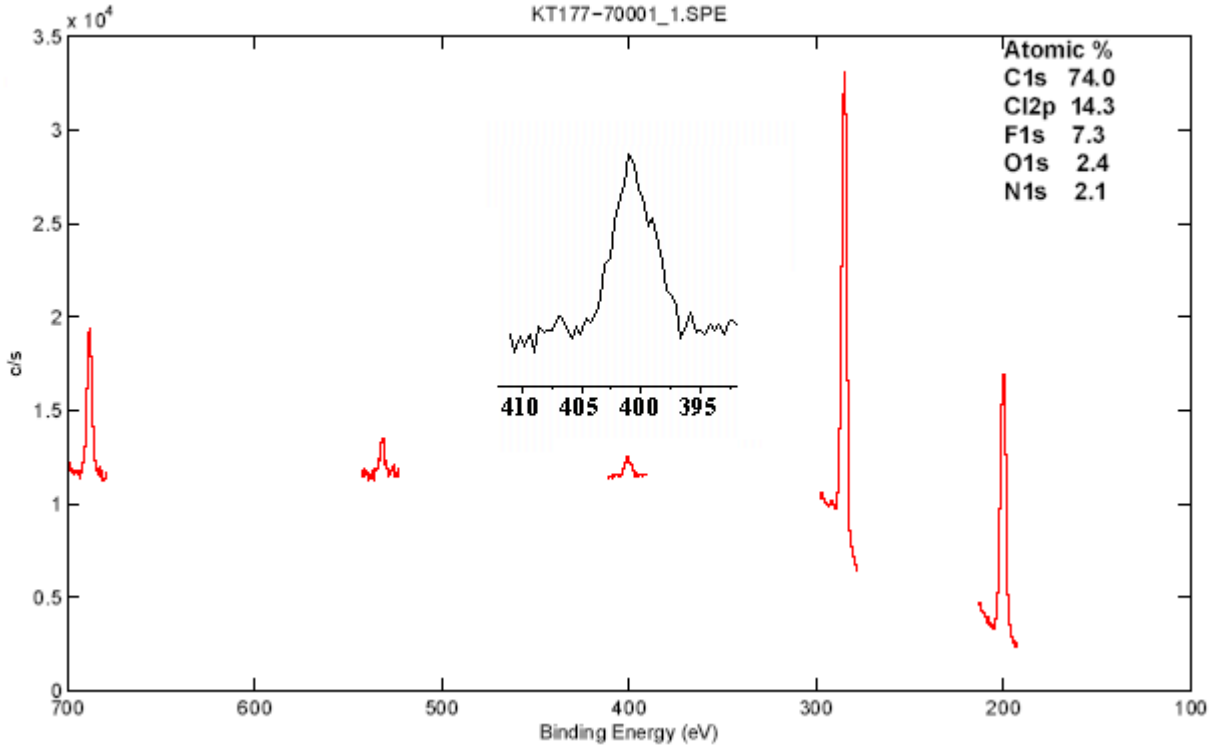

Figure A.11. XPS spectrum for PVC-*g*-P4VP48hF-72h6C film. Elements were probed 20 eV of their specific energies for F (688), O (530), N (401), C (284), and Cl (199).

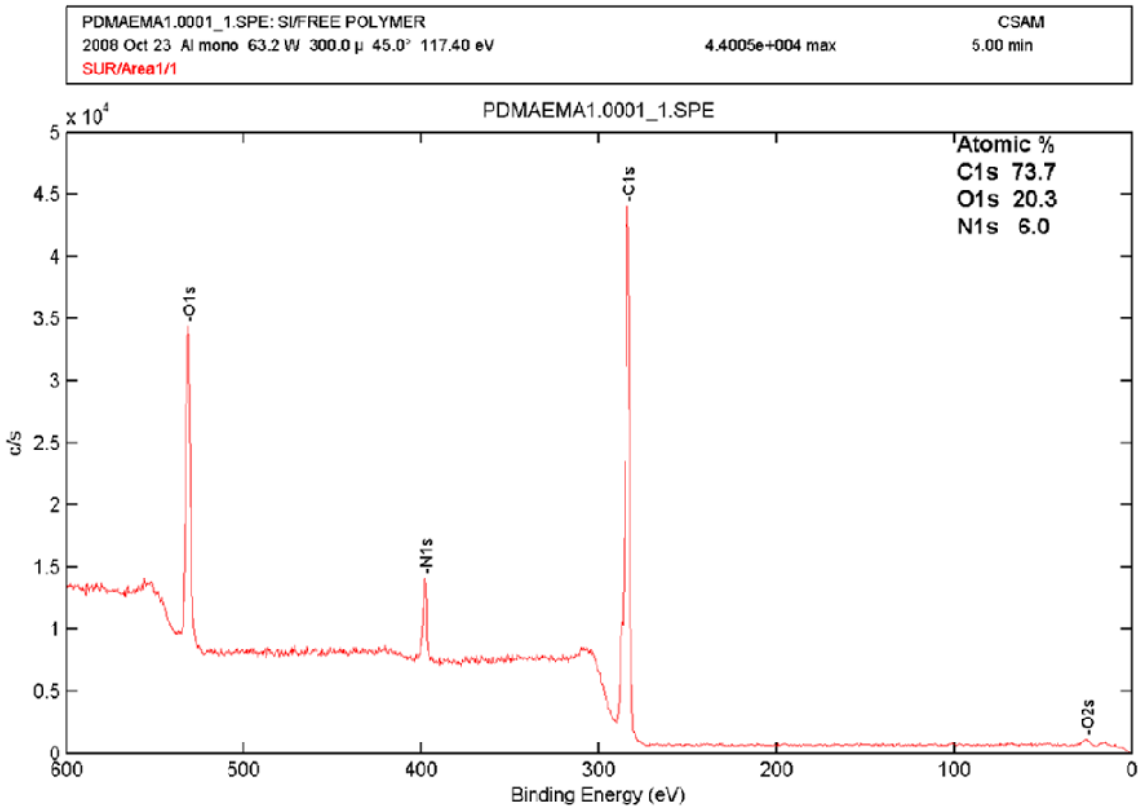

Figure A.12. XPS spectrum of free PDMAEMA in the range of 0-600 eV.

APPENDIX B.

IR CALIBRATION DATA

PHEMA 1733 cm^{-1}		PHEMA 1078 cm^{-1}	
Thickness (x)	Absorbance (y)	Thickness (x)	Absorbance (y)
0.208	0.0393	0.208	0.0142
0.202	0.0366	0.202	0.0131
0.167	0.0312	0.167	0.0115
0.167	0.0293	0.167	0.0112
0.164	0.0292	0.164	0.0112
0.161	0.0291	0.161	0.0112
0.218	0.0382	0.218	0.0146
0.197	0.0361	0.197	0.0147
0.109	0.0210	0.109	0.00791
0.105	0.0213		
0.100	0.0195		

Figure B.1. Thickness and absorbance data for PHEMA IR calibration curve based on the absorbance at 1733 cm^{-1} and 1078 cm^{-1}.

PHEA 1167 cm^{-1}		PHEA 1731 cm^{-1}	
Thickness (x)	Absorbance (y)	Thickness (x)	Absorbance (y)
0.134	0.0192	0.134	0.0384
0.128	0.0179	0.128	0.0317
0.102	0.0147	0.102	0.0306
0.0832	0.0113	0.0963	0.0257
0.0712	0.0106	0.0832	0.0266
0.0708	0.00941	0.0708	0.0231
0.0601	0.00871	0.0523	0.0210
0.0523	0.00702	0.0424	0.0147
0.0424	0.00492	0.0350	0.0141
0.0350	0.00375	0.0266	0.00834
0.194	0.0244	0.194	0.0542
0.135	0.0187	0.135	0.0405
0.135	0.0191		

Figure B.2. Thickness and absorbance data for PHEA IR calibration curve based on the absorbance at 1731 cm^{-1} and 1167 cm^{-1}.

PDMAEMA 1733 cm^{-1}		PDMAEMA 1457 cm^{-1}	
Thickness (x)	Absorbance (y)	Thickness (x)	Absorbance (y)
0.1669	0.03878	0.0986	0.008581
0.0861	0.0179	0.1648	0.013303
0.0771	0.0163	0.084	0.006891
0.093	0.01951	0.0909	0.00899
0.1578	0.035764	0.1318	0.0123
0.1765	0.041518	0.0837	0.006617
0.1125	0.025948		
0.1339	0.033987		
0.0858	0.017993		
0.1022	0.026963		

Figure B.3. Thickness and absorbance data for PDMAEMA IR calibration curve based on the absorbance at 1733 cm^{-1} and 1457 cm^{-1}.

PDMA 1640 cm^{-1}		P4VP 1600 cm^{-1}		PAA 1687 cm^{-1}	
Thickness (x)	Absorbance (y)	Thickness (x)	Absorbance (y)	Thickness (x)	Absorbance (y)
15.3	0.04911	0.0307	0.005	0.0234	0.0105
16.1	0.06254	0.0501	0.00615	0.0205	0.00764
7.12	0.02466	0.127	0.041	0.0114	0.00302
5.02	0.02037	0.0781	0.0222	0.0134	0.00369
4.57	0.01477	0.1275	0.03575	0.0139	0.00614
		0.09258	0.02641		

Figure B.4. Thickness and absorbance data for PDMA, P4VP and PAA IR calibration curve based on the absorbance at 1640, 1600 and 1687 cm^{-1}, respectively.

APPENDIX C.

CALCULATIONS

Gravimetric Analysis: Error by Propagation

$$x = a * (b/c) \quad \text{(EQ.C.1)}$$

$$s_x = x ((s_a/a)^2 + (s_b/b)^2 + (s_c/c)^2 + ...)^{1/2} \quad \text{(EQ.C.2)}$$

PHEMA: W = 0.3438 ± .001; A = 92.1 ± 0.1; ρ = 1.15 ± 0.01; H = 0.00162 cm)

$(0.00162) ((0.001 / 0.3438)^2 + (0.1 / 92.1)^2 + (.01 / 1.15)^2)^{1/2}$

$= 16.2 \pm 0.1$ μm

IR Calibration: Error by Standard Deviation

	PDMA	PDMA FD	PDMAEMA 1457	PHEMA 1078	P4VP	PAA	PHEA 1167
	0.378	2.3	1.9	3.724	3.919	2.012	3.433
	0.375	0.729	2.781	3.726	3.024	1.766	3.683
	1.067	1.118	2.596	3.214	3.752	1.761	3.07
	1.219	0.828	2.916	3.516	3.856	2.295	1.697
	1.057			4.165	3.525	3.765	2.205
				4.228	3.603	3.803	
				4.127	2.744		
					2.47		
					1.495		
					2.832		
Ave. Abs.	0.819	1.244	2.548	3.814	3.122	2.567	2.818
STDEV	**0.409**	**0.723**	**0.452**	**0.242**	**0.765**	**0.963**	**0.840**

Calculated by adding error to average absorbance to get thickness range :

PDMA : 0.819 / 2 + 0.409 = 0.819 = y

y = 0.3565 x

x = 2.408

2.408 – 1.26 (thickness) = 1.2 μm error

UV-Vis Calibration

$$y = 10.845x + 0.2548 \quad \text{(EQ.C.3)}$$

Absorbance of PVC-*g*-P4VP (y): 0.983

Concentration (x) = 0.0672 mg/mL

Concentration (mg/mL) / DMF (mL) / 1000 (mg) = WP4VP (g) (EQ.C.4)
0.0672 (mg/mL) / 13.9 (mL) / 1000 (mg) = 0.000933g

(WP4VP * ρ-1 * A-1)/ 2= H (EQ.C.5)
0.000933 * (1g / 1000 mg) * (1 / 1.153 (g/cm^3)) * (1/0.2183 (cm^2))
H = 0.003695 cm / 2
Thickness of P4VP = 18.5 μm

Calculation for % PVC in PVC-*g*-PHEMA

PHEMA theoretical $C_6H_{10}O_3$ (130.148 g/mol):
C: 55.37
H: 7.74
O: 36.88

GIVEN ELEMENTAL Analysis of sample #114 –

C: 57.83	59.50
H: 8.00	8.20
O: 29.76	**30.60**
Cl: 1.67	1.70 .
97.26%	100%

With O known to be 30.60% of the sample, the parts oxygen in the chemical formula is:

(15.9994 (X)) / 130.148 = **0.306**

X = **2.49**

The chemical formula for PHEMA ($C_6H_{10}O_3$) claims 3 parts Oxygen. Therefore, the ratio of calculated O to actual O is (2.49/ 3). This ratio can be multiplied by the actual parts H (10) and C (6) to get the calculated value of parts H and C:

(2.49/ 3) x 3 = 8.3 H

(2.49/ 3) x 2 = 4.98 C

The new formula that represents the 'parts' of elements in the sample for PHEMA is:

$C_{4.98}H_{8.3}O_{2.49}$

The mass %C: (4.98)(12.0107)/ 130.148 = **46 %**
The mass %H: (8.3)(1.00794)/ 130.14 = **6.4%**
The mass % O: **30.60%**

Now, the % of PVC can be calculated by subtracting the PHEMA elemental % from the GIVEN elemental analysis.

C: 59.50% - **46%** = % C_{PVC} = 13.5% C_{PVC}
H: 8.20% - **6.4%** = % H_{PVC} = 1.8% H_{PVC}
Cl: 1.7% - 0% = % Cl_{PVC} = 1.7% Cl

The total % PVC in the sample is **17%**, and the total %PHEMA in the sample is **83%, if the amount of oxygen is solely for PHEMA.**